Antifungal activity of rationally designed γ-core peptide derivatives of ascomycetous antifungal proteins

Ph.D. dissertation

KAREMERA K John

Supervisors:

Dr. Norbert László Galgóczi and Dr. Attila Borics

Doctoral School of Biology

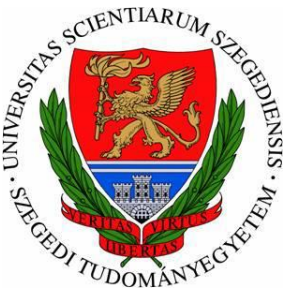

Department of Microbiology and Biotechnology

Faculty of Science and Informatics

University of Szeged

2026

TABLE OF CONTENTS

LIST OF ABBREVIATIONS

5-FC:	5-fluorocytosine
5-FU:	5-fluorouracil
AFPg:	*Aspergillus giganteus* antifungal protein
AFPs:	Antifungal proteins
AgNPs:	Silver nanoparticles
AI:	Artificial Intelligence
AmB:	Amphotericin B
AMP:	Antimicrobial proteins/peptides
AFG:	Anidulafungin
AuNPs:	Gold nanoparticles
BP:	Bubble-protein
CAS:	Caspofungin
DIC:	Diisopropylcarbodiimide
DNA:	Deoxyribonucleic acid
ECD:	Electronic circular dichroism spectroscopy
FACS:	Fluorescence-activated cell sorting
FDA:	Food and Drug Administration
FLC:	Fluconazole
FPPL:	Fungal priority pathogen list
GAFFI:	Global Action Fund for Fungal Infections
GP:	Growth percentage
GRAVY:	Grand average of hydropathy
HIV:	Human immunodeficiency virus
HIV-AOIs:	Human immunodeficiency virus-AIDS- associated opportunistic infections
$I_{0:}$	Observed percentage inhibition
I*e:*	Expected percentage inhibition
IP:	Inhibition percentage
IPS:	Insect physiological saline-treated control
IR:	Interaction ratio
ITZ:	Itraconazole
LCM:	Low cationic medium

MFG:	Micafungin
MIC:	Minimum inhibitory concentration
NFAP2*:*	*Neosartorya fischeri* antifungal protein 2
OD_{620}:	Optical density at 620 nm
PAF*:*	*Penicillium chrysogenum* antifungal protein
PDA:	Potato dextrose agar
pI:	Isoelectric point
PLGA:	Poly (lactic-co-glycolic acid)
RNA:	Ribonucleic acid
RP-HPLC:	Reverse-phase high-performance liquid chromatography
SEM:	Scanning electron microscopy
SLNPs:	Solid lipid nanoparticles
TFA:	Trifluoroacetic acid
TRB:	Terbinafine
U.S:	United States
UK:	United Kingdom
USD:	United States Dollar
UT:	Untreated control
WHO:	World Health Organisation
YPDA*:*	Yeast extract peptone, dextrose agar
ZnONPs:	Zinc oxide nanoparticles
γAFPs:	Gamma-core antifungal peptides

1. INTRODUCTION

1.1. Fungi as a neglected problem in human medicine

Data on the prevalence and mortality rates of fungal infections have become increasingly available over the past few decades. However, inadequate surveillance and persistent data gaps continue to hinder a comprehensive global understanding of fungal infections, which pose significant health burdens, ranging from serious, life-threatening illnesses to chronic conditions (Denning, 2024). It is estimated that over 150 million fatal cases occur annually. Factors such as long-term medication use, societal changes, and medical advancements have all contributed to their accelerated spread. The emergence of drug-resistant strains of fungal species (e.g. *Aspergillus fumigatus*, *Candida albicans*, *Candidozyma auris* [formerly, *Candida auris*]) underscores the urgent need for effective research and development in antifungal therapeutics (Kainz et al., 2020). Resistance to conventional antifungal drugs, along with the emergence of strains exhibiting reduced susceptibility, are key drivers behind the rising incidence of fungal infections (Datta et al., 2013). Currently, only four major classes of compounds (azoles, echinocandins, polyenes, and flucytosine) are used in antifungal therapies to treat invasive fungal infections, when the whole body is affected by the infectious agent (Wall & Lopez-Ribot, 2020). The widespread use of triazole fungicides in agriculture has made the problem of rising resistance even worse, due to the extensive and prolonged use of them (Khanna & Bharti, 2014; Antibiotic Resistance Threats in the United States, 2019; Kainz et al., 2020). Historically, fungal infections were considered rare and did not significantly impact human health. However, according to the Global Action Fund for Fungal Infections (GAFFI), this situation has drastically changed due to the rising number of immunocompromised individuals who are especially susceptible to such infections (Rodrigues & Nosanchuk, 2020). The health of these people is seriously threatened by invasive fungal infections. Furthermore, GAFFI notes that even immunocompetent individuals can experience severe outcomes from localized fungal infections (Tufa et al., 2023). For instance, fungal keratitis causes over a million cases of blindness each year (Bongomin et al., 2017; Fisher & Denning, 2023). Nearly one billion individuals globally suffer from skin mycoses (Urban et al,2020), which are slightly more prevalent than tooth decay and headaches (Rodrigues & Nosanchuk, 2020). Moreover, over 10 million people suffer from reactive airway diseases triggered by exposure to fungal spores (Bongomin

et al., 2017). In response to growing concerns, the World Health Organisation (WHO) published the first Fungal Priority Pathogen List (FPPL) in October 2022(Fisher & Denning, 2023, GAFFI, 2020), to guide scientific research and policy initiatives targeting serious fungal infections. The list focuses on 19 fungal species and is based on several criteria, including mortality, incidence, global distribution, trends, hospitalisation needs, comorbidities, antifungal resistance, preventability, diagnostic accessibility, and evidence-based treatments. Concerns have been raised that the current ranking may not accurately reflect the true burden of certain fungal infections. Therefore, a revised list using WHO regional classifications is recommended to better account for specific regional contexts (Sekkides, 2015; Parums, 2022). In response to the growing threat, scientists are collaborating to establish a multifaceted approach that integrates advanced diagnostic techniques such as next-generation sequencing and molecular diagnostics (Naik et al., 2024) and conduct studies aimed at developing new antifungal treatments and improving existing ones (Fisher and Denning, 2023). Antifungal proteins and peptides (AFPs) are being evaluated in clinical trials to assess their safety and efficacy in treating fungal infections (Li et al., 2021; Puumala et al., 2024). The structural characteristics of AFPs, found in both plants and animals, yare critical determinants of their antimicrobial efficacy. Among these, the γ-core motif (GXC-X_{3-6}-C signature, where X represents any amino acid) is a key structural element of AFPs from both sources and it is essential to their antifungal activity (Sagaram et al., 2011; Li et al., 2021). According to Chagri et al. (2024), synthetic peptides spanning the γ-core motif can disrupt internal cellular functions, potentially raise intracellular ATP levels and induce cell death. Synthetic peptides designed on the γ-core motifs of plant and animal AFPs demonstrate broad-spectrum antifungal activity, making them promising candidates for novel therapeutic development. These peptides exert their effects by either damaging the fungal cell membrane, leading to cell lysis, or causing reduced hyphal growth with excessive branching (Slezina et al., 2022a; Sonderegger et al., 2018).

1.2. Antifungal Therapy

The rising frequency of fungal infections has become a major public health concern, driven by an increase in host predisposition factors. While numerous antifungal drugs available, their efficacy remains debatable, and the limited number of broad-spectrum agents along with associated side effects cannot be overlooked. To counter emerging fungal pathogens and stop the spread of resistant strains, it is essential to develop

innovative drugs and delivery systems (Sousa et al., 2020). Antifungal drug discovery flourished during the 1990s, driven by increased interest from major pharmaceutical companies in developing novel antifungal therapies (**Fig. 1**). However, echinocandins have only been available for the past two decades, and progress in drug development has since slowed. Currently, the U.S. Food and Drug Administration (FDA) has approved four classes of antifungal agents for the treatment of invasive fungal infections: azoles, flucytosine, echinocandins, and polyenes (Odds et al., 2003; Wall & Lopez-Ribot, 2020).

Effective use of these antifungal drugs approved for human treatment requires understanding of the structural differences between pathogenic fungi and healthy human cells. In particular, unique fungal enzymes involved in the ergosterol biosynthesis, as well as distinct components of the fungal cell wall (mannans, glucans, and chitins) are commonly targeted in antifungal drug development (Georgiev, 2000; Hossain et al., 2022).

1.2.1. Polyenes

Macrolides and amphipathic organic compounds, such as amphotericin B (AMB), which was first isolated from *Streptomyces* in the 1940s and 1950s (Hossain et al., 2022), are examples of polyenes. These represent the earliest broad-spectrum antifungal medicine approved for human use (Odds et al., 2003; Vandeputte et al., 2011). Polyenes bind to ergosterol, leading to pore formation in the fungal plasma membrane. According to Grey et al. (2012) (**Fig. 1**), this disruption compromises ionic homeostasis, ultimately resulting in cell death. Consequently, polyenes are considered fungicidal and exhibit broad activity against a wide range of fungal species. Despite their effectiveness, AMB has long been associated with significant toxicity, particularly nephrotoxicity, which may lead to renal failure (**Table 1**). To address this limitation, several lipid-based formulations have been developed, including liposomal AMB, AMB lipid complex, and AMB colloidal dispersion. These formulations typically demonstrate better pharmacokinetics and reduced toxicity, largely dependent on the composition and particle size of the nanoformulations (Wall & Lopez-Ribot, 2020).

1.2.2. Azoles

Although azoles were first discovered in 1944, they were not approved for human use until the late 1950s (Odds et al., 2003). Azoles act by inhibiting the cytochrome P450 enzyme 14-sterol demethylase, thereby blocking the synthesis of ergosterol (**Fig. 1**). This leads to accumulation of toxic sterol intermediates and compromises membrane integrity (Chang et al., 2016; Pianalto & Alspaugh, 2016; Wall & Lopez-Ribot, 2020). Most azoles exhibit a broad-spectrum activity (**Table 1**) against yeasts and filamentous fungi and are typically fungistatic. Fluconazole (FLC) has been the most widely used azole for systemic fungal infections since the 1990s, especially for those caused by *Candida* species. However, certain fungi including *Aspergillus* and other emerging moulds, display intrinsic resistance to FLC. As a result, newer derivatives effective against *Aspergillus*, such as voriconazole and itraconazole (ITZ) have been developed. Resistance to azoles often arises during treatment, largely due to their fungistatic effect. Mutations in the target gene *ERG11* and the overexpression of efflux pumps that transport azole molecules outside of cells are common mechanisms underlying resistance (Sanglard & Coste, 2015). Despite the resistance, azoles remain one of the most widely used antifungal agents for treating various fungal infections.

1.2.3. Echinocandins

Lipopeptide echinocandins constitute a relatively new class of antifungal medications, initially developed in the 1970s but only introduced into clinical practice in the early 2000s (Cappelletty & Eiselstein-McKitrick, 2007; Emri et al., 2013). These compounds target 1,3-β-D-glucan synthase, an essential enzyme responsible for the synthesis of 1,3-β-D-glucan, a major polysaccharide component of fungal cell walls (Johnson & Perfect, 2003) (**Fig. 1**). Caspofungin (CSP) became the first echinocandin approved for human use in 2001, followed by micafungin (MFG) in 2005 (Chen et al., 2011), anidulafungin in 2006 (Hossain et al., 2022), and rezafungin in 2023 (Wall & Lopez-Ribot, 2020; Hossain et al., 2022). Compared to other antifungal therapies, echinocandins exhibit reduced toxicity and fewer drug-drug interactions. Notably, they were initially licensed for the treatment of aspergillosis refractory to conventional antifungal agents (Wall & Lopez-Ribot, 2020) (**Table 1**).

1.2.4. Pyrimidine analogues

5-fluorocytosine (5-FC) and 5-fluorouracil (5-FU) are pyrimidine analogues, synthetic counterparts of the nucleotide cytosine. Initially developed in 1957 as a potential antitumor agent, 5-FC was approved for antifungal use in humans in 1968 (Vermes, 2000). The enzyme cytosine deaminase converts 5-FC into 5-FU, which is then incorporated into DNA and RNA during synthesis, disrupting cellular function by inhibiting DNA replication and protein synthesis (Sanglard et al., 2009) (**Fig. 1**). These analogues exhibit remarkable antifungal activity against *Candida* and *Cryptococcus* species (**Table 1**). 5-FC demonstrates high bioavailability due to its rapid absorption (Hossain et al., 2022).

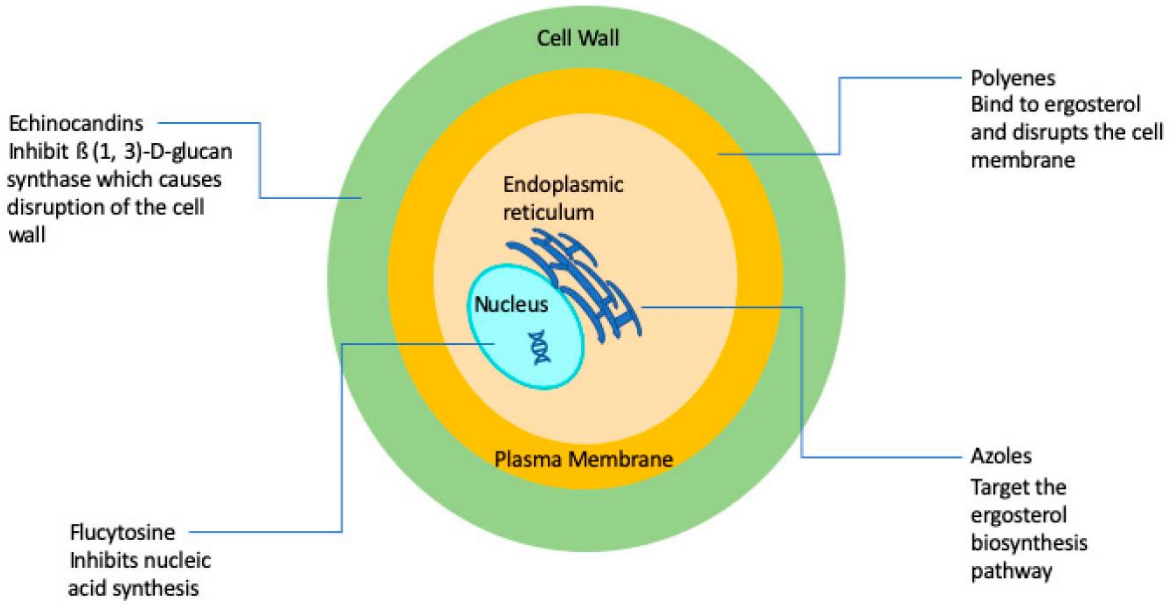

Figure 1: Simplified schematic overview depicting the principal mechanisms of action of current antifungal agents, highlighting their effects on fungal plasma membrane integrity, cell wall biosynthesis, and critical intracellular pathways. Source: Wall & Lopez-Ribot (2020).

Table 1: Major classes of antifungal agents and their characteristics. Adapted from Niño-Vega et al. (2024).

Class	Mode of Action	Use	Restrictions
Polyenes	Makes membrane pores and binds ergosterol	Broad-spectrum, *Aspergillus, Candida*	High toxicity (nephrotoxicity)
Azoles	Prevents the synthesis of ergosterol	Broad-spectrum, *Aspergillus, Candida*	Resistance and interactions with drugs
Echinocandins	Inhibits β-(1,3)-glucan synthase	*Candida, Aspergillus*	Emerging resistance and ineffectiveness against certain species
Flucytosine	Disrupts the DNA and RNA syntheses	*Cryptococcus* treatment in combination therapy	Bone marrow toxicity and rapid resistance

1.3. Challenges in Antifungal Therapy

There is no doubt that new antifungal therapies are urgently needed to combat pathogenic fungi. Fungal infections, now recognized as significant contributors to morbidity and mortality, particularly among immunocompromised individuals, have escalated markedly over recent decades. Furthermore, the application of currently approved antifungal drug classes, including azoles, echinocandins, polyenes, allylamines, and pyrimidine analogues, presents numerous challenges (Fuentefria et al., 2017).

1.3.1. Changes in epidemiology

Until recent decades, fungal infections were considered relatively rare causes of clinically significant illnesses compared to bacterial and viral pathogens (Seagle et al., 2021; Richardson, 2005). This trend shifted in the latter half of the 20th century, as the number of immunocompromised individuals, particularly following advancements in medical care and the HIV/AIDS pandemic, thereby increasing susceptibility to opportunistic fungal infections (Richardson, 2005, Casadevall, 2018; Seagle et al., 2021). Once

regarded as rare infectious agents, fungi such as *Cryptococcus* species are now major contributors to invasive fungal diseases, commonly referred to as systemic mycoses in immunocompromised hosts (Pfaller PGP et al., 2006). As morbidity and mortality related to these infections have risen, fungal diseases have drawn greater epidemiologic attention and now pose substantial changes in diagnosis and clinical management (Webb et al., 2018).

Over the past decade, an increasing diversity of fungal species has been recognized as causative agents of human disease, accompanied by a broader spectrum of clinical manifestations. Improved access to antiretroviral therapy has led to a decline in Human Immunodeficiency Virus-associated opportunistic infections, such as *cryptococcosis*, in North America (Alsuhibani et al., 2025). However, the expansion of at-risk populations has significantly contributed to a rise in healthcare-associated fungal infections, notably those caused by *Aspergillus*, *Candida* species, and other moulds (Seagle et al., 2021). Furthermore, the clinical relevance of geographically restricted dimorphic fungi, such as *Blastomyces*, *Coccidioides*, and *Histoplasma*, as well as moulds like Mucoromycetes, *Fusarium*, and *Scedosporium* species, has increased substantially (Webb et al., 2018, Singh, 2001). Geographic expansion of fungal infections is often linked to environmental changes (Maiga et al., 2018; Webb et al., 2018, Singh, 2001). Epidemiologic data also reveal a sharp increase in drug-resistant fungal infections and the emergence of novel multidrug-resistant fungal pathogens (Forsberg et al., 2019). Severe fungal diseases are estimated to affect approximately 300 million people globally each year, with infection rates continuing to rise (Richardson, 2005). Annual worldwide deaths are estimated at 3.8 million, with invasive fungal diseases causing mortality in over 50% of affected high-risk populations. In the United States alone, fungal infections accounted for over 70,000 hospitalizations and roughly more than $7 billion in healthcare expenditures in 2017 (Benedict et al., 2019; Denning, 2024). The complexity of disease mitigation is compounded by a constellation of socioeconomic, environmental, and healthcare-related factors (Seagle et al., 2021). While increased use of prophylactic antifungals has reduced the prevalence of candidemia in certain populations, it has simultaneously contributed to rising resistance rates of other fungal infections (Perlin et al., 2017). Timely detection, effective clinical intervention, and appropriate antifungal therapy remain critical for reducing the burden of fungal diseases. However, despite advancements in diagnostic capabilities, limitations persist in treatment options, alongside with high morbidity and mortality rates, and low public and clinical awareness (Webb et al., 2018). A

comprehensive understanding of fungal epidemiology and emerging trends is essential for effective prevention, diagnosis, therapeutic management, and improved patient outcomes.

1.3.2. Antifungal Drug Resistance

Antifungal treatment failure is multifactorial and influenced by both host-related (clinical resistance) and pathogen-related (microbiological resistance) factors. Antifungal resistance refers to the inherent or acquired lack of susceptibility of fungi to antifungal agents (Cowen et al., 2014). It may develop in response to drug exposure and typically involves altered gene expression. Clinical outcomes are influenced by a combination of variables including the host's immune system, drug penetration and distribution at the site of infections, adherence to prescribed therapy, and susceptibility of the pathogen to the treatment (Cowen et al., 2014).

Moreover, widespread use of antifungal agents at suboptimal concentrations can result in prolonged exposure of microorganisms to the drugs, potentially allowing resistant cells to survive and propagate. A better understanding of resistance mechanisms and fungal treatment adaptability is critical for the development of novel therapeutics, as antifungal resistance in common infections limits treatment efficacy and underscores the urgent need for new antifungal agents (Cowen et al., 2014; Campoy & Adrio, 2016) **(Table 2**).

Several contributing factors are known to promote the development of fungal resistance, including:

- Misuse of antifungal drugs: Resistance may arise when medications taken incorrectly, for example through missed doses, premature discontinuation of therapy, or subtherapeutic dosing (Perea & Patterson, 2002).
- Agricultural fungicide use: Fungicidal agents are extensively applied in plant and crop protection (Hossain et al., 2022). This increased environmental exposure may contribute to resistance development in fungi.
- Spontaneous resistance: In some cases, fungal infection fungal infections stop responding to previously effective therapies without a clear external cause. Mechanisms may include target site modifications (*e.g.*, mutations in ribosomal proteins), efflux pump overexpression, reduced membrane permeability, or enzymatic drug inactivation (Robbins et al., 2017).

- Transmitted resistance: Resistant fungal strains can be spread between individuals. This means that recipients may harbour infections that are unresponsive to certain antifungal agents, even without prior drug exposure (Mayr & Lass-Flörl, 2011; Hossain et al., 2022).
- Prolonged treatment: Extended exposure to the antifungal (as often required for persistent infections) can create selective pressure that fosters resistance (Hossain et al., 2022; Robbins et al., 2017).
- Biofilm formation: Sessile microbial communities known as biofilms strongly adhere to surfaces and each other, and are encased within a polymeric extracellular matrix primarily composed of polysaccharide (Costa-Orlandi et al., 2017). These cells exhibit morphological diversity and display enhanced resilience compared to planktonic cells, contributing to the persistence of fungal infections (Verstrepen & Klis, 2006). Pathogenic fungi can form biofilms on abiotic surfaces, such as catheters and prosthetic devices—a trait particularly exploited by yeasts to access the bloodstream and disseminate to internal organs. Biofilms, not only provide resistance to most standard antifungal treatments but also markedly diminish the effectiveness of host immune defence. This resistance complicates clinical management and contributes elevated mortality rate. In the United States, biofilms are implicated in approximately 80% of all infections. Notably, Kumar et al. (2017) reported that biofilms exhibit nearly a thousand-fold greater resistance to antifungal drugs compared to planktonic cells. Biofilms pose a dual threat by evading host immunity and diminishing antifungal efficacy, making treatment of fungal infections more challenging and often less successful. Elucidating the molecular mechanisms that govern biofilm formation and persistence could pave the way for developing innovative therapeutic strategies to combat these challenging infections (Costa-Orlandi et al., 2017; Kumar et al., 2017).

Fungi have developed several molecular mechanisms of resistance to antifungal agents, including the following:

- Alterations to drug targets: Genetic modification in drug-binding sites is among the most common causes of antifungal resistance. For example, point mutations in two highly conserved hotspot regions of *FKS* genes that play a vital role in the integrity of fungal cell wall encoding glucan synthase can confer echinocandin resistance by significantly reducing the sensitivity of the enzyme by over a

thousand-fold. These mutations interfere with the biosynthesis of the essential cell wall polymer (1,3)-β-D-glucan (Niimi et al., 2006; Perlin et al., 2015).

- Regulation of drug transporters: *C. albicans* can become resistant to azoles through overexpression of multidrug transporter genes such as *CDR1*, *CDR2*, or *MDR1*, or through overexpression of *ERG11*, which encodes the enzyme Ionosterol 14α-demethylase involved in the synthesis of ergosterol, thus targeting azole antifungal drugs (**Table 2**). These changes lead to reduced drug accumulation and decreased susceptibility (Perlin et al., 2015).
- Stress responses and adaptive mechanisms: Stress conditions (including oxidative, translational, and endoplasmic reticulum stress) can induce chromosome loss and drive karyotype diversification in *Saccharomyces cerevisiae*, contributing to antifungal adaptation and resistance (Forche et al., 2011; Perlin et al., 2015).
- Other findings are supported by the observation that passage through a murine host promotes genome rearrangements even in *C. albicans*, even in the absence of antifungal treatment, suggesting that host-related conditions drive underlying genetic instability (Forche et al., 2009). Similarly, analysis of clinical isolates of *Nakaseomyces glabratus* (formerly *Candida glabrata*) reveals extensive genomic alterations, including multiple chromosomal translocations and the emergence of novel chromosomes (Ahmad et al., 2013). Such data indicate that this species possesses adaptive mechanisms that enable cells to tolerate significant stress-induced genetic changes and potentially modulate their response to antifungal agents.
- Genetic plasticity as a driver of resistance: Chromosomal disomies or segmental duplications, which generate extra copies of genes including those encoding drug efflux pumps like azole targets (ERG11), have been associated with the development of azole resistance in Candida albicans (Selmecki et al., 2006). Similarly, exposure to azoles can induce multiple chromosomal mutations and disomies in *Cryptococcus neoformans* (Sionov et al., 2010). Importantly, such extensive genomic alterations may also occur in response to non-antifungal stressors, underscoring the broader role of environmental and therapeutic pressures in accelerating fungal adaptation. These mechanisms contribute

significantly to the mounting challenge of antimicrobial resistance, a growing crisis in global health.

Table 2: Mechanisms of fungal resistance across the five major classes of antifungal agents. Adapted from Bondaryk et al. (2017).

Group Name	Group Member/s	Resistance Mechanism
Fluorinated pyrimidine analogs	Flucytosine	Enzyme deficiencies in flucytosine metabolism and pyrimidine salvage. Mutations in *FCA1*, *FUR1*, *FCY21*, and *FCY22*.
Polyenes	Natamycin Amphotericin B Nystatin	*ERG3* gene defects (decreased ergosterol content in cell membrane). Modified membrane composition replaced. Lipids and non-ergosterol cytoplasmic membrane sterols (such as squalene and zymosterol). Enlargement of *Cryptococcus neoformans* capsules
Echinocandins	Micafungin Caspofungin Anidulafungin	*FKS1* and *FKS2* gene mutation. Absence of 1,3-glucan in the *C. neoformans* cell wall.
Allylamines	Naftifine Terbinafine	Drug target modification (missense mutation or *ERG1* substitution). Degradation of the terbinafine naphthalene ring.
Azoles	Fluconazole	*ERG11* mutations or overexpression (which is a gene responsible for encoding the enzyme Ionosterol 14α-demethylase involved in the biosynthesis of ergosterol).
	Voriconazole	Decreased azole uptake and efflux through ATP-binding cassette transporters, which results in less azole accumulation inside fungal cells.
	Posaconazole	*ERG3* mutation-induced tolerance to methylated sterols (a gene responsible for encoding enzyme C-5 sterol desaturase involved in the conversion of episterol to 5,7,24(28)-ergostatrienol in the ergosterol biosynthesis pathways)

1.3.3. Price and accessibility

Significant global disparities in the cost and availability of antifungal medications directly affect patient outcomes. Although antifungal drugs can be life-saving, their accessibility remains limited in many regions, particularly in low-income countries. According to Kneale et al. (2016), analysis of data from 155 countries with populations over one million shows that fungal infectious diseases are responsible for roughly 1.5 million deaths each year. Critically, two-thirds of these deaths could be prevented with proper diagnosis and treatment. Cryptococcal meningitis alone is estimated to cause more than 15% of HIV/AIDS-related deaths (Denning, 2015), while survivors of *Pneumocystis* pneumonia, disseminated histoplasmosis, invasive aspergillosis, candidiasis, and cryptococcal meningitis typically recover and lead healthy lives if treated promptly. However, drug shortages remain a major barrier: for example, limited access to AMB contributes to poor outcomes in cases of candidiasis, mucormycosis, disseminated histoplasmosis, cryptococcal meningitis, and other fungal infections. A deficiency in flucytosine can reduce the primary treatment responses and culture conversion rates in cryptococcal meningitis, increasing mortality by 25% over 10 months (Hamill, 2013). In 42 of 155 surveyed countries, AMB was entirely unavailable, affecting an estimated 481 million people (Kneale et al., 2016). Flucytosine was not licenced in 89 countries, impacting over 2.5 billion individuals. The cost of AMB deoxycholate varied widely, from as little as $1 to as much as $171 per day (Kneale et al., 2016).

In regions such as Africa, when AMB and flucytosine are completely unavailable, the three-month survival rates for cryptococcal meningitis drop from about 75% to just 30%. The average cost of AMB and flucytosine for two-weeks of induction regimen is approximately $450, although prices vary significantly depending on region and supply chain factors (Jackson et al., 2012).

While FLC was found to be licensed in all 141 assessed countries (88.6%), its daily price ranged from less than $1 to $31. In contrast, flucytosine was unlicensed in 71.2% of 125 countries and unavailable in 76%, affecting nearly 2.9 billion people. Regarding ITZ, 2.4% of 123 countries lacked licensing, while 4.0% reported complete unavailability, collectively leaving 78 million individuals without access. Prices for ITZ ranged from under $1 to $102 daily (Kneale et al., 2016).

In the United States, healthcare expenditures on systemic fungal infection drugs rose from USD 121.9 million in 2009 to USD 155 million in 2023, while spending on invasive fungal infection prescriptions decreased from USD 156.8 million in 2022 to USD 80.7

million in 2023 (Alsuhibani et al., 2025), thus questioning the affordability for middle and low-income countries.

Table 3: Availability and licensing status of systemic antifungal agents by country. Adapted from Kneale et al. (2016).

	Intravenous only	**Intravenous and oral**		
Disease/status	**Amphotericin B**	**Fluconazole**	**Itraconazole**	**Flucytosine**
Countries where not licensed	22/155 (14.2%)	0/151	3/123 (2.4%)	89/123 (72.4%)
Countries where not available	42/155 (27.1%)	0/143 [a]	5/125 (4.0%)	94/120 (78.3%)
World population unable to receive antifungals [b]	481 million (6.62%)	none	78 million (1.07%)	2898 million (39.9%)

[a] Availability in five countries is limited to the Dipeptidyl peptidase (HIV only).

[b] Assumes that all countries for which we have no data have access, which is unlikely.

To address the critical barriers to antifungal treatment-particularly in middle- and low-income nations GAFFI recommends the following strategic measures (Sekkides, 2015): Expand access to affordable diagnostic tests, emphasizing rapid, non-culture-based methods for detecting both common and rare fungal diseases.

Establish a global network of trained medical professionals, supported by train the trainer programs and standardized clinical guidelines. Ensure universal distribution of antifungal medications included in the WHO Essential Medicine List, prioritizing availability in underserved populations.

Trained specialists in the field of public health mycology, a field currently underrepresented due to the non-communicable nature of most fungal diseases.

Maintain continuous surveillance of high-burden fungal infections to inform clinical practice, shape educational programs, and guide research priorities. Implement at least one diagnostic laboratory for fungal diseases in every country, led by a specialist with broad diagnostic capabilities and supported by a critical mass of healthcare professionals. Countries with populations over 5 million should host multiple such facilities.

1.4. New Possibilities in Antifungal Therapy

Novel antifungal treatments are advancing rapidly in response to the rising incidence of fungal infections and the growing prevalence of resistant strains. Current efforts are

focused on developing new antifungal agents, repurposing existing drugs, and applying advanced technologies to improve treatment outcomes. Emerging options in antifungal therapy include the following:

1.4.1. New antifungal agents

Ibrexafungerp is the first non-azole oral antifungal approved specifically for the treatment of vaginal yeast infections. It is a terpenoid compound and inhibits 1,3-β-D-glucan synthase, key enzyme in fungal cell wall synthesis. Notably, it has shown efficacy against azole-resistant *C. auris* strains (Aimbatov, 2023).

Rezafungin is the next-generation echinocandin that demonstrates potent antifungal activity against candidemia. It offers enhanced pharmacokinetic properties and greater dosing convenience compared to conventional echinocandins, potentially improving patient adherence and outcomes (Aimbatov, 2023).

Olorofim represents a novel class of antifungals targeting dihydroorotate dehydrogenase—an enzyme essential for pyrimidine biosynthesis in fungi. This unique mechanism offers promising activity against resistant fungal pathogens and hard-to-treat moulds (Aimbatov, 2023).

1.4.2. Drug repurposing

Repositioning existing drugs with known safety profiles for antifungal applications can accelerate therapeutic development. One notable example is sertraline, an antidepressant, which has demonstrated inhibitory effects against *C. neoformans*. Its ability to cross the blood–brain barrier makes it particularly effective in the treatment of cryptococcal meningitis (Pianalto & Alspaugh, 2016).

1.4.3. Nanotechnology-based strategies

Nanoparticles are increasingly being explored to overcome the limitations of conventional antifungal drugs. These nanoscale delivery systems aim to enhance drug bioavailability, reduce toxicity, and improve targeted efficacy, particularly in drug-resistant infections (Nino-Vega et al., 2024).

1.4.4. Artificial intelligence (AI)

AI technologies are increasingly being applied in antifungal drug discovery to identify novel molecular targets. By analysing fungal genomes and protein structures, AI models

can predict resistance patterns and streamline the development of new antifungal therapies (Niño-Vega et al., 2024). This data-driven approach represents a contemporary and promising strategy for addressing emerging fungal pathogens and overcoming therapeutic limitations (Niño-Vega et al., 2024).

1.5. Antifungal Proteins

Antifungal proteins (AFPs) represent a promising class of agents for combating fungal infections, which constitute a serious threat to human health. Owing to their potent antifungal properties (acquired through diverse mechanisms related to their function, structure, and origin) these proteins which are derived from a variety of sources, including plants, fungi, and animals, are suitable for medical use (Selitrennikoff, 2001). Classification of these proteins reveals considerable diversity, particularly among those originating from fungi and plants (Wong & Ng, 2011).

1.5.1. AFPs from plants

These AFPs are vital for preventing fungal infections due to their diverse structures and mechanisms of action. For instance, lipid transfer proteins disrupt fungal cell walls, while reactive oxygen species contribute to cell proliferation and induce apoptosis in fungal cells (Wong & Ng, 2011; Ng et al., 2013). Plant AFPs are classified into several groups, including thaumatin-like proteins, lipoxygenases, protease inhibitors, defensins, and pathogenesis-related proteins (Hermanova et al., 2006). Moreover, certain AFPs found in plant latex exhibit strong efficacy against both human and phytopathogenic fungal strains (Barbosa et al., 2020).

1.5.2. AFPs from animals

These AFPs are known to possess potent antifungal properties. Notable examples include broad-spectrum human cathelicidins, such as LL-37, histatins that selectively target *C. albicans (*Pinilla et al., 2022*),* as well as lysozymes, and lactoferrins found in human tears and mucosal secretions. These latter hydrolyse β-1,4 glycosidic bonds in the fungal cell wall, contributing to their antifungal efficacy (Singh & Rani, 2016).

1.5.3. AFPs from fungi

These AFPs are small, stable, secreted, cationic, and cysteine-rich proteins that are promising candidates for the development of next-generation antifungal medications.

Many of these features like β-strand structures typical to filamentous ascomycetes, stabilized by disulfide bonds (Garrigues et al., 2017; Váradi et al., 2018). Phylogenetic analyses have identified four distinct classes of cysteine-rich AFPs from ascomycetes, namely *Penicillium chrysogenum* antifungal protein (PAF), *Aspergillus giganteus* antifungal protein (AFPg), *Penicillium brevicompactum* "bubble-protein"(BP), and *Aspergillus fischeri* (formerly, *Neosartorya fischeri*) antifungal protein 2 (NFAP2) (Sonderegger et al., 2018) (**Fig. 2**). Despite differences in their primary sequences, these AFPs, found in Eurotiomycetes, share a conserved γ-core motif (G-X-C-$X_{3–9}$-C, where X denotes any amino acid). Their structure and antifungal efficacy is influenced by the physical and chemical properties of the γ-core motif and surrounding regions (Sonderegger et al., 2018).

In addition to defensins, proline-rich peptides, and cysteine-rich antifungal peptides derived from plants and animals, recent studies have shown that bacteria, particularly species of *Bacillus*, produce antifungal lipopeptides, bacteriocins, and cell wall degrading enzymes. These bioactive molecules are increasingly recognized as promising candidates for the development of next-generation antifungal therapies in response to raising antimicrobial resistance (Bravo et al.,2011).

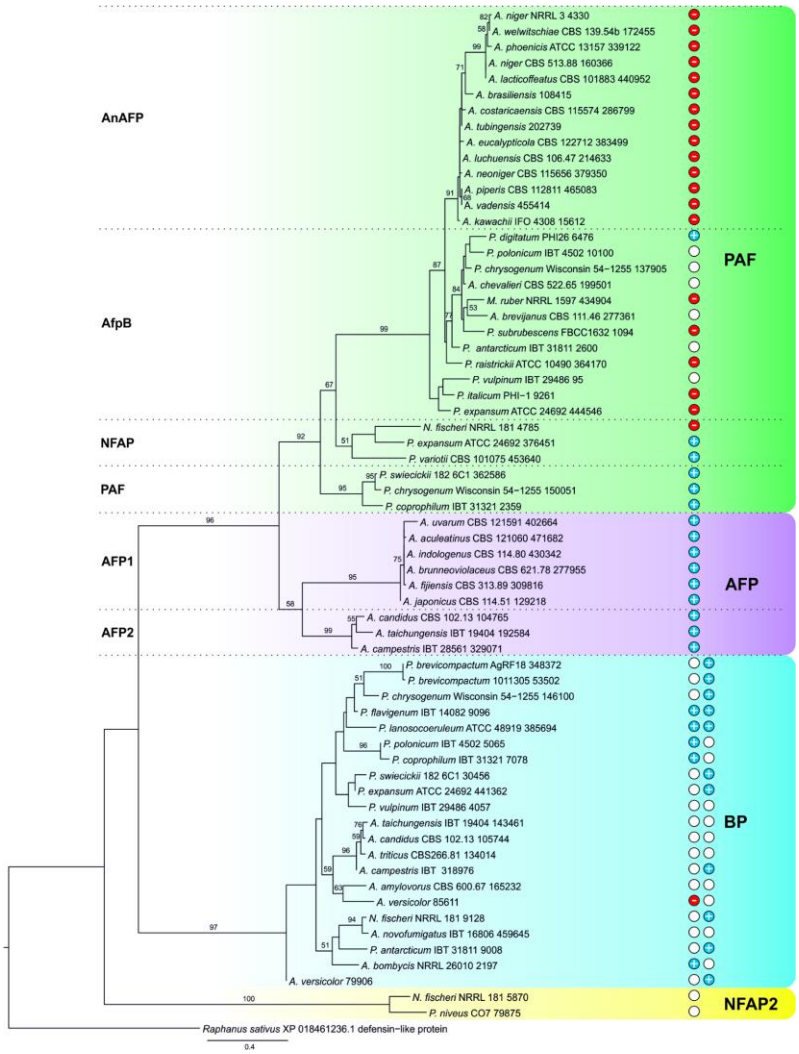

Figure 2: AFPs from Eurotiomycetes containing the conserved γ-core motif. Isolate names are listed alongside the accession numbers of the corresponding AFPs. The net charge of each γ-core motif at pH 7.0 is indicated: blue discs represent positively charged motifs, red discs indicate negatively charged motifs, and white discs denote near-neutral motifs, BP: *Penicillium brevicompactum*, "bubble" protein; NFAP: Neosartorya fischeri antifungal proteins, PAF: *Penicilium chrysogenum* antifungal proteins, AFP: *Aspergillus niger* antifungal protein, Double disc: two distinct γ-cores located at different loci, with the same or different charge. Source: Sonderegger et al. (2018).

1.5.1. Mode of action of antifungal proteins

AFPs exert their activity through intricate interactions with fungal cells, ultimately leading to cell death via diverse mechanisms (Giner-Llorca et al., 2023;). Recent research has elucidated these mechanisms, highlighting the potential of AFPs as powerful agents

against fungal infections. The key modes of action employed by AFPs are the following (**Table 5**).

Plasma membrane permeabilization: AFPs bind electrostatically to negatively charged components of fungal membranes, such as phospholipids and sphingolipids, causing membrane permeabilization. This disruption leads to the formation of pores or channels in the fungal plasma membrane, resulting in ion leakage, membrane depolarization, and ultimately, cell lysis (Theis et al.,2003; Hagen et al., 2007). A well-characterized example of such activity is exhibited by the AFP from *A. giganteus*.

Induction of programmed cell death: Once internalized, AFPs initiate a programmed cell death in fungal cells, a process often mediated by reactive oxygen species, which triggers transcriptional reprogramming and ultimately lead to cell death (Bugeda et al., 2020). The ability of AfpB produced by *Penicillium digitatum* exemplifies this multifaceted mechanism, demonstrating the ability to suppress toxin-encoding genes and induce apoptosis, thereby reinforcing its regulatory influence on fungal cell integrity (Ropero-Pérez et al., 2023).

Inhibition of cell wall biosynthesis: Research on the inhibition of fungal cell wall biosynthesis by AFPs is of high importance, as the cell wall is essential for fungal viability and represents a uniquely exploitable therapeutic target. In susceptible fungal strains, the AFP from *A. giganteus* has been shown to suppress chitin biosynthesis, paralleling the activity of echinocandins, which inhibit β-1,3-D-glucan synthesis, as well as newly identified compounds that affect mannan and chitin synthesis pathways (Giner-Llorca et al., 2023).

Intracellular targeting: AFPs, such as AfpB from *P. digitatum*, exhibit a multifaceted mode of action involving cell wall interactions, energy-dependent internalisation, subsequent intracellular effects that culminate in fungal cell death. This mechanism is pivotal to the development of effective antifungal therapies. As described by Ropero-Pérez et al. (2023), AFPs initiate their antifungal activity by binding to the mannosylated outer layer of the fungal cell wall. Following adhesion, they are internalised via an energy-dependent process, enabling them to access intracellular targets such as RNA and protein synthesis machinery, as well as mitochondrial function (Bugeda et al., 2020).

Chelation of essential metal ions: Multifunctional lactoferrin is a glycoprotein that binds iron and is mainly found in milk. It is important for many biological processes, including immunomodulatory processes that increase the host's immune response and

antimicrobial, antiviral, anti-inflammatory, and anticancer properties (Legrand et al., 2008; Guo-Xiang, 2006).

Table 4: Mechanisms of action of antifungal proteins.

Mode of Action	Mechanism shown with pertinent examples	Reference
Membrane disruption	Plant defensins, like RsAFP2, cause membranes to permeate.	Hagen et al., 2007; Theis et al.,2003
Inhibition of cell wall synthesis	AFP from *A. giganteus* inhibits chitin synthesis, a structural polysaccharide necessary for fungal cell walls.	Bugeda et al., 2020, Ropero-Pérez et al., 2023
Intracellular targeting	AFP interferes with expression by binding nucleic acids.	Giner-Llorca et al., 2023
Induction of apoptosis	PAF from *Penicillium chrysogenum* momentarily raises intracellular calcium (Ca^{2+}), a signalling molecule that starts apoptotic processes.	Leiter et al., 2008, Ropero-Pérez et al., 2023
Ion chelation	Lactoferrin binds iron.	Legrand et al., 2008; Guo-Xiang, 2006
Immune activation	Histatin-5 boosts immune response.	Legrand et al., 2008

1.5.2. Biological role of ascomycetous antifungal proteins

Subsequent research has demonstrated that fungal species producing AFPs may exhibit sensitivity to their own AFPs during specific developmental stages. This sensitivity has been linked to the biological activity of AFPs within the native producer fungus (Meyer and Jung, 2018). The present study also highlights that PAFis involved in the initiation of conidiogenesis, as well as the induction of apoptosis and autophagy, under nutrient-deprived conditions following the attainment of a certain biomass level (Hegedüs et al., 2011). Additionally, AFPs are involved in stress response mechanisms, which limit the growth of pathogenic fungi and enhance the capacity of native fungal producers to tolerate abiotic stresses, such as temperature changes and oxidative damage (Kaiserer et al., 2003). In the cases of AnAFP from *Aspergillus niger* and AFPg from *A. giganteus*, it has been hypothesized that these proteins similarly contribute to the activation of autophagy under nutrient-limiting conditions (Paege et al., 2016; Meyer and Jung, 2018), an

observation recently confirmed experimentally in a study published this year (Starke et al., 2025). AfpB, secreted by *P. digitatum*, induces regulated cell death in the producer fungus and is likely involved in population density regulation (Gandía et al., 2019; Bugeda et al., 2020). Collectively, these findings refute the earlier assumption that AFPs derived from Eurotiomycetes cannot harm their native producers. Nevertheless, exceptions exist—such as PeAfpA secreted by *Penicillium expansum*, which does not induce cell death in its native host (Ropero-Pérez et al., 2023).

1.5.3. Structure and the γ-core motif of ascomycetous antifungal proteins

AFPs, particularly those derived from Ascomycetous fungi, are small (approximately 5 to 6 kDa), cysteine-rich, cationic proteins that typically contain 6–8 cysteine residues, forming disulfide bridges that stabilize their tertiary structure. Most AFPs adopt a compact β-barrel-like structure composed of five β-strands, stabilized by four disulfide bonds (Zhao et al., 2022). A conserved structural element frequently found in the loop regions or embedded within β-strands is the γ-core motif, which plays a critical role in antifungal activity even under harsh environmental conditions (Sonderegger et al., 2018; Slezina et al., 2022). These structural components of the γ-core motif facilitate interaction with fungal membranes and disrupt membrane integrity, thereby killing fungal cells (Sonderegger et al., 2018). Consequently, they have emerged as a promising target for the development of next-generation antifungal therapeutics. The synthetic peptides spanning the γ-core motif exhibit broad-spectrum antimicrobial action and immunomodulatory effects, making them a valuable tool against various pathogens, including fungi and viruses. It exerts its function by binding to microbial membranes, disrupting the integrity, and ultimately causing cell death (Utesch et al., 2018). Altering the γ-core motif through amino acid substitutions that increase the overall positive charge or improve hydrophilicity has been demonstrated to improve the antifungal efficacy of AFPs. To be more precise, modified PAF from *P. chrysogenum*, specifically the $P\gamma^{var}$ and $P\gamma^{opt}$ variants, exhibits a 10-fold increase in antifungal activity against *C. albicans* (Sonderegger et al., 2018; Utesch et al., 2018).

1.5.4. Potential application of antifungal proteins from Eurotiomycetes and their γ-core peptide derivatives in human medicine

The AFPs of Eurotiomycetes and their γ-core peptide derivatives offer promising solutions for human medicine to address the rapidly growing challenges of fungal

infections and drug resistance. These AFPs and their γ-core peptide derivatives represent attractive targets for the development of novel antifungal therapies. Their relevance to human health lies in their potent antifungal properties, as they are typically small, cysteine-rich, and often cationic proteins that have evolved as defence mechanisms, targeting fungal pathogens (Sonderegger et al., 2018). These AFPs containing γ-core motif(s) are increasingly recognized as promising therapeutic candidates due to their specific arrangement of cysteine residues, which enables structural stability through the formation of disulfide bond. This stability is essential for maintaining protein structure and function under environmental conditions. These AFPs exhibit novel modes of action with low toxicity to human cells and are characterised by broad-spectrum activity against various fungal pathogens, including *C. albicans* and *A. fumigatus*. Moreover, their structural features may confer antifungal transferability to other fungal species (Varadi et al., 2024). Understanding the structural features that allow antifungal transferability to other fungal species is important for creating new antifungal treatments. Insights into the structure of fungal proteins and enzymes can help design broad-spectrum antifungal agents by targeting shared elements across different species. This method can address the shortcomings of current antifungal drugs, including resistance and a narrow therapeutic spectrum. This approach can overcome limitations of current antifungal drugs, such as resistance and a restricted therapeutic range. One potential application involves γ-core peptide derivatives derived from Eurotiomycetes AFPs, which can disrupt cell-cell interactions and effectively prevent fungal biofilm formation by coating the surfaces of medical devices, such as implants and catheters, thereby reducing the incidence of nosocomial fungal infections, particularly those caused by *Candida* species (Guevara-Lora et al., 2023). AFPs and their γ-core peptide derivatives may also be used in combination with conventional antifungal agents, especially in immunocompromised patients, to enhance treatment efficacy, delay the development of resistance, and achieve therapeutic effects at lower dosages (Rochard et al., 2024). $P\gamma^{opt}$, a rationally designed γ-core peptide derivative of PAF, demonstrates enhanced antifungal efficacy (Sonderegger et al., 2018). Despite the promising potential of Eurotiomycetes AFPs and their γ-core motif peptide derivatives as novel antifungal agents, challenges remain regarding their stability under physiological conditions and the feasibility of large-scale synthesis. Further research is necessary to fully understand their therapeutic applications and overcome these limitations.

2. OBJECTIVES

The increasing prevalence of drug-resistant fungal strains has led to the escalating rise in global fungal infection cases. In response, Sonderegger et al. (2018) carried out a phylogenetic analysis and found that, despite differences in their primary structure, antifungal proteins (AFPs) in Eurotiomycetes share a conserved γ-core motif (G-X-C-X_{3-9}-C). The study, conducted at the University of Szeged, Department of Microbiology and Biotechnology, is consistent with recent research demonstrating the antimicrobial activity of a variety of synthetic and natural antimicrobial peptides (AMPs) against microbial pathogens. The main objective of the present PhD thesis was to investigate the antifungal properties and potential medical application of peptide derivatives designed on the γ-core motifs of various AFPs from Eurotiomycetes. Considering this main objective, the aims of our study were as follows:

- To design a series of synthetic peptides incorporating the γ-core motifs of antifungal proteins from Eurotiomycetes (γAFPs).
- To evaluate the *in vitro* antifungal efficacy of γAFPs against a panel of human and phytopathogenic fungal species.
- To assess the *in vitro* efficacy and antifungal activity of the most potent γAFPs, both alone and in combination with conventional antifungal agents, against human pathogenic fungi.
- To characterize the structure of γAFPs in the presence of conventional antifungal drugs, fungal cells, and conidia.
- To examine the potential toxicological effects of the most effective γAFPs and their combinations with conventional antifungal agents in an animal model.
- To determine the therapeutic efficacy of the most effective γAFPs and their combinations with conventional antifungal agents in an animal model.

3. MATERIALS AND METHODS

3.1. *In silico* Analysis

Amino acid sequences of AFPs from various Eurotiomycetes were retrieved from the UniProt database (UniProt Consortium, 2025). Sequence alignment was performed using BioEdit (Hall, 1999) and visualized with Jalview Version 2 (Waterhouse et al., 2009). Signal sequence cleavage sites were predicted using SignalP 5.0 (Armenteros et al., 2019).

A maximum likelihood phylogenetic tree was constructed using MEGA11, applying the WAG substitution model, gamma-distributed rate variation, and the nearest-neighbor interchange algorithm, with 1,000 bootstrap replicates (Tamura et al., 2021; Whelan and Goldman, 2001). Defensin-like proteins from *Raphanus sativus* (UniProt IDs: P69241, P30230) were used as an outgroup.

Physicochemical properties of γAFPs were determined using the ExPASy ProtParam tool (Duvaud et al., 2021) and the Antimicrobial Peptide Calculator and Predictor available from the Antimicrobial Peptide Database (Wang and Wang, 2016). Tertiary structures of AFPs were obtained from AlphaFold via UniProt (Jumper et al., 2021; Varadi et al., 2024), while those of γAFPs were predicted using PEP-FOLD3 (Lamiable et al., 2013).

All tertiary structures were visualized with UCSF Chimera (Pettersen et al., 2004). The model reliability was assessed through Ramachandran plot analysis generated via MolProbity (Williams et al., 2018).

3.2. Peptide Synthesis

The γAFPs were produced through microwave-assisted, stepwise solid-phase peptide synthesis employing Fmoc/S-tBu chemistry on a Liberty Blue synthesizer (CEM Corporation, Matthews, NC, USA). The synthesis was carried out using TentaGel S RAM resin (loading: 0.2 mmol/g) with coupling facilitated by ethyl 2-cyano-2-(hydroxyimino)acetate (Oxyma) and diisopropylcarbodiimide (DIC). Peptides were cleaved from the resin using a mixture containing trifluoroacetic acid (TFA), water, and dithiothreitol (DTT) at a ratio of 95:5:3 (v/v/v), incubated for three hours. Post-cleavage, TFA was evaporated, and peptides were precipitated using ice-cold diethyl ether, subsequently dissolved in 10% acetic acid (v/v) and freeze-dried. The resulting crude peptides were purified through semipreparative reverse-phase high-performance liquid chromatography (RP–HPLC), utilizing a solvent system of 0.1% TFA (v/v) as solvent A

and 80% acetonitrile containing 0.1% TFA (v/v) as solvent B. A linear gradient from 0% to 30% of solvent B over 60 minutes was applied. The purification process was conducted on a Phenomenex Jupiter Proteo 90 Å column (250 mm × 10 mm) with a Shimadzu HPLC system (Berlin, Germany), monitoring absorbance at 220 nm. Peptide purity was assessed using analytical RP–HPLC on a Phenomenex Luna 10 μm C18 100 Å column operated with an Agilent 1100 HPLC system (Palo Alto, CA, USA). Lyophilized γAFPs were stored at −20°C pending further application. Peptide synthesis was carried out by Györgyi Váradi (Department of Medical Chemistry, Albert Szent-Györgyi Medical School, University of Szeged).

3.3. Fungal Strains and Inoculum Preparation

Fresh conidial suspensions of molds (*A. fumigatus* CBS 101355, *Botrytis cinerea* SZMC 21472, *Cladosporium herbarum* FSU 1148, *Fusarium subglutinans* CBS 747.97) and cells of mid-log phase yeast cultures (*C. albicans* SC5314, *S. cerevisiae* SZMC 0644) were used for all experiments. Yeasts were maintained on yeast extract peptone dextrose (YPD) agar slants (1% yeast extract, 2% peptone, 2% glucose, 2% agar [w/v]), while molds were maintained on potato dextrose agar (PDA) (Sigma–Aldrich, St. Louis, MO, USA) at 4°C. Fresh conidia were harvested from the surface of seven days old mold cultures grown on PDA at 25°C or 30°C (*A. fumigatus*), suspended in spore buffer (0.9% NaCl, 0.01% Tween [v/v]), and filtered using a 40 μm pore-size cell strainer (VWR, Radnor, PA, USA). Conidia were subsequently washed twice in spore buffer (900 × g for 5 min) and resuspended in spore buffer. To generate mid-log phase yeast cultures, cells were inoculated from YPD agar slants into low cationic medium (LCM) (0.5% glucose, 0.25% yeast extract, 0.0125% peptone [w/v]) and incubated at 30°C for 8 h with continuous shaking (200 rpm). Cultures were then inoculated at a 1:100 dilution into fresh LCM and further incubated under the same conditions for 16 h. Finally, both conidia and yeast cells were diluted in LCM to achieve the concentrations required for the experiments.

3.4. *In vitro* antifungal susceptibility tests

A broth microdilution susceptibility assay was conducted according to Tóth et al. (2016) to evaluate the antifungal efficacy of synthetic γAFPs against four molds (A. *fumigatus* CBS 101355, *B. cinerea* SZMC 21472, *C. herbarum* FSU 1148, *F. subglutinans* CBS 747.97) and two yeasts (*C. albicans* SC5314, *S. cerevisiae* SZMC 0644) in LCM. Briefly,

100 µL of γAFPs (25–400 µg/mL, twofold serial dilutions in LCM) were combined with 100 µL of fungal suspensions (2×10^5 conidia or yeast cells/mL) in flat-bottom 96-well microtiter plates (TC Plate 96 Well, Suspension, F; Sarstedt, Nümbrecht, Germany). LCM without γAFP served as the untreated control. The plates were statically incubated at 25°C for 72 h (*B. cinerea* SZMC 21472, *C. herbarum* FSU 1148, *F. subglutinans* CBS 747.97), or at 30°C for 48 h (*C. albicans* SC5314, *S. cerevisiae* SZMC 0644) or 72 h (*A. fumigatus* CBS 101355). Absorbance at 620 nm (OD_{620}) was recorded using a SPECTROstar Nano plate reader (BMG Labtech, Ortenberg, Germany). Fresh LCM (200 µL) was used for background calibration. The minimum inhibitory concentration (MIC) of γAFPs was defined as the lowest concentration that reduced fungal growth to ≤5% relative to the untreated control (OD_{620} set to 100%). In cases where no MIC was observed, the growth inhibition percentage (IP) at 200 µg/mL γAFP was calculated as follows: IP = 100% - ([absorbance of treated culture × 100] / absorbance of untreated culture). For this calculation, the absorbance of the untreated culture was set to 100% growth, and fresh medium (200 µL) was used for spectrophotometric calibration. Susceptibility tests were conducted twice, including two technical replicates.

The broth microdilution method, as described earlier, was applied to determine the MICs of conventional antifungal drugs, including amphotericin B (AMB), fluconazole (FLC), micafungin (MFG), and terbinafine (TRB) (MedChemExpress, Monmouth Junction, NJ, USA), against *C. albican*s SC5314 and *A. fumigatus* CBS 101355. The tested concentration ranges were 0.125–32 µg/mL for AMB, 2–32 µg/mL for FLC, 0.078–32 µg/mL for MFG, and 0.125–32 µg/mL for TRB.

3.5. *In vitro* Interaction Between γAFPs and Antifungal Drugs

The checkerboard titration method (Eliopoulos et al., 1996) was employed to investigate the interaction between γAFPs and antifungal drugs against *C. albicans* SC5314 and *A. fumigatus* CBS 101355. In this experiment, 100 µL of two-fold serial dilutions of γAFP (ranging from 4×MIC, prepared in 10 steps in LCM) were combined with 100 µL of two-fold serial dilutions of the antifungal drug (4×MIC, prepared in 10 steps in LCM containing 2×10^5 fungal cells or conidia / mL). Plates were incubated statically at 30°C for 48 h (*C. albicans* SC5314), or at 25°C for 72 h (*A. fumigatus* CBS 101355). Following the incubation, growth percentages (GP) in the presence of γAFP were calculated based on absorbance at 620 nm (OD_{620}) using the formula: GP = (absorbance of treated culture × 100) / absorbance of untreated culture. For this calculation, the absorbance of the

untreated culture was set to 100% growth, and fresh medium (200 µL) was used for spectrophotometric calibration. The interaction ratio (IR) was determined using the Abbott formula (Moreno et al., 2003): $IR = I_0 / I_e$, where $I_e = X + Y – (XY / 100)$ (expected percentage inhibition for a given interaction), X and Y represent the percentage inhibitions of the individual compounds used alone, and I_0 is the observed percentage inhibition. The nature of the interaction was considered additive if IR is between 0.5 and 1.5, synergy if IR > 1.5, and antagonistic if IR < 0.5. There is no interaction when the combined effect is similar to the stronger individual compound. Interaction experiments were repeated twice, including two technical replicates.

3.6. Electronic Circular Dichroism Spectroscopy

The secondary structural features of γAFPs were characterized using electronic circular dichroism (ECD) spectroscopy. Spectral data were recorded between 185 and 260 nm with the aid of a Jasco-J815 spectropolarimeter (JASCO, Tokyo, Japan). Prior to measurement, peptide solutions were prepared at a concentration of 100 µg/mL in bidistilled H_2O and placed in quartz cuvettes with a 1 mm optical path length. Temperature control was maintained at 25°C throughout the acquisition process using a Peltier thermoelectric unit (TE Technology, Traverse City, MI, USA). Each spectrum represents an average of ten consecutive scans per sample, with solvent spectra subtracted to isolate peptide-specific signals.

Ellipticity values are expressed in mean residue molar ellipticity units. Estimations of secondary structural content, reflecting canonical motifs, were performed via the DichroWeb server (Miles et al., 2022) using the CDSSTR analytical method (Sreerama et al., 2000).

The conformational changes in the secondary structure of γAFP^{B6GXZ8} and $\gamma AFP^{A0A2J5HZT4}$ in the presence of *C. albicans* SC5314 cells, *A. fumigatus* CBS 101355 conidia, TRB, FLC, and their respective synergistic combinations (TRB + *C. albicans* SC5314 cells, and FLC + *A. fumigatus* CBS 101355 conidia) were investigated using ECD spectroscopy, following the previously described measurement conditions. For this analysis, conidia or yeast cells were washed three times and resuspended in bidistilled H_2O or an aqueous solution of γAFP^{B6GXZ8} (200 µg/mL), $\gamma AFP^{A0A2J5HZT4}$ (200 µg/mL), TRB (1 µg/mL) or FLC (32 µg/mL), and γAFP^{B6GXZ8} (200 µg/mL) + TRB (0.5 µg/mL) or $\gamma AFP^{A0A2J5HZT4}$ (200 µg/mL) + FLC (32 µg/mL) combination at a final concentration

of 2×10^7 cells or conidia/mL. Spectra of bidistilled H_2O, aqueous solutions of γAFPs, antifungal drugs, and their combinations were also acquired for background subtraction.

3.7. Fluorescence-Activated Cell Sorting

The antifungal efficacies of γAFP^{B6GXZ8}, $\gamma AFP^{A0A2J5HZT4}$, TBF, FLC, and their respective synergistic combinations (γAFP^{B6GXZ8} + TBF, $\gamma AFP^{A0A2J5HZT4}$ + FLC) were evaluated using fluorescence-activated cell sorting (FACS). *C. albicans* SC5314 cells and *A. fumigatus* CBS 101355 conidia (2×10^5) were treated with 200 μg/mL $\gamma AFP^{A0A2J5HZT4}$, 200 μg/mL γAFP^{B6GXZ8}, 32 μg/mL FLC, 1 μg/mL TRB, and combinations namely 200 μg/mL $\gamma AFP^{A0A2J5HZT4}$ + 32 asμg/mL FLC and 200 μg/mL γAFP^{B6GXZ8} + 0.5 μg/mL TRB, in LCM at 30°C for 1 h with shaking (160 rpm). The treated cells were then stained with 5 μg/mL propidium iodide (PI; Sigma-Aldrich, St. Louis, MO, USA) for 10 min at room temperature in the dark, washed twice in PBS (9000 × *g* for 5 min), and resuspended in PBS. For positive PI staining and calibration controls, cells or conidia were treated with 70% ethanol (v/v) for 10 minutes at room temperature under shaking conditions (160 rpm). Untreated cells or conidia functioned as controls to reflect spontaneous cell death. Detection of PI-positive signals was performed using a FlowSight imaging flow cytometer (Amins, Merck Millipore, Billerica, MA, USA) equipped with excitation lasers at wavelengths of 405 nm (violet), 488 nm (blue), and 642 nm (red). Calibration procedures were included to avoid fluorescence channel oversaturation and prevent artifact signals due to spectral spillover. Each experimental run analyzed a total of 5000 cells. PI-associated fluorescence was detected at 642 nm, with excitation lasers and emission in channel 2 window.

Gating strategies were refined to include at least 96% of the untreated population, while excluding cellular debris from data collection. Flow cytometry datasets were processed and interpreted using Image Data Exploration and Analysis Software (IDEAS) (Amins, Millipore, Billerica, MA, USA). All FACS experiments were repeated three times independently.

3.8. Scanning Electron Microscopy

Scanning electron microscopy (SEM) analysis was performed to examine the morphological effects of γAFP^{B6GXZ8} (200 μg/mL), $\gamma AFP^{A0A2J5HZT4}$ (200 μg/mL), TRB (1 μg/mL), FLC (32 μg/mL), and their respective synergistic combinations (γAFP^{B6GXZ8} [200 μg/mL] + TBF [0.5 μg/mL], $\gamma AFP^{A0A2J5HZT4}$ [200 μg/mL] + FLC [32 μg/mL]) on *C.*

albicans SC5314 cells and *A. fumigatus* CBS 101355 conidia (4×10^6 cells or conidia)/ml under the following conditions: LCM, incubation at 30 °C for 16 hours with shaking at 160 rpm for *C. albicans*, and under static conditions for *A. fumigatus*. Untreated conidia or cells served as morphology controls. Cells or conidia were harvested (9,000 × *g* for 5 min), washed twice, and resuspended in PBS. For SEM, 8 µL aliquots were dispensed onto silicon discs pre-coated with 0.01% (w/v) poly-L-lysine (Merck Millipore, Billerica, MA, USA). Samples were fixed overnight at 4°C in 2.5% (v/v) glutaraldehyde with 0.05 M cacodylate buffer (pH 7.2) in PBS. Post-fixation, specimens were rinsed twice with PBS and dehydrated through a graded ethanol series (30%–100%, v/v; 4 h per concentration at 4°C). The samples were dried with a Quorum K850 critical-point dryer (Quorum Technologies, Laughton, UK), and coated with a 12 nm layer of gold, and imaged using a JEOL JSM-7100F/LV field emission SEM (JEOL Ltd., Tokyo, Japan).

3.9. Hemolysis Assay

The hemolytic activities of aqueous solutions containing γAFP^{B6GXZ8} (200 µg/mL), γAFP^{A0A2J5HZT4} (200 µg/mL), TRB (1 µg/mL), FLC (32 µg/mL), and their respective synergistic combinations [γAFP^{B6GXZ8} (200 µg/mL) + TRB (0.5 µg/mL), γAFP^{A0A2J5HZT4} (200 µg/mL) + FLC (32 µg/mL)] were assessed using Columbia blood agar plates (5% (v/v) sheep blood; VWR, Radnor, PA, USA). Sterile filter paper disks (6 mm diameter) were impregnated with 10 µL of each solution and placed onto agar plates. Sterile bidistilled H_2O and 20% (v/v) Triton X-100 were used as negative and positive hemolysis controls, respectively. The presence of clear zones surrounding the filter disks was examined after 24 h incubation at 37°C. The experiment was conducted in triplicate.

3.10. *Galleria mellonella* Toxicity Assay

The potential *in vivo* toxic effects of γAFP^{B6GXZ8}, γAFP^{A0A2J5HZT4}, TRB, FLC, and their respective synergistic combinations (γAFP^{B6GXZ8} + TRB, γAFP^{A0A2J5HZT4} + FLC) were investigated in *G. mellonella* larvae at concentrations used in the hemolysis assay. Twenty microliters of each test solution, prepared in insect physiological saline (IPS) (50 mM NaCl, 5 mM KCl, 10 mM EDTA, and 30 mM sodium citrate in 0.1 M Tris-HCl, pH 6.9), were injected intrahemocoelically using 29-gauge insulin needles (BD Micro-Fine, Franklin Lakes, NJ, USA) through the last right pro-leg of twenty larvae. Larvae were incubated at 37°C, and survival was monitored every 24 hours for 6 days. IPS- and 20% (v/v) Triton X-100-treated larvae served as nontoxic and positive toxicity controls,

respectively, while larvae without any interventions as untreated controls. The toxicity assay was repeated twice.

3.11. *In vivo* Therapeutic Efficacy of γAFP-Antifungal Drug Combinations

The *in vivo* therapeutic efficacies of γAFP^{B6GXZ8}, $\gamma AFP^{A0A2J5HZT4}$, TRB, FLC, and their respective combinations (γAFP^{B6GXZ8} + TRB, $\gamma AFP^{A0A2J5HZT4}$ + FLC) used in the hemolysis assay were evaluated in *G. mellonella* larvae following the toxicity assay protocol. In addition to the previously described procedure, 20 µL of fungal cell or conidial suspension (2×10^7 conidia or cells/mL) were injected into the last left pro-legs of larvae, whereas in the case of the nontoxic and positive toxicity controls, 20 µL of IPS were injected. This experiment was repeated twice.

3.12. Statistical Analysis

For growth inhibitory activity one-way ANOVA and Tukey's HSD post-hoc tests (Statistics Kingdom, https://www. statskingdom.com/index.html) were applied to determine significant differences ($p \leq 0.05$) regarding the proportion of dead cells following various treatments (Statistics Kingdom, 2022). To assess statistically significant differences in the FACS results, Pearson's chi-squared test was applied, and the Phi coefficient was calculated to evaluate the strength of association between the two treatment groups (Statistic Kingdom online platform, 2025; https://www.statskingdom.com/310GoodnessChi.html). To assess *G. mellonella* survival, log-rank (Mantel–Cox) and Gehan–Breslow–Wilcoxon tests were performed using GraphPad Prism 7.00 (GraphPad Software, Boston, MA, USA). Survival differences were deemed statistically significant if $p \leq 0.05$ in both tests. All statistical analyses were conducted using GraphPad Prism 7.00 (GraphPad Software, Boston, MA, USA).

4. RESULTS

4.1. AFP Selection for Peptide Design, and Physicochemical Properties of γAFPs

Previous studies have demonstrated that net charge and hydrophobicity significantly influence the antifungal efficacy of synthetic peptides designed based on the γ-core motif of AFPs from *P. chrysogenum* and *Aspergillus fischeri* (Sonderegger et al., 2018; Tóth et al., 2020, 2022; Váradi et al., 2024). Considering these findings, γ-core motifs from representative AFPs belonging to four phylogenetically distinct groups within Eurotiomycetes (**Fig.3**) were selected for γAFP design, based on their differences in physicochemical properties (**Table 6)**. To optimize antifungal activity, the designed γAFPs incorporated three additional amino acids from the N-terminus and one extra amino acid from the C-terminus according to Sonderegger et al. (2018) (**Table 6**). The γAFPs encompassing the γ-core motifs from the *P. chrysogenum* AFP (PAF group) exhibited net charge variations between –1.5 and +4.0, with grand average of hydropathy value (GRAVY) ranging from –1.814 to –0.607. For γAFPs derived from *Aspergillus giganteus* AFP group, net charge ranged between +2.0 and +4.25, with GRAVY from –2.271 to –1.421. For γAFPs from *Penicillium brevicompactum* 'bubble' protein (BP) group, net charge varied between –0.75 and +2.0, whereas GRAVY ranged from –1.350 to –0.275. Finally, the γAFP of *A. fischeri* NFAP2 group exhibited a neutral charge and an almost zero GRAVY (0.075) (**Table 6**). The Boman Index, a parameter used to predict peptide protein-binding propensity from amino acid composition and side-chain transfer free energy, was determined. The elevated Boman index (> 2.50) observed in certain members of the PAF- (*i.e.*, γAFP^{A0A0A2K0J0}, γAFP^{A1D8H8}, γAFP^{B6HWK0}), AFPg- (*i.e.*, γAFP^{P17737}, γAFP^{A0A2V5H6U3}, γAFP^{A0A2J5HZT4}), and BP- (*i.e.*, γAFP2^{A0A1V6NXI2}) groups suggests high binding potential to membranes, supporting the hypothesis of their membrane interaction activity (Boman, 2003).

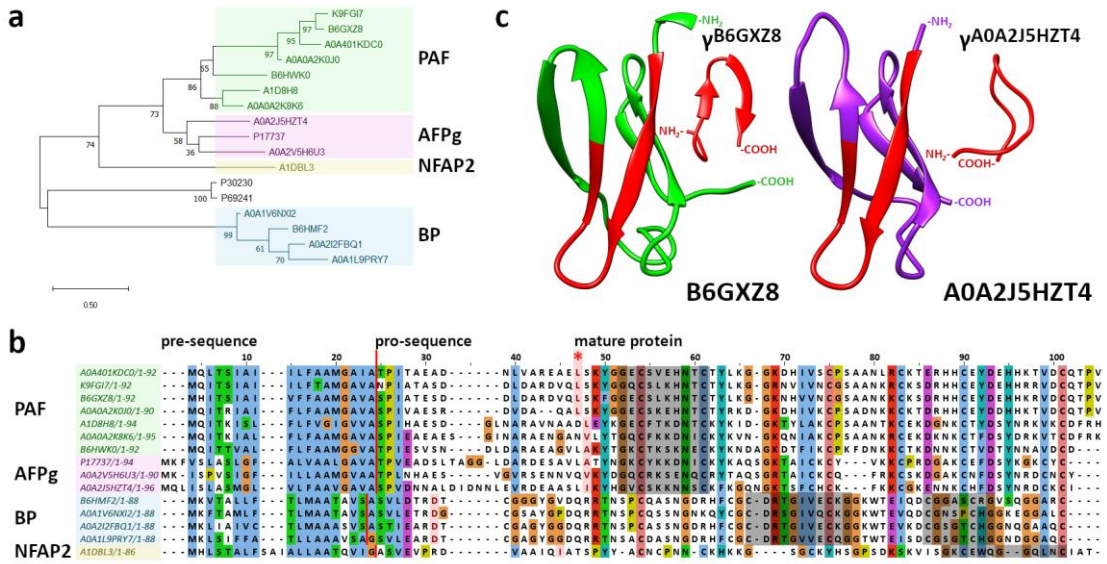

Figure 3: Phylogenetic and *in silico* structural analyses of AFPs from Eurotiomycetes involved in this study. Maximum likelihood tree (a), and ClustalW multiple alignment of AMPs (b), whereon the UniProt database accession numbers of the respective AFPs are indicated (for further information see **Table 6**). The *Penicillium chrysogenum* antifungal protein (PAF), *Aspergillus giganteus* antifungal protein (AFPg), *Aspergillus fischeri* antifungal protein 2 (NFAP2), and the *Penicillium brevicompactum* 'bubble' protein (BP) subclades are highlighted in green, purple, yellow, and blue, respectively. In panel (b), red line indicates the predicted cleavage site of the signal sequence, and the first amino acid of the mature AFP is highlighted in red and indicated with red asterisk, the conserved γ-core motif (GXC-X_{3-9}-C) is highlighted in grey. AlphaFold and PEP-FOLD3 predicted tertiary structure of *Penicillium rubens* Wisconsin 54-1255 PAF-like (B6GXZ8), and *Aspergillus taichungensis* IBT 19404 AFP-like (A0A2J5HZT4) proteins, and the synthetic peptides designed on the γ-core motifs (γ^{B6GXZ8} and $\gamma^{A0A2J5HZT4}$) (c).

Table 5: Amino acid sequences of antifungal proteins (AFPs) from Eurotiomycetes involved in the study, and physicochemical properties of synthetic peptides spanning the γ-core motif (γAFP).

Peptide	Length (aa)	Mw (Da)	Theoretical pI	Net charge (pH = 7.0)	GRAVY	Boman index (kcal/mol)
PAF-group						
Aspergillus awamori (A0A401KDC0) MQLTSIAIILFAAMGAIATPITAEADNLVAREAELS**KYGGECSVEHNTCT**YLKGGKDHIVSCPSAANLRCKTERHHCEYDEHHKTVDCQTPV						
γAFP^{A0A401KDC0}: KYGGECSVEHNTCT						
γAFP^{A0A401KDC0}	14	1527.64	5.40	-0.75	-0.907	2.19
Penicillium digitatum (K9FGI7) MQITSIAIILFTAMGAVANPIATASDDLDARDVQLS**KYGGQCSLKHNTCT**YLKGGRNVIVNCGSAANKRCKSDRHHCEYDEHHRRVDCQTPV						
γAFP^{K9FGI7}: KYGGQCSLKHNTCT						
γAFP^{K9FGI7}	14	1539.74	8.86	+2.5	-0.964	1.94
Penicillium rubens (B6GXZ8) MHITSIAIVFFAAMGAVASPIATESDDLDARDVQLS**KFGGECSLKHNTCT**YLKGGKNHVVNCGSAANKKCKSDRHHCEYDEHHKRVDCQTPV						
γAFP^{B6GXZ8}: KFGGECSLKHNTCT						
γAFP^{B6GXZ8}*	14	1524.73	8.06	+1.25	-0.671	1.81
Penicillium expansum (A0A0A2K0J0) MQITRIAIFLFAAMGAVASPIVAESRDVDAQALS**KYGGECSKEHNTCT**YRKDGKDHIVKCPSADNKKCKTDRHHCEYDDHHKTVDCQTPV						
γAFP^{A0A0A2K0J0}: KYGGECSKEHNTCT						
γAFP^{A0A0A2K0J0}	14	1556.69	6.74	+0.25	-1.486	2.87
Neosartorya fischeri (A1D8H8) MQITKISLFLFVGIGVVASPIHAESDGLNARAVNAADL**EYKGECFTKDNTCK**YKIDGKTYLAKCPSAANTKCEKDGNKCTYDSYNRKVKCDFRH						
γAFP^{A1D8H8}: EYKGECFTKDNTCK						
γAFP^{A1D8H8}	14	1665.85	6.26	-1.5	-1.500	3.17
Penicillium expansum (A0A0A2K8K6) MQITKIALFLFAAMGAVASPIEAEAESGINARAENGANV**LYTGQCFKKDNICK**YKVNGKQNIAKCPSAANKRCEKDKNKCTFDSYDRKVTCDFRK						
γAFP^{A0A0A2K8K6}: LYTGQCFKKDNICK						
γAFP^{A0A0A2K8K6}	14	1660.97	8.82	+2.0	-0.607	1.71
Penicillium rubens (B6HWK0) MQITTVALFLFAAMGGVATPIESVSNDLDARAEAGVLA**KYTGKCTKSKNECK**YKNDAGKDTFIKCPKFDNKKCTKDNNKCTVDTYNNAVDCD						
150051_ γAFP^{B6HWK0}: KYTGKCTKSKNECK						
γAFP^{B6HWK0}	14	1617.90	9.51	+4.0	-1.814	3.31
AFPg-group						
Aspergillus giganteus (P17737) MKFVSLASLGFALVAALGAVATPVEADSLTAGGLDARDESAVLA**TYNGKCYKKDNICK**YKAQSGKTAICKCYVKKCPRDGAKCEFDSYKGKCYC						
γAFP^{P17737}: TYNGKCYKKDNICK						
γAFP^{P17737}	14	1677.95	9.18	+3.0	-1.450	2.75
Aspergillus violaceofuscus (A0A2V5H6U3) MKISPVSIGFILLAAMGVAATPLNHAESVGVRSENNVQV**KYDGQCRKSENQCR**YTAQSGRTAICKCQFRKCSKDGAKCNFDSYNRDCNCY						
γAFP^{A0A2V5H6U3}: KYDGQCRKSENQCR						
γAFP^{A0A2V5H6U3}	14	1714.89	8.86	+2.0	-2.271	5.30
Aspergillus taichungensis (A0A2J5HZT4) MQLISLASMGLVLFAAVGAVASPVDNNALDIDNNLEVRDEAASLI**KYHGVCSKKNNSCK**FKGQNGKTSFCHCKFKKCGKENNKCHFDSYNRDCKCI						
γAFP^{A0A2J5HZT4}: KYHGVCSKKNNSCK						
γAFP^{A0A2J5HZT4}*	14	1595.85	9.60	+4.25	-1.421	2.82

BP-group						
Penicillium rubens (B6HMF2)						
MKVTALLFTLMAATAVSASVLDTRDTCGGGYGVDQRRTNSPCQASNGDRHFC**<u>GCDRTGIVECKGGKW</u>**TEIQ**<u>DCGGASCRGVSQ</u>**GGARC						
γAFP1^{B6HMF2}: WKGGKCEVIGTRDCG, γAFP2^{B6HMF2}: QSVGRCSAGGCD						
γAFP1^{B6HMF2}	15	1608.85	8.05	+1.0	-0.587	1.76
γAFP2^{B6HMF2}	12	1139.22	5.82	0.00	-0.275	2.06
Penicillium polonicum (A0A1V6NXI2)						
MKFTAMLFTLMAATAVSASVLETRDGCGSAYGPDQRRTNSPCQSSNGNKQYC**<u>GCDRSGIVQCKGGKW</u>**TEVQD**<u>CGNSPCHGGKE</u>**GGALC						
γAFP1^{A0A1V6NXI2}: WKGGKCQVIGSRDCG, γAFP2^{A0A1V6NXI2} EKGGHCPSNGCD						
γAFP1^{A0A1V6NXI2}	15	1593.84	8.90	+2.0	-0.593	1.73
γAFP2^{A0A1V6NXI2}	12	1203.27	5.32	-0.75	-1.350	2.53
Aspergillus candidus (A0A2I2FBQ1)						
MKLIAIVCTLMAAASVSASTIEARDTCGAGYGGDQRRTNSPCASSNGDRHFC**<u>GCDRTGIVECKGGKW</u>**TEVK**<u>DCGSGTCHGGNQ</u>**GAAQC						
γAFP1^{A0A2I2FBQ1}: WKGGKCEVIGTRDCG, γAFP2^{A0A2I2FBQ1}: QNGGHCTGSGCD						
γAFP1^{A0A2I2FBQ1}	15	1608.85	8.05	+1.0	-0.587	1.76
γAFP2^{A0A2I2FBQ1}	12	1135.15	5.08	-0.75	-0.983	2.1
Aspergillus versicolor (A0A1L9PRY7)						
MKLSIFFATLLAAAVSAGSVLEARDTCGAGYGGDQRRTNSACDASNGDRHFC**<u>GCDRTGVVECQGGTW</u>**TEIS**<u>DCGSGTCHGGND</u>**GGAQC						
γAFP1^{A0A1L9PRY7}: WTGGQCEVVGTRDCG, γAFP2^{A0A1L9PRY7}:DNGGHCTGSGCD						
γAFP1^{A0A1L9PRY7}	15	1567.71	4.37	-1.0	-0.367	1.62
γAFP2^{A0A1L9PRY7}	12	1122.11	4.20	-1.75	-0.983	2.36
NFAP2-group						
Neosartorya fischeri (A1DBL3)						
MHLSTALFSAIALLAATQVIGASVEVPRDVAAIQIATSPYYACNCPNNCKHKKGSGCKYHSGPSDKSK**<u>VISGKCEWQGGQLNCI</u>**AT						
γAFP^{A1DBL3}: VISGKCEWQGGQLNCI						
γAFP^{A1DBL3}	16	1735.01	5.96	0.00	0.075	0.43

After the species name, the UniProt database accession number is indicated. Amino acid sequence regions used for γAFP design are indicated with bold and underlined letters in the primary structure. γAFPs selected for drug interaction analysis are highlighted in grey. γAFPs selected for comprehensive investigations are marked with asterisk. GRAVY: grand average of hydropathy value.

4.2. Antifungal Activity of γAFPs

The *in vitro* antifungal efficacy of γAFPs was evaluated against a diverse set of yeasts and molds, including human and plant pathogenic isolates, using a broth microdilution assay (**Table 6**). None of the tested γAFPs achieved complete growth inhibition at concentrations up to 200 µg/mL (MIC > 200 µg/mL). However, several γAFPs exhibited significant antifungal activity at the highest tested concentration (200 µg/mL). γAFP^{B6HWK0} displayed remarkable inhibitory effects against *A. fumigatus*. γAFP^{B6GXZ8}, γAFP2^{A0A2I2FBQ1}, and γAFP^{A0A0A2K0J0} demonstrated strong activity against *B. cinerea*, *F. subglutinans,* and S. *cerevisiae*, respectively (IP ≥ 50%, **Table 6**). Conversely, γAFP^{A1D8H8}, γAFP1^{B6HMF2}, γAFP2^{A0A1V6NXI2}, and γAFP1^{A0A1L9PRY7} were considered as inactive, exhibiting IP values between 0% and 14±5% (**Table 6**). The remaining γAFPs inhibited growth of at least one fungal species, with IP values ranging from 25% to 50% (**Table 6**). Statistical analysis of growth percentages at various concentrations of the most effective γAFPs revealed that their inhibitory activity was not dose-dependent within the investigated concentration range (**Fig. 4**). Their efficacy remained constant beyond a certain threshold and further increases in concentration did not yield statistically significant differences in growth reduction ($p \geq 0.05$, **Fig.4**). The effective concentrations were 100 µg/mL for γAFP^{B6HWK0} against *A. fumigatus*, γAFP^{A0A0A2K0J0}, and γAFP2^{A0A2I2FBQ1} against *S. cerevisiae*, 25 µg/mL for γAFPB^{6GXZ8} against *B. cinerea* (**Fig.4**). An exception was γAFP2^{A0A2I2FBQ1}, which exhibited non-linear concentration-dependent inhibition against *F. subglutinans* (**Fig.4**).

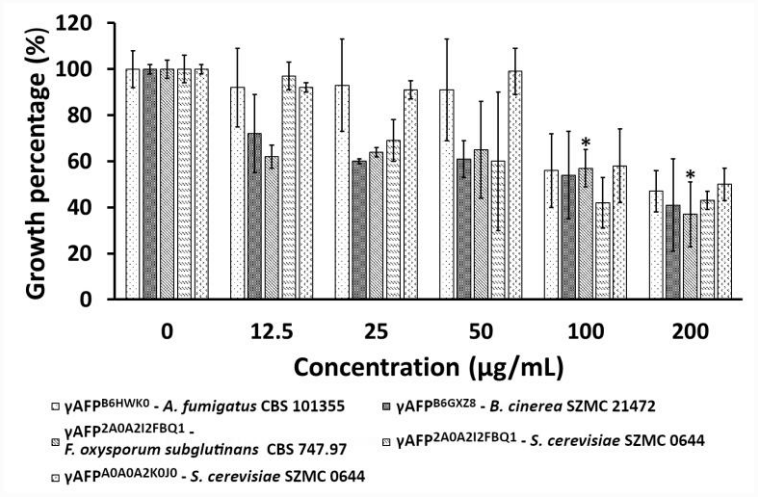

Figure 4: Growth percentages of fungi at various concentrations of the most effective γAFPs. Asterisk indicates not gradual dose-dependent inhibitory activity.

Table 6: Growth inhibition percentages (IP) of 200 µg/mL γAFPs on the tested fungal isolates compared to the untreated control cultures.

Fungus / Peptide	***Aspergillus fumigatus* CBS 101355^{+}**	***Botrytis cinerea* SZMC 21472^{++}**	***Candida albicans* SC5314^{+}**	***Cladosporium herbarum* FSU 1148^{++}**	***Fusarium subglutinans* CBS 747.97^{++}**	***Saccharomyces cerevisiae* SZMC 0644**
PAF-group IPs						
γAFP^{A0A401KDC0}	**26±12**	n.d.	10±3	n.d.	n.d.	n.d.
γAFP^{K9FGI7}	n.d.	n.d.	n.d.	35±2	n.d.	n.d.
γAFP^{B6GXZ8}*	n.d.	**59±20**	9±12	14±14	n.d.	**43±1**
γAFP^{A0A0A2K0J0}	**37±17**	**26±3**	n.d.	n.d.	n.d.	**50±7**
γAFP^{A1D8H8}	n.d.	n.d.	n.d.	n.d.	n.d.	n.d.
γAFP^{A0A0A2K8K6}	12±5	20±8	14±12	n.d.	n.d.	**33±3**
γAFP^{B6HWK0}	**53±9**	18±9	n.d.	n.d.	n.d.	18±4
AFPg-group IPs						
γAFPP^{17737}	9±7	n.d.	n.d.	23±18	n.d.	n.d.
γAFP^{A0A2V5H6U3}	24±0	20±1	13±0	18±6	n.d.	15±10
γAFP^{A0A2J5HZT4}*	22±1	24±14	13±4	n.d.	**42±8**	17±3
BP-group IPs						
γAFP1^{B6HMF2}	7±1	n.d.	n.d.	n.d.	n.d.	15±0
γAFP2^{B6HMF2}	8±3	**45±3**	n.d.	n.d.	n.d.	20±3
γAFP1^{A0A1V6NXI2}	n.d.	**27±1**	n.d.	**33±1**	20±4	7±10
γAFP2^{A0A1V6NXI2}	n.d.	n.d.	n.d.	n.d.	7±5	n.d.
γAFP1^{A0A2I2FBQ1}	8±1	n.d.	n.d.	n.d.	n.d.	n.d.
γAFP2^{A0A2I2FBQ1}	14±2	n.d.	21±7	n.d.	**63±14**	**57±4**
γAFP1^{A0A1L9PRY7}	13±3	n.d.	6±4	14±5	n.d.	11±1
γAFP2^{A0A1L9PRY7}	n.d.	11±5	15±4	n.d.	21±6	**34±4**
NFAP2-group IPs						
γAFP^{A1DBL3}	n.d.	n.d.	n.d.	n.d.	10±4	44±4

γAFPs selected for drug interaction analysis are highlighted in grey. γAFPs selected for comprehensive investigations are marked with asterisk. $^{+}$: human pathogenic fungus, $^{++}$ plant pathogenic fungus n.d.: Growth inhibition was not detected.

4.3. Interaction Between γAFPs and Conventional Drugs Against *C. albicans* and *A. fumigatus*

The MICs of conventional antifungal drugs, including FLC, AMB, MFG, and TRB, were determined using an *in vitro* broth microdilution assay against two human pathogenic fungal isolates, *C. albicans* and *A. fumigatus*. Under the applied test conditions AMB (MIC = 1 µg/mL), MFG (MIC = 0.0156 µg/mL), and TRB (MIC = 1 µg/mL) effectively inhibited *C. albicans*, while FLC did not (MIC > 32 µg/mL). Complete growth inhibition of *A. fumigatus* was not achieved with AMB, MFG, TRB, or FLC (MICs > 32 µg/mL). Considering these MIC values, AMB, MFG, and TRB were included in combination

experiments against *C. albicans* to assess whether the presence of γAFPs could enhance efficacy and lower the effective concentration, thereby reducing potential side effects in long-term, high-dosage therapies (Lu et al., 2023). Previous studies have demonstrated that co-administration of antimicrobial peptides can make the resistant fungal strains susceptible to conventional antifungal drugs (Zhu et al., 2022). Given that *A. fumigatus* exhibits intrinsic resistance to the generic FLC (Leonardelli et al., 2016), FLC was tested in combination with γAFPs to evaluate its potential effectiveness against *A. fumigatus*. In this experiment, conventional antifungal drugs were combined with an effective representative of each fungal AFPs group with various physicochemical properties, *i.e.* γAFP^{B6GXZ8}, $\gamma AFP^{A0A0A2K0J0}$, $\gamma AFP^{A0A2J5HZT4}$, $\gamma AFP2^{A0A2I2FBQ1}$, γAFP^{A1DBL3} (**Table 5**). Most antifungal drug + γAFP combinations exhibited indifferent interactions, and no antagonistic effects were observed (data not shown). However, two notable exceptions emerged, as γAFP^{B6GXZ8} + TRB and $\gamma AFP^{A0A2J5HZT4}$ + FLC combinations demonstrated synergy against *C. albicans* (**Table 7**) and *A. fumigatus* (**Table 8**), respectively. That synergistic combinations were subsequently included in further experiments, where the highest IR and IP values were detected below the individual MICs **(Table 7**). These were 200 µg/ml γAFP^{B6GXZ8} + 0.5 µg/ ml TRB against *C. albicans*, and 200 µg/ml γAFPA0A2J5HZT4 + 32 µg/ml FLC against *A. fumigatus* (**Table 9**)

Table 7: Inhibition percentages (IP, %) of *Candida albicans* SC5314 in the combinatorial application of γAFP^{B6GXZ8} + terbinafine (TRB).

Candida albicans SC3514												
$\gamma^{AFPB6GXZ8}$ + TRB	**400 µg/ml**	**200 µg/ml**	**100 µg/ml**	**50 µg/ml**	**25 µg/ml**	**12.5 µg/ml**	**6.25 µg/ml**	**3.125 µg/ml**	**1.56 µg/ml**	**0.78 µg/ml**	**0.39 µg/ml**	**0**
2 µg/ml	94±1.2% IR:1.02±0.0	94±1% IR:1.02±0.01	93±0.8% IR: 1.02±0.01	94±1.3% IR: 1.02±0.03	94±1.9% IR: 1.0±0.04	93±1.9% IR: 1.02±0.01	93±1.5% IR: 1.02±0.01	93±0.6% IR: 1.02±0.04	92±0.5% IR: 1.0±0.01	92±1% IR: 1.0±0.01	92±1% IR: 1.01±0.01	92±1.3%
1 µg/ml	94±0.6% IR: 1.01±0.01	95±1% IR: 1.03±0.01	93±0.5% IR: 1.01±0.01	93±1.2% IR: 1.01±0.015	92±0.5% IR: 1.03±0.05	93±0.6% IR: 1.01±0	93±1.3% IR: 1.01±0.01	93±0.6% IR: 1.01±0.01	92±0.6% IR:1.0±X0.0	92±0.5% IR: 0.99±0.01	92±0.5% IR: 1.0±0	92±0.5%
0.5 µg/ml	73±4.8% IR: 2.83±1.08	**68±7.1% IR: 2.7±0.73**	55±6.8% IR: 2.08±0.45	52±6.7% IR: 2.02±0.49	47±6.6% IR: 1.68±0.35	40±2.4% IR: 1.58±0.29	36±4.5% IR: 1.48±0.33	33±5.9% IR: 1.17±0.01	32±4.9% IR: 1.06±0.24	28±7% IR: 0.93±0.1	24±6.3% IR: 0.94±0.27	24±6.1%
0.25 µg/ml	33±9.1% IR: 1.89±0.23	24±2.4% IR: 1.83±1.0	20±2.2% IR: 1.29±0.3	24±10.4% IR: 1.61±0.5	16±8.5% IR: 0.96±0.31	21±4.9% IR: 1.56±0.37	18±3% IR: 1.32±0.32	20±2.4% IR: 1.19±0.28	13±2.8% IR: 0.71±0.25	17±2.6% IR: 0.88±0.15	18±2.2% IR: 1.19±0.15	12±2.8%
0.125 µg/ml	18±6.8% IR: 0.92±0.34	14±5.1% IR: 0.81±0.14	21±4% IR: 1.16±0.25	18±4.2% IR: 1.04±0.2	24±2.8% IR: 1.36±0.31	11±2.6% IR: 0.63±0.03	14±3.1% IR: 0.84±0.14	17±2.8% IR: 0.86±0.08	16±2.6% IR: 0.75±0.23	11±3.3% IR: 0.47±0.05	20±3.1% IR: 1.21±0.24	15±2.6%
0.0625 µg/ml	12±3.7% IR: 0.8±0.23	10±3.3% IR: 0.77±0.1	9±2.6% IR: 0.62±0.07	17±2.6% IR: 1.40±0.53	12±3.1% IR: 0.76±0.1	14±2.9% IR: 1.23±0.33	15±2.6% IR: 1.28±0.39	16±2.8% IR: 1.07±0.22	14±3.3% IR: 0.89±0.45	6±2.9% IR: 0.34±0.09	13±3.1% IR: 0.93±0.22	9±2.3%
0.03125 µg/ml	14±2.6% IR: 0.99±0.32	15±2.8% IR: 1.42±0.55	13±2.6% IR: 0.97±0.22	13±2.6% IR: 1.15±0.4	11±2.8% IR: 0.93±0.32	15±2.9% IR: 1.49±0.51	13±3.3% IR: 1.19±0.36	12±2.6% IR: 0.82±0.15	13±2.9% IR: 0.87±0.39	11±2.4% IR: 0.7±0.14	10±1.3% IR: 0.7±0.21	9±2.8%
0 µg/ml	6±3.7%	4±2.9%	5±2.4%	4±2.9%	5±3.7%	3±2.5%	3±3.9%	7±2.9%	9±6.4%	9±3.4%	4±2.8%	0±0%

Interaction ratio (IR) calculated according to the Abbot-formula presented below IP. Red cells indicate synergy (IR >1.5), while orange cells additive interaction. The untreated control was defined as 100% of growth.

Table 8: Inhibition percentages (IP, %) of *Aspergillus fumigatus* CBS 101355 in the combinatorial application of and γAFP^{B6GXZ8} + fluconazole (FLC).

Aspergillus fumigatus CBS 101355												
$\gamma^{AFPB6GXZ8}$ + FLC	**400 µg/ml**	**200 µg/ml**	**100 µg/ml**	**50 µg/ml**	**25 µg/ml**	**12.5 µg/ml**	**6.25 µg/ml**	**3.125 µg/ml**	**1.56 µg/ml**	**0.78 µg/ml**	**0.39 µg/ml**	**0**
64 µg/ml	58±8.2% IR: 1.59±0.46	65±7.2% IR: 2.51±0.23	54±2.6% IR: 2.14±0.44	13±11.3% IR: 0.37±0.29	23±4.3% IR: 1.77±1.43	23±3.6% IR: 0.88±0.4	8±10% IR: 0.72±0.84	4±4.7% IR: 0.4±0.59	1±1% IR: 0.1±0.1	4±4.8% IR: 0.21±0.24	7±2.5% IR: 0.22±0.25	4±4.3%
32 µg/ml	62±5.7% IR: 1.91±0.67	**70±5.9% IR: 2.99±0.15**	65±3.3% IR: 2.84±0.28	33±25.8% IR: 1.33±1.18	48±1% IR: 4.03±3.36	39±14.8% IR: 1.51±0.21	19±8.5% IR: 2.55±3.14	00±0% IR: 0.0±0	4±4.2% IR: 0.1±0.17	00±0.0% IR: 0.0±0	00±00% IR: 0.0±0	00±0.0%
16 µg/ml	67±3.2% IR: 1.79±0.56	73±4.8% IR: 2.79±0.42	71±0.8% IR: 2.79±0.56	38±29.2% IR: 1.35±1.13	43±8.5% IR: 3.05±2.73	36±12.1% IR: 1.59±1.09	22±10.7% IR: 2.33±1.93	38±19.8% IR: 3.35±3.12	29±8.1% IR: 2.0±2.14	37±19.1% IR: 2.52±3.51	14±15.9% IR: 1.1±2.2	4±2.9%
8 µg/ml	58±8.5% IR: 1.67±0.81	72±5.2% IR: 2.88±0.28	64±1.3% IR: 2.74±0.49	33±37.8% IR: 1.38±1.64	46±21.4% IR: 4.01±3.88	49±17.9% IR: 2.22±1.61	49±7.3% IR: 7.13±6.11	18±10.9% IR: 1.32±0.51	21±5.9% IR: 2.15±2.69	31±16% IR: 3.59±4.9	16±23.1% IR: 3.1±6.12	2±2.6%
4 µg/ml	59±4.1% IR: 1.46±0.46	72±5% IR: 2.85±0.36	66±4.6% IR: 2.41±0.24	22±25.4% IR: 0.67±0.82	54±0.5% IR: 2.36±1.41	55±3.3% IR: 1.95±0.84	32±11.5% IR: 4.2±1.81	12±12.2% IR: 0.51±0.34	32±17.3% IR: 3.29±2.42	33±20.7% IR: 3.5±2.95	16±10.3% IR: 1.67±1.91	4±2.9%
2 µg/ml	53±5.2% IR: 1.33±0.47	76±3.9% IR: 2.66±0.37	67±2.9% IR: 2.48±0.53	62±1.2% IR: 1.88±0.2	39±11.6% IR: 1.86±1.6	44±3.7% IR: 1.5±0.62	30±10% IR: 5.33±3.51	12±13.3% IR: 0.32±0.38	30±11.1% IR: 3.9±4.1	4±5.1% IR: 0.56±0.82	11±3.8% IR: 1.22±0.79	6±11.6%
1 µg/ml	63±1.3% IR: 1.62±0.53	76±2.8% IR: 3.26±0.23	72±3.2% IR: 3.14±0.37	56±7.3% IR: 2.1±0.69	53±4.8% IR: 4.18±3.35	55±3.4% IR: 2.33±0.95	27±25.4% IR: 0.31±0.62	10±4.1% IR: 0.78±0.97	10±8.5% IR: 0.0±0	15±13% IR: 0.15±0.21	20±12.7% IR: 0.41±0.73	00±0.0%
0 µg/ml	38±14.2%	24±2.1%	23±3.6%	29±5.4%	24±19.1%	27±12.9%	2±2.6%	15±14.6%	6±6.4%	3±3.5%	7±8.5%	00±0%

Interaction ratio (IR) calculated according to the Abbot-formula presented below IP. Red cells indicate synergy (IR >1.5), orange cells additive interaction (IR between 0.5 and 1.5), while green cells antagonism (IR < 1.5). The untreated control was defined as 100% of growth**.**

Table 9: Synergy between antifungal peptides (γAFP^{B6GXZ8}, γAFP^{A0A2J5HZT4}) and conventional antifungal drugs where the highest interaction ratios (IRs) and growth inhibitory percentages were detected below the individual MICs against *C. albicans* or *A. fumigatus*. IRs were calculated according to the Abbott-formula.

Combination	X and Y	I_e	I_o	IR	Type
Candida albicans SC5314					
γAFP^{B6GXZ8} (200 µg/ml) + TRB (0.5 µg/ml)	4±3% 24±6%	27±7%	68±7%	2.7±0.7	Synergy
Aspergillus fumigatus CBS 101355					
γAFP^{A0A2J5HZT4} (200 µg/ml) + FLC (32 µg/ml)	24±2% 0±0%	24±2%	70±5.9%	3.0±0.2	Synergy

FLC: fluconazole, I*e*: expected percentage inhibition, I_0: observed percentage inhibition. IR: interaction ratio, TRB: terbinafine, X and Y: percentage inhibitions for the individual compounds used alone.

The analysis revealed a non-linear relationship between net charge and GRAVY score. The fitted quadratic model $y=0.11x^2-0.92x-0.73$ showed a minimum GRAVY value at net charge +4.2. This suggests that peptides with moderately positive net charge tend to be more hydrophilic, which may enhance their antifungal efficacy. The model achieved an R^2 value of 0.65, indicating a moderate fit to the data.

These results were obtained using γAFPs with antifungal activity (**Tables 5** and **6**) that were analyzed for net charge and GRAVY scores using standard bioinformatics tools. A quadratic regression model was fitted to the data using least squares estimation to explore the relationship between net charge and hydropathy. The model equation was derived and visualized using Python-based scientific plotting libraries.

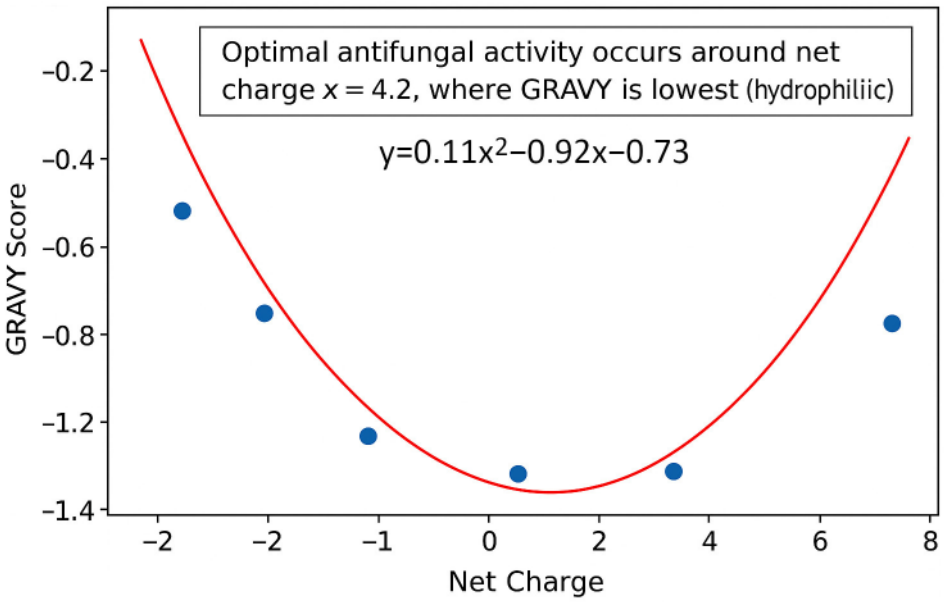

Figure 5: Quadratic relationship between net charge and GRAVY score in antifungal active γAFPs. Blue dots represent antifungal active γAFPs highlighted in gray in Tables 1 and 2. The red curve shows a quadratic regression model.

4.4. ECD Spectroscopy

Previously, it was observed that synthetic γAFPs do not have an ordered structure, and a conformation change is not necessary for them to exert an antifungal effect (Tóth et al. 2020a; Váradi et al. 2024). Both γAFP^{B6GXZ8} and γAFP^{A0A2J5HZT4} exhibited class D ECD spectra in all applied conditions, indicative of unordered structures, or, more precisely, high conformational flexibility and an ensemble of dynamic, fast interconverting structural states (**Fig. 5**). Spectral deconvolution of the ECD spectra indicated contributions from all canonical secondary structural elements; however, approximately 60% of the contributions emerged from the turn structures and non-canonical, unordered conformations (**Table 10**). No considerable differences in spectral features and contributions were observed between the two peptides regardless of the applied experimental conditions. This indicates that the interactions of these peptides with fungal cells do not induce notable conformational reorganization. The obtained results support the *in silico*-predicted unordered structure of γAFP^{A0A2J5HZT4}, but they contradict the predicted β-pleated conformation of γAFP^{B6GXZ8} (**Fig. 3c**).

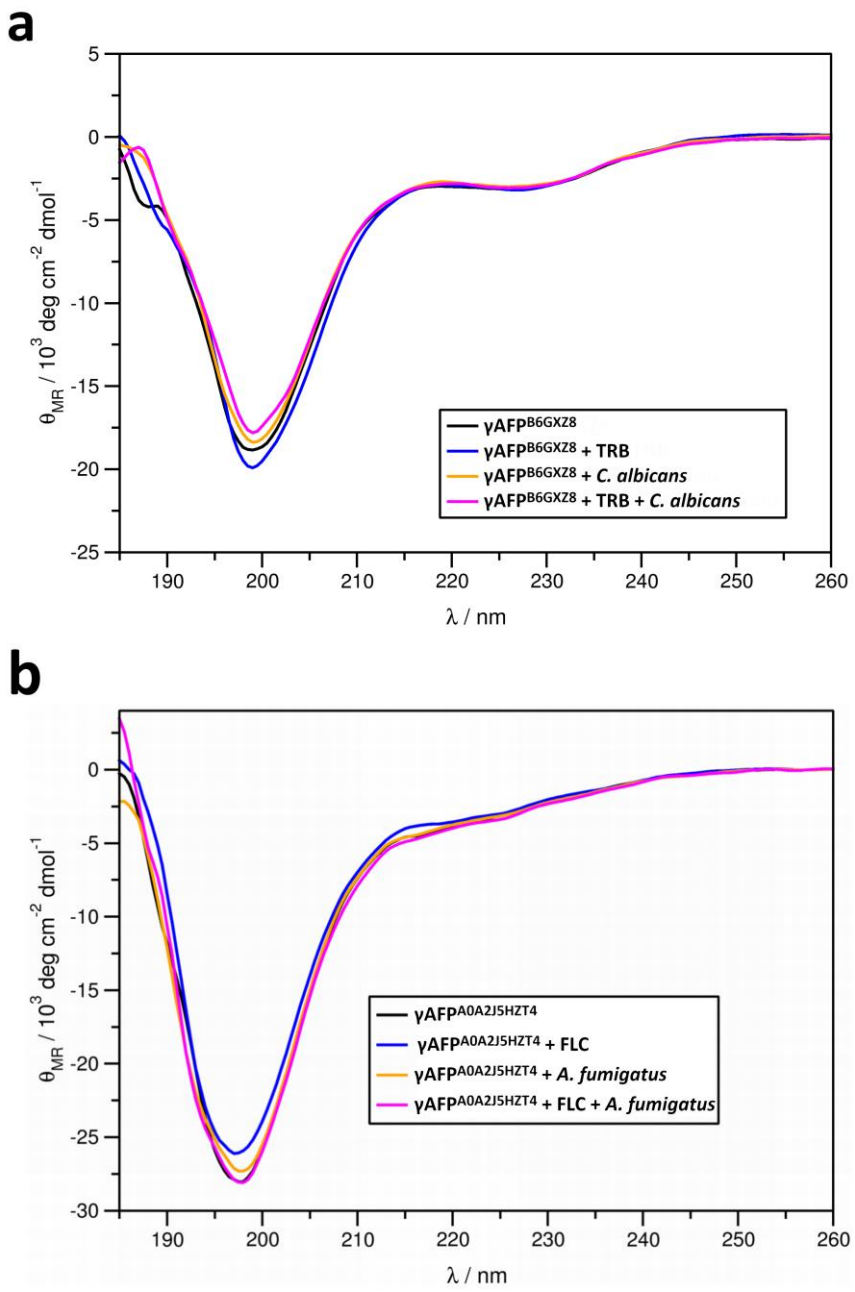

Figure 6: ECD spectra of γAFP^{B6GXZ8} (a) and γAFP^{A0A2J5HZT4} (b) in bidistilled H_2O, and in the presence of terbinafine (TRB), *Candida albicans* SC5314, and TRB and *C. albicans* SC 3514 (a); and in the presence of fluconazole (FLC), *Aspergillus fumigatus* CBS 101355, and FLC and *A. fumigatus* CBS 101355 (b), respectively.

Table 10: Secondary structural contributions to the observed ECD spectra of γAFP^{B6GXZ8} and γAFP^{A0A2J5HZT4} obtained from spectral deconvolution

	Helix1	**Helix2**	**Strand1**	**Strand2**	**Turns**	**Unordered**	**Total**
γAFP^{B6GXZ8}	0.01	0.08	0.18	0.11	0.26	0.36	1
γAFP^{B6GXZ8} + TRB	0.02	0.09	0.18	0.11	0.26	0.35	1.01
γAFP^{B6GXZ8} + *C. albicans*	0.01	0.08	0.19	0.11	0.25	0.36	1
γAFP^{B6GXZ8} + TRB + *C. albicans*	0.01	0.08	0.19	0.11	0.25	0.35	0.99
γAFP^{A0A2J5HZT4}	-.01	0.10	0.17	0.11	0.25	0.37	0.99
γAFP^{A0A2J5HZT4} + FLC	-.01	0.08	0.19	0.11	0.24	0.37	0.98
γAFP^{A0A2J5HZT4} + *A. fumigatus*	-.01	0.10	0.16	0.10	0.25	0.39	0.99
γAFP^{A0A2J5HZT4} + FLC + *A. fumigatus*	-.01	0.09	0.18	0.10	0.24	0.39	0.99

4.5. Fungal Cell Killing Efficacy of γAFP + Antifungal Drug Combinations

One of the primary antifungal mechanisms of AFPs is the disruption of the plasma membrane of the target fungus (Struyfs et al., 2021). This membrane-compromising effect can be evaluated using PI staining. PI is a red-fluorescent, membrane-impermeant dye that selectively binds to nuclear and chromosomal DNA and only enters cells with compromised membrane integrity. FACS was utilized to quantify the cell-killing and membrane-disrupting capabilities of two potent γAFPs in combination with conventional antifungal agents (TRB and FLC). These combinations were compared to the standalone application of each compound to elucidate the observed synergistic interactions (**Table 10**). The γAFP^{B6GXZ8} + TRB combination demonstrated significantly higher cell-killing efficacy than either compound alone (**Table 11**). The γAFP^{A0A2J5HZT4} + FLC combination also showed enhanced cell-killing activity compared to FLC alone. However, its efficacy was lower than that of the γAFP^{A0A2J5HZT4} peptide when applied individually (**Table 11**). Table 12 provides a detailed summary of the statistical analysis results.

Table 4: FACS analysis of cell death (propidium iodide positive cells/conidia, PI+) treated with γAFP, antifungal drug (TRB, FLC) and their combination

Treatment	PI+ (%)	p-value	
Candida albicans SC5314			
Untreated	0.2% ± 0.1	-	p= 0.072 ns
γAFP^{B6GXZ8}	46.3% ± 24.6	$p= 6.5 \times 10^{-16}$ *	
TRB	44.5% ± 17.4	$p= 2.4 \times 10^{-11}$ *	
γAFP^{B6GXZ8} + TRB	51.1% ± 23.9	-	
Aspergillus fumigatus CBS 101355			
Untreated	0.3% ± 0.18		$p= 2.48 \times 10^{-36}$ +
$\gamma AFP^{A0A2J5HZT4}$	15.1% ± 6.1	$p= 3.52 \times 10^{-5}$ *	
FLC	4.6% ± 1.3	$p= 2.52 \times 10^{-12}$ *	
$\gamma AFP^{A0A2J5HZT4}$ + FLC	8.3% ± 0.9		

FLC: fluconazole, TRB: terbinafine.

*: significant differences ($p \leq 0.05$) between the standalone and combination treatment, +: significant differences ($p \leq 0.05$) between the standalone treatments, ns: no significant difference.

Table 12: Statistical analysis (Pearson's chi-squared test and the Phi coefficient) of FACS results.

Comparison	p-value	Significance ($p \leq 0.05$)	φ (phi)	Effect size
Candida albicans SC5341				
Combination vs. $\gamma AFPB^{6GXZ8}$	2.4×10^{-11}	Yes	0.0421	Small
Combination vs. TRB	6.5×10^{-16}	Yes	0.0521	Small
$\gamma AFPB^{6GXZ8}$ vs. TRB	0.072	No	0.018	Negligible
Aspergillus fumigatus CBS 101355				
Combination vs. $\gamma AFP^{A0A2J5HZT4}$	3.5×10^{-5}	Yes	0.0414	Small
Combination vs. FLC	2.5×10^{-12}	Yes	0.0695	Small
$\gamma AFP^{A0A2J5HZT4}$ vs. FLC	2.5×10^{-36}	Yes	0.125	Medium

FLC: fluconazole, TRB: terbinafine

4.6. SEM analysis

SEM further evidenced the antifungal activity of γAFP^{B6GXZ8}, TRB, and their synergistic combination, while revealing the associated morphological alterations (**Fig. 7a**). Treatment with γAFP^{B6GXZ8} induced notable surface changes in *C. albicans* cells, characterized by a coarse, dense surface with textured projections, deviating from the smooth, ovoid morphology typical of untreated yeast-phase cells. Some cells appeared partially deformed or aggregated, suggesting stress-induced responses, membrane disruption, or direct interaction with the peptide. Exposure to TRB produced similarly distinct alterations, including roughened and corrugated cell surfaces, indicative of membrane remodeling commonly observed under antifungal stress. Additionally, some cells exhibited shrinkage, potentially resulting from TRB-induced membrane permeabilization. Prominent cell aggregation and visible interfacial adhesion further pointed toward the initiation of biofilm-like architecture under TRB pressure. Cells subjected to the combination treatment displayed morphological hallmarks attributable to both γAFP^{B6GXZ8} and TRB exposure. These included irregular surfaces with multiple protrusions and the presence of intercellular filamentous connections, suggestive of biofilm-associated growth. SEM analysis demonstrated distinct morphological alterations in *A. fumigatus* conidia after antifungal treatments (**Fig. 7b**). Untreated spores maintained their characteristic smooth and rounded appearance, consistent with healthy, dormant conidia. Exposure to γAFP^{A0A2J5HZT4} alone resulted in moderate surface damage, indicative of membrane perturbation and partial structural compromise. The FLC-treated conidia showed minimal deformation, underscoring the reduced susceptibility of dormant conidia to azoles. Notably, the combination of γAFP^{A0A2J5HZT4} and FLC produced extensive morphological disruption, including collapsed and conidial structural integrity (**Fig. 7b**).

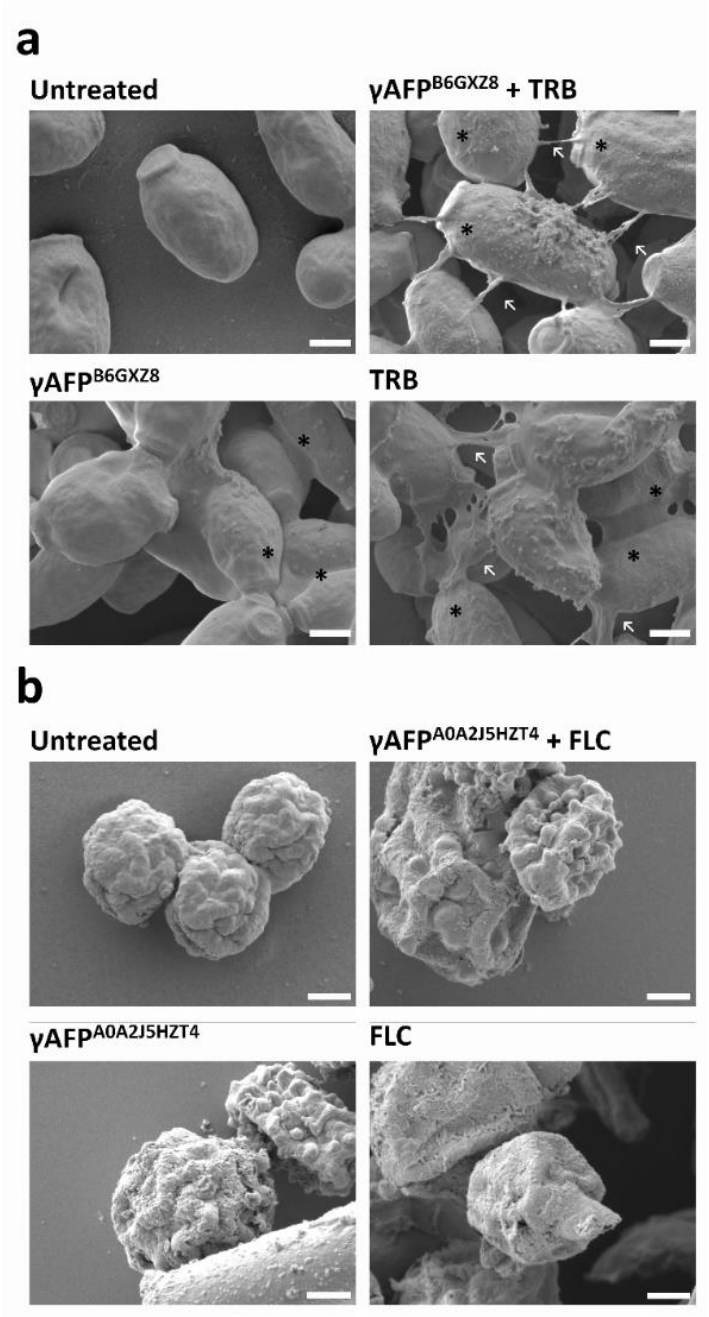

Figure 7: Scanning electron microscopy of *Candida albicans* SC5314 and *Aspergillus fumigatus* CBS 101355 treated with γAFP (γAFP^{B6GXZ8}, γAFP^{A0A2J5HZT4}), terbinafine (TRB), fluconazole (FLC), and their combination (AFP^{B6GXZ8} + TRB and γAFP^{A0A2J5HZT4} + FLC) (4×106 cells or conidia) in LCM, incubated at 30 °C for 16 hours with shaking at 160 rpm for *C. albicans*, and under static conditions for *A. fumigatus*). Asterisks indicate representative cells with membrane perturbation, while arrows the intercellular filamentous connections. Scale bars represent 1 μm

4.7. Hemolytic Activity and Toxicity of γAFP + Antifungal Drug Combinations

The therapeutic application of antimicrobial peptides is often limited by their potential to induce hemolysis in red blood cells (Abdelbaky et al., 2024). A well-established *G. mellonella* acute toxicity assay serves as a reliable model to assess the *in vivo* harmful effects of drug candidates (Ignasiak et al., 2017). To evaluate the hemolytic activity and toxic effects, γAFP^{B6GXZ8} + TRB and γAFP^{A0A2J5HZT4} + FLC combinations were tested *in vitro* on sheep blood agar plates and *in vivo* using *G. mellonella* larvae. None of the sole applications of γAFPs and antifungal drugs, nor their combinations, caused hemolysis or significantly reduced the survival of larvae (Fig. 8). These findings support the conclusion that γAFPs and their combinations with antifungal drugs can be safely utilized for therapeutic purposes.

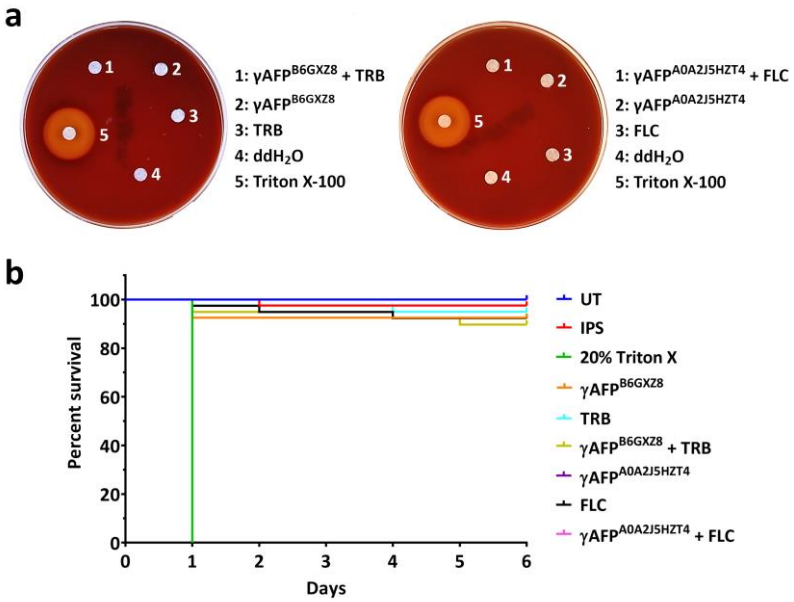

Figure 8: Hemolytic activity of γAFP^{B6GXZ8} (200 µg/mL), γAFP^{A0A2J5HZT4} (200 µg/mL), TRB (1 µg/mL), FLC (32 µg/mL), and their respective synergistic combinations (γAFP^{B6GXZ8} [200 µg/mL] + TRB [0.5 µg/mL], γAFP^{A0A2J5HZT4} [200 µg/mL] + FLC [32 µg/mL]) on Columbia blood agar plates after incubation for 24 h at 37°C (a). Triton X-100 [20% (v/v)] and ddH2O were used as the positive and negative lysis controls, respectively. Sterile filter paper disks (diameter: 6 mm) were impregnated with 10 µL of each solution and placed onto agar plates. Survival of *Galleria mellonella* larvae after injection with 20 µL IPS solution of peptides, antifungal drugs, and their combinations in concentration that used in hemolytic activity test (b). UT: untreated control, IPS: insect

physiological saline-treated control. *: $p \leq 0.05$ from both Log rank (Mantel-Cox) and Gehan-Breslow-Wilcoxon tests.

4.8. *In vivo* Therapeutic Potential of γAFP + Antifungal Drug Combinations

The in vivo efficacy of γAFP^{B6GXZ8}, TRB, and their combined treatment was assessed using a *G. mellonella* infection model with *C. albicans* SC5314 (**Fig. 9a**). Infection led to a marked decrease in larval survival relative to the IPS-treated control group ($p = 0.0001$). Comparable reductions in survival were observed when infected larvae received γAFP^{B6GXZ8} or TRB alone ($p = 0.0047$ and $p = 0.0336$, respectively). In contrast, no significant decline in survival was detected following combined treatment with γAFP^{B6GXZ8} and TRB ($p = 0.0533$). When compared with infected, untreated larvae, the combination therapy demonstrated a significantly stronger therapeutic effect than either monotherapy ($p = 0.024$ for γAFP^{B6GXZ8} and $p = 0.0015$ for TRB, compared with $p = 0.0004$). Overall, larval survival increased and was prolonged in the order γAFP^{B6GXZ8} < TRB < γAFP^{B6GXZ8} plus TRB ($p = 0.0245$, 0.001, and 0.0002, respectively), although differences among treatment groups were not statistically significant ($p > 0.05$; **Table S1**). Collectively, these results indicate that the combined administration of TRB and γAFP^{B6GXZ8} confers greater therapeutic benefit than either agent alone and may help prevent disease progression. The in vivo therapeutic activity of the $\gamma AFP^{A0A2J5HZT4}$–FLC combination against *A. fumigatus* CBS 101355 was assessed (**Fig. 9b**). Infection with A. fumigatus conidia caused a significant reduction in larval survival compared with the IPS-treated control group ($p < 0.0001$). Neither $\gamma AFP^{A0A2J5HZT4}$ nor FLC, administered alone ($p < 0.0001$) or in combination ($p = 0.0009$), fully prevented this infection-induced mortality. Relative to infected, untreated larvae, FLC monotherapy had no significant effect on survival ($p = 0.9503$). In contrast, treatment with $\gamma AFP^{A0A2J5HZT4}$ alone, as well as in combination with FLC, significantly prolonged ($p = 0.0375$ and $p = 0.0045$, respectively) and increased ($p = 0.0442$ and $p = 0.0063$, respectively) larval survival, with the combined treatment producing a more pronounced effect. Although no statistically significant difference was observed between $\gamma AFP^{A0A2J5HZT4}$ monotherapy and the combination treatment ($p > 0.05$), the combined regimen significantly outperformed FLC alone ($p = 0.0085$; **Table S2**). Overall, these results suggest that $\gamma AFP^{A0A2J5HZT4}$ exhibits moderate therapeutic efficacy as a single agent, which can be enhanced in the presence of FLC, leading to improved and prolonged larval survival.

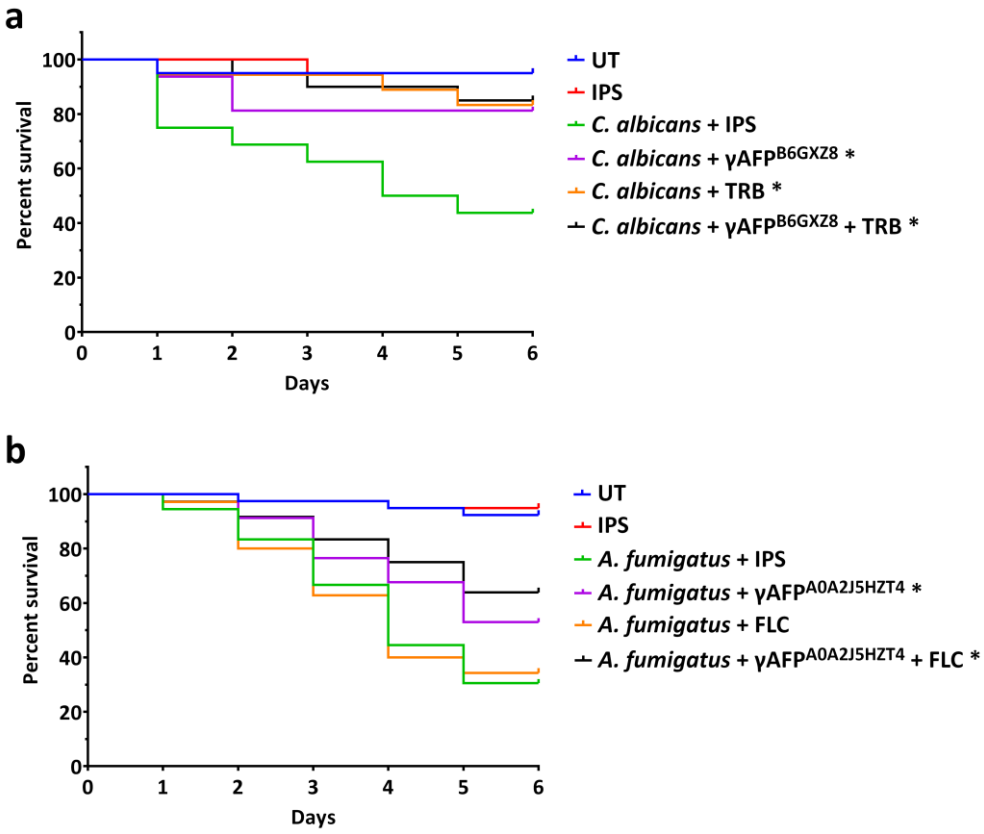

Figure 9: *In vivo* therapeutic potential of γAFP^{B6GXZ8}, γAFP^{A0A2J5HZT4}, terbinafine (TRB), fluconazole (FLC), AFP^{B6GXZ8} + TRB and γAFP^{A0A2J5HZT4} + FLC combinations in *Galleria mellonella* larval infection model. Larvae were infected with *Candida albicans* SC5314 then treated with, γAFP^{B6GXZ8}, TRB, or their synergistic combination (a). Larvae were infected with *Aspergillus fumigatus* CBS 101355 then treated with γAFP^{A0A2J5HZT4}, FLC or their synergistic combination (b). UT: not infected and untreated control, IPS: insect physiological saline-treated control, *C. albicans* + IPS: *C. albicans* infected and IPS-treated (untreated), *C. albicans* + γAFP^{B6GXZ8}: *C. albicans* infected and γAFP^{B6GXZ8}-treated (200 µg/mL), *C. albicans* + TRB: *C. albicans* infected and TRB-treated (1 µg/mL), *C. albicans* + γAFP^{B6GXZ8} + TRB: *C. albicans* infected and γAFP^{B6GXZ8} (200 µg/mL) - TRB (0.5 µg/mL) combination-treated and, *A. fumigatus* + IPS: *A. fumigatus* infected and IPS-treated (untreated), *A. fumigatus* + γAFP^{A0A2J5HZT4}: *A. fumigatus* infected and γAFP^{A0A2J5HZT4}-treated (200 µg/mL), *A. fumigatus* + FLC: *A. fumigatus* infected and FLC-treated (32 µg/mL), *A. fumigatus* + γAFP^{A0A2J5HZT4} + FLC: *A. fumigatus* infected and + γAFP^{A0A2J5HZT4} (200 µg/mL) – FLC (32 µg/mL) combination-treated groups. IPS: insect physiological saline-treated control. *: $p \leq 0.05$ from both Log rank (Mantel-Cox) and Gehan-Breslow-Wilcoxon tests in compared to the infected *(C. albicans* or *A. fumigatus* + IPS), not treated group.

5. DISCUSSION

The γ-core motif is a conserved structural feature present in numerous cysteine-rich antimicrobial peptides across a wide range of organisms, including plants, fungi, and animals. In higher organisms (i.e., plants and animals), it plays a pivotal role in the innate immune system, providing defense against microbial pathogens (Slezina et al., 2022a b; Andrés et al., 2024). Beyond its functional significance, the γ-core motif contributes to the structural stability of antimicrobial peptides by facilitating the formation of disulfide bonds between cysteine residues (Slezina et al., 2022b). However, current knowledge regarding the role of this motif in fungal AFPs remains limited and somewhat contradictory. Some studies suggest that the γ-core motif enhances the antifungal activity of *A. giganteus* AFP by interacting with the fungal cell membrane (Utesch et al., 2018), and that it can be modified through amino acid substitutions without significantly altering the overall structure of *P. chrysogenum* PAF (Sonderegger et al., 2018) and *P. expansum* PeAfpB (Giner-Llorca et al., 2023). Conversely, other research indicates that the γ-core region of *A. fischeri* NFAP2 does not mediate fungal membrane interaction or damage (Pavela et al., 2024), and that amino acid substitutions within this motif disrupt the overall structure of the protein, thereby reducing its antifungal efficacy (Váradi et al., 2023).

Given their functional significance, γ-core motifs of plant and animal antimicrobial peptides are being actively explored for their potential in designing novel synthetic peptide-based antimicrobial agents (Slezina et al., 2022a,b). The γ-core motifs of AFPs also represent promising candidates in this regard. However, most synthetic peptides encompassing the native γ-core region have exhibited no antifungal activity (Garrigues et al., 2017; Huber et al., 2020; Tóth et al., 2020a, 2022), suggesting that only highly hydrophilic and positively charged γ-core peptides demonstrate antifungal efficacy (Sonderegger et al., 2018; Huber et al., 2020). This conclusion is further supported by findings indicating that amino acid substitutions increasing the positive net charge of the native γ-core peptide can confer antifungal activity or enhance its pre-existing efficacy (Sonderegger et al., 2018; Huber et al., 2020; Tóth et al., 2020, 2020b, 2022). In the present study, we investigated a set of synthetic fungal γAFPs, exhibiting diverse physicochemical properties. Susceptibility test data suggest that not only positively charged/hydrophilic γAFPs (*i.e.*, γAFP^{B6GXZ8}, $\gamma AFPB^{6HWK0}$, $\gamma AFP^{A0A2J5HZT4}$) inhibit fungal growth (IP ≥ 40%), but also their neutral/hydrophilic or hydrophobic counterparts (*i.e.*, $\gamma AFP^{A0A0A2K0J0}$, $\gamma AFP2^{B6HMF2}$, γAFP^{A1DBL3}) and even negatively

charged/hydrophilic variants (*i.e.*, γAFP^{A0A401KDC0}, γAFP2^{A0A2I2FBQ1}) (**Tables 5** and **6**). Interestingly, some positively charged/hydrophilic γAFPs failed to exhibit growth inhibition in the tested fungal isolates (**Tables 5** and **6**). This suggests that antifungal activity is not solely determined by net positive charge and hydrophilicity, but rather by additional factors such as amino acid sequence, net charge-to-hydropathy ratio, and other physicochemical properties. Comprehensive and comparative bioinformatics analyses are required to uncover these determinants. However, it was observed that enhanced net positive charge increases the antifungal activity of γ-core peptides up to a certain threshold by promoting membrane binding or membrane permeabilization (van der Weerden et al., 2013; de Oliveira Mello et al., 2019), and in some cases, by facilitating access to intracellular targets as well (Li et al., 2021). However, achieving optimal biological activity requires a proper balance between positive charge and other structural properties, such as hydrophobicity and amphipathicity (Fernández de Ullivarri et al., 2020). The varying efficacies of γAFPs against different fungal species may be explained by species-specific differences in plasma membrane lipid composition, which are known to influence antifungal peptide-mediated cell killing (Kodedová et al. 2019).

In recent antifungal therapy, the combined application of different drug classes is increasingly considered to overcome resistance, improve therapeutic outcomes, broaden spectrum and activity, and minimize adverse effects (Zhu et al., 2023). Combinations of AFPs with conventional antifungal drugs have shown promise in achieving these objectives (de Ullivarri et al., 2020; Li et al., 2021). To the best of our knowledge, the efficacy of conventional antifungal drugs has not yet been investigated in the presence of synthetic fungal γAFPs. To address this gap, we examined the interactions between various fungal γAFPs and antifungal agents representing polyenes, allylamines, triazoles, and echinocandins against two prevalent human pathogenic fungi, *C. albicans* and *A. fumigatus* (**Table 5**). Among the tested peptides, only the positively charged and hydrophilic γAFP^{B6GXZ8} and γAFPA^{0A2J5HZT4} enhanced the efficacy of the allylamine TRB and the triazole FLC against *C. albicans* and *A. fumigatus*, respectively, demonstrating *in vitro* synergy **(Tables 7 and 9**). Both TRB and FLC exert their antifungal effects by disrupting fungal cell membrane synthesis - TRB inhibits squalene epoxidase, while FLC targets lanosterol 14-α-demethylase (Houšť et al., 2020). FACS and SEM analyses suggest that γAFP^{B6GXZ8} and γAFP^{A0A2J5HZT4} compromise cell membrane integrity and may induce membrane perturbation (**Table 9** and **Fig. 7**). This effect appeared to be amplified in the presence of TRB due to its membrane-weakening

properties (**Fig. 7**), potentially explaining the observed synergy (**Tables 6 and 8**). However, the results obtained from FACS and SEM analyses, and the *G. mellonella* infection model contradicted this assumption in the case of FLC, as this antifungal drug did not enhance the antifungal efficacy of γAFP^{A0A2J5HZT4} under these experimental conditions (**Fig. 7**, **Fig. 8b, Table 11**).

Our ECD spectroscopic analyses revealed that none of the investigated γAFPs undergo significant structural rearrangements in the presence of fungal cells or conidia, antifungal agents, or their combined exposure. Consistent with previous studies, it is well-established that short, linear AFPs retain a disordered conformation in solution, even in the presence of fungal cells (Tóth et al. 2020, van der Weerden et al., 2013). Although adopting an ordered structure may enhance the stability and specificity of AFPs, it is not necessarily a prerequisite for antifungal activity, particularly in the case of peptides that exert their effects through direct membrane disruption rather than receptor-mediated mechanisms (van der Weerden et al., 2013). This mode of action is characteristic of the modified peptides synthesized in this and in previous studies, which encompass the γ-core region (Tóth et al. 2020a; Váradi et al. 2024). SEM observations supported the membrane compromising effects of both γAFP^{B6GXZ8} and γAFP^{A0A2J5HZT4} (**Fig. 7**).

FACS analysis revealed that membrane disruption is the primary antifungal mechanism of the examined γAFPs indicated by the high proportion of PI-positive cells and conidia in comparison with the untreated samples (**Table 11**). This cell-killing efficacy was markedly enhanced in the presence of TRB, corroborating the *in vitro* synergy observed in the checkerboard titration assay (**Table 9**). In contrast, no such enhancement was detected with fluconazole (FLC), which appeared to compromise the antifungal activity of the γAFP (**Table 11**). This discrepancy may be attributable to differences in incubation conditions and the higher cell concentrations employed in the assay.

G. mellonella infection model experiments corroborated the FACS analysis findings, supporting the *in vitro* synergistic interactions between γAFP^{B6GXZ8} and TRB. This combination produced a markedly superior therapeutic effect compared to their individual administration (**Fig. 9a**). In contrast, no statistically significant difference was observed between the efficacy of γAFP^{A0A2J5HZT4} alone and its combination with FLC (**Fig. 9b**), which exclude the *in vivo* synergy between these two compounds. Notably, both the standalone and combined application of γAFP^{B6GXZ8} with TRB effectively prevented infection progression (**Fig. 9a**), whereas γAFP^{A0A2J5HZT4} and its combination with FLC merely extended larval survival without complete protection (**Fig. 9b**). These findings

underscore the potential of γAFPs as standalone antifungal agents or as adjuvants to enhance the efficacy of conventional therapeutics. It should be noted that TRB is not typically employed in the treatment of systemic fungal infections, though it demonstrates high efficacy in topical applications against superficial *Candida* infections (Ryder et al. 1998). Likewise, FLC, despite being a member of the azole class, is not generally used as a first-line treatment for aspergillosis due to its limited activity against *Aspergillus* species, which possess intrinsic or acquired resistance mechanisms (Leonardelli et al., 2016). Nonetheless, our results offer valuable insights into the possible role of AFP–conventional drug combinations in the management of systemic fungal infections and highlight their promise as topical antifungal formulations.

6. CONCLUSIONS

Numerous previous studies have demonstrated that synthetic peptides encompassing the evolutionarily conserved γ-core regions of antifungal proteins possess pronounced antifungal efficacy and may hold therapeutic potential. Based on the findings of this study, we propose that the antifungal efficacy of these peptides is determined by the magnitude of the net positive charge and hydrophilicity in addition to the charge-to-hydropathy ratio. A preliminary quadratic regression analysis revealed that the net charge critically influences the hydropathy profile of γAFPs (**Fig. 5**), which might contribute to their enhanced antifungal activity. The observed minimum GRAVY at a net charge of +4.2 suggests an optimal balance between electrostatic interactions and solubility, thereby facilitating membrane penetration and target engagement (**Fig. 5**). Among the peptides designed from the native γ-core regions of 19 Eurotiomycetes-derived antifungal proteins, only a subset fulfilled this criterion and exhibited notable antifungal activity (**Tables 5** and **6**), implying that in general, these regions do not directly determine antifungal potency but instead support structural stability and proper folding. Furthermore, our observations suggest that when these peptides are active against fungal pathogens, their antifungal mechanism likely involves plasma membrane disruption. Additionally, γAFPs can enhance the efficacy of antifungal agents targeting membrane biosynthesis, both *in vitro* and *in vivo*, supporting their applicability as standalone or adjuvant treatments for systemic and superficial fungal infections. However, definitive validation requires further *in vivo* studies employing relevant animal models.

7. SUMMARY

In recent years, fungal infections caused by human pathogens have risen sharply, largely due to the rapid emergence and spread of resistance to the antifungal agents commonly used in clinical practice. This escalating resistance, together with the appearance of fungal strains displaying diminished susceptibility to standard treatments, has become a major driver of the increasing global burden of fungal diseases. Currently, therapeutic options remain limited only to four principal classes of antifungal compounds (azoles, echinocandins, polyenes, and flucytosine) that are routinely used to manage invasive fungal infections. It has been noticed that heavy and prolonged use of triazole fungicides in agriculture has further intensified the resistance problem, expanding selective pressure across environmental reservoirs and ultimately contributing to treatment failures in clinical settings. As a result, the World Health Organization has emphasized the urgent need for antifungal therapies based on novel molecular scaffolds with mechanisms of action fundamentally different from existing drugs.

Among the promising candidates to address this challenge are synthetic peptides (γAFPs) derived from the evolutionarily conserved γ-core motifs of antifungal proteins (characterized by the GXC-X_{3-9}-C signature) found in Eurotiomycetes. In this motif, "X" denotes any amino acid, serving as a key structural element necessary for antifungal function.

Synthetic peptides engineered around this γ-core region have shown the capacity to disrupt essential intracellular processes, elevate intracellular ATP levels, and ultimately trigger fungal cell death. Importantly, γ-core motif–based peptides originating from plant and animal AFPs often display broad-spectrum antifungal effects while maintaining low toxicity toward mammalian cells, positioning them as attractive leads for next-generation antifungal therapeutics.

Despite their potential, significant gaps remain in our understanding of the physicochemical determinants that govern the antifungal potency of γAFPs, as well as their therapeutic performance *in vivo*, either as monotherapies or in combination with established antifungal agents. To bridge these knowledge gaps, the present study focused on a systematic evaluation of the antifungal properties and potential clinical applications of 19 peptide derivatives designed from γ-core motifs of AFPs derived from Eurotiomycetes. The specific aims were to:

- To design a set of synthetic peptides that integrate the γ-core motifs found in antifungal proteins of Eurotiomycetes (γAFPs)
- Assess the *in vitro* antifungal activity of γAFPs against a diverse panel of clinically relevant human fungal pathogens and agriculturally important phytopathogens.
- Examine the in vitro interaction patterns, synergistic, additive, or antagonistic, between the most active γAFPs and conventional antifungal drugs commonly used against human pathogenic fungi.
- Determine the *in vitro* antifungal potency of leading γAFPs, both as standalone agents and in combination with conventional antifungals.
- Characterize the structural behaviour of γAFPs in the presence of antifungal drugs, fungal cells, and conidia to better understand structure-function relationships.
- Evaluate potential toxicological effects of leading γAFPs and their drug combinations in an animal model.
- Assess therapeutic efficacy *in vivo*, focusing on fungal infection outcomes and survival in the same animal system.

Our findings demonstrate that the antifungal activity of γAFPs *in vitro* is governed not merely by overall net positive charge or hydrophilicity; instead, it is heavily influenced by the net charge-to-hydropathy ratio. This ratio strongly influences peptide fungus interactions and helps to explain functional differences among γAFP derivatives. For the most active peptides, we confirmed that their mechanism of action involves plasma membrane disruption and that they can act synergistically with antifungal agents targeting membrane biosynthesis. Using the *Galleria mellonella* larval model, we demonstrated that these potent γAFPs can prevent *Candida albicans* infection or extend survival in larvae infected with *Aspergillus fumigatus*. Notably, the synergistic effects observed in vitro were also confirmed *in vivo*.

Using the *G. mellonella* infection model, we further confirmed that the most active γAFPs provide meaningful protection against fungal pathogens. Specifically, these peptides prevented infection by *C. albicans* or significantly prolonged survival in larvae challenged with *A. fumigatus*. Notably, the synergistic interactions observed during *in vitro* testing were also reproduced *in vivo*, offering robust evidence that γAFPs can enhance the performance of conventional antifungals under physiological conditions.

Taken together, these findings underscore the therapeutic potential of γAFPs as both standalone antifungal agents and as adjuvants that improve the efficacy of existing drugs for systemic and superficial fungal infections. The identification of two leading γAFP candidates, characterized by strong antifungal activity, low toxicity, and consistent synergistic effects with conventional antifungal drugs, provides a compelling foundation for further development of peptide-based antifungal therapies. These advances contribute significantly to the broader effort to expand the antifungal drug pipeline and offer new strategies for combating the growing threat posed by resistant fungal pathogens.

8. ÖSSZEFOGLALÁS

Az elmúlt években a humán patogén gombák által okozott fertőzések száma meredeken emelkedett, elsősorban a klinikai gyakorlatban rutinszerűen alkalmazott gombaellenes szerekre kialakuló és gyorsan terjedő rezisztencia miatt. Ez a fokozódó rezisztencia, valamint az olyan gombatörzsek megjelenése, amelyek a standard terápiákkal szemben csökkent érzékenységet mutatnak – napjainkra a gombás megbetegedések globális terhének egyik fő hajtóerejévé vált. Jelenleg mindössze négy fő gombaellenes gyógyszerosztály (azolok, echinokandinok, polién makrolidok és flucitozin) áll rendelkezésre az invazív gombafertőzések kezelésére. Tovább súlyosbítja a problémát, hogy a mezőgazdaságban alkalmazott triazol fungicidek intenzív és tartós használata növeli a szelekciós nyomást a környezetben, ami végső soron a klinikai kezelések sikertelenségéhez is hozzájárul. Ennek következtében az Egészségügyi Világszervezet hangsúlyozza, hogy sürgősen szükség van olyan új antifungális terápiákra, amelyek teljesen új molekuláris vázakon alapulnak, és hatásmechanizmusuk alapvetően eltér a jelenleg alkalmazott szerekétől.

A kihívás megoldására ígéretes jelöltcsoportként tűnnek fel a szintetikus peptidek (γAFP-k), amelyek az Eurotiomycetes osztályba tartozó antifungális fehérjék evolúciósan konzervált γ-mag (γ-core) motívumaiból származtathatók (amelyet a GXC-$X_{3–9}$-C jelsor jellemez). Ebben a motívumban az „X” bármely aminosavat jelöl, és olyan szerkezeti elemet képez, amely elengedhetetlen az antifungális aktivitáshoz.

A γ-core régióra tervezett szintetikus peptidek képesek megzavarni létfontosságú intracelluláris folyamatokat, növelni az intracelluláris ATP-szintet, és végső soron gombasejt-elhalást indukálni. Különösen fontos, hogy a növényi és állati AFP-k γ-core motívumából származó peptidek gyakran széles spektrumú antifungális hatást fejtenek ki, miközben alacsony toxicitást mutatnak emlőssejteken, így ígéretes vezető molekulákká válnak a következő generációs antifungális terápiák fejlesztésében.

Potenciáljuk ellenére még mindig jelentős tudásbeli hiányosságok vannak azzal kapcsolatban, hogy mely fizikai-kémiai tényezők határozzák meg a γAFP-k antifungális hatékonyságát, illetve hogyan teljesítenek ezek a peptidek *in vivo* önmagukban vagy kombinációban a jelenleg alkalmazott antifungális szerekkel. Ezeknek a hiányosságoknak a csökkentésére jelen tanulmányunk 19, Eurotiomycetes eredetű AFP-k γ-core motívumaiból tervezett peptid derivátum antifungális tulajdonságainak és

potenciális klinikai alkalmazásának szisztematikus vizsgálatára fókuszált. Konkrét céljaink a következők voltak:

- Az Eurotiomycetes antifungális fehérjéiben található γ-core motívumokat (γAFP-ket) integráló szintetikus peptidsorozat megtervezése
- *In vitro* antifungális aktivitás vizsgálata klinikailag releváns humán kórokozó gombák és mezőgazdasági jelentőségű fitopatogének széles paneljén
- A legaktívabb γAFP-k és a klinikumban használatos antifungális gyógyszerek közötti *in vitro* kölcsönhatások (szinergizmus, additivitás, antagonizmus) feltérképezése
- A vezető γAFP-jelöltek *in vitro* hatékonyságának meghatározása önmagukban és konvencionális antifungális szerekkel kombinálva
- A γAFP-k szerkezeti viselkedésének jellemzése gombaellenes gyógyszerek, gombasejtek és konídiumok jelenlétében a szerkezet–funkció kapcsolatok megértése céljából
- A vezető γAFP-k és kombinációik potenciális toxikológiai hatásainak értékelése állatmodellben
- A terápiás hatékonyság *in vivo* vizsgálata, különös tekintettel a fertőzéskimenetelre és a túlélésre ugyanebben az állatrendszerben

Vizsgálataink azt mutatják, hogy a γAFP-k in vitro antifungális aktivitását nem pusztán a nettó pozitív töltés vagy a hidrofilitás határozza meg; sokkal inkább a nettó töltés és a hidropátia aránya befolyásolja. Ez az arány döntően formálja a peptid–gomba kölcsönhatásokat, és magyarázza a különböző γAFP derivátumok hatásbeli különbségeit. A legaktívabb peptidek esetében igazoltuk, hogy hatásmechanizmusuk a plazmamembrán károsítását foglalja magában, és hogy szinergizmust képesek kialakítani a membrán-bioszintézist gátló gombaellenes szerekkel.

A *Galleria mellonella* lárvamodellt alkalmazva kimutattuk, hogy ezek az erőteljes γAFP-k képesek megelőzni a *Candida albicans* fertőzést, illetve növelni az *Aspergillus fumigatus*-szal fertőzött lárvák túlélését. Figyelemre méltó módon az *in vitro* szinergista hatások *in vivo* is megerősítést nyertek.

A *G. mellon*ella fertőzésmodell további bizonyítékkal szolgált arra, hogy a legaktívabb γAFP-k érdemi védelmet nyújtanak gombapatogénekkel szemben. Konkrétan ezek a peptidek vagy teljesen megelőzték a *C. albicans* fertőzést, vagy jelentősen meghosszabbították az *A. fumigatus* által kihívott lárvák túlélését. Fontos megfigyelés,

hogy az in vitro azonosított szinergista kölcsönhatások in vivo is visszaköszöntek, erős bizonyítékot szolgáltatva arra, hogy a γAFP-k képesek fokozni a konvencionális antifungális szerek hatékonyságát fiziológiás körülmények között is.

Összességében eredményeink kiemelik a γAFP-k terápiás potenciálját mind önmagukban alkalmazható antifungális ágensként, mind pedig olyan adjuvánsként, amely javítja a meglévő gyógyszerek hatásosságát szisztémás és felszíni gombafertőzések esetén. A két vezető γAFP jelölt azonosítása – amelyek erős antifungális aktivitással, alacsony toxicitással és konzisztens szinergizmussal rendelkeznek a konvencionális antifungális szerekkel – meggyőző alapot teremt a peptidalapú gombaellenes terápiák további fejlesztéséhez. E fejlemények jelentősen hozzájárulnak az antifungális hatóanyag-fejlesztési pipeline bővítéséhez, és új stratégiákat kínálnak a rezisztens gombapatogének jelentette egyre növekvő fenyegetés elleni küzdelemben.

9. ACKNOWLEDGEMENTS

I would like to take this opportunity to express my heartfelt gratitude to all those who played a role in the successful completion of my PhD journey.

First and foremost, I am profoundly thankful to my supervisor **Dr. László Galgóczi**, for his exceptional guidance, for providing me with the freedom to develop independently, and for his steadfast patience as I gradually progressed in hand zone analysis. His commitment and support were instrumental in bringing this work to completion.

I am also grateful to my co-supervisor **Dr. Attila Borics**, for his expert direction and insights, particularly during the ECD experiments.

I am grateful to **Dr. Gábor Rákhely**, former Head of the Department of Biotechnology, who passed away in 2023, for giving me the opportunity to begin my PhD work under his leadership. I would also like to thank **Prof. Dr. Csaba Vágvölgyi**, who took over the responsibilities of department head as acting director and ensured the smooth continuation of my work until 2024, when the Department of Biotechnology and Microbiology was established under the leadership of **Prof. Dr. Tamás Papp**. I am equally thankful to him for enabling me to complete my PhD studies there.

My sincere thanks go to **Liliána Tóth**, **Kinga Dán**, **Richárd Merber**, and **Rebeka Papp** for their meaningful contributions and ongoing support throughout the course of my research.

I am truly grateful to **Gábor Bende** for his support and for patiently guiding me through experimental techniques that were completely unfamiliar to me, always offering his time and encouragement.

I would also like to thank **Csaba Papp, Györgyi Váradi**, and **Attila Farkas** for their assistance with Fluorescence-Activated Cell Sorting, Peptide Synthesis, and Scanning Electron Microscopy analysis, respectively.

Special thanks to the administration and staff of the Department of Microbiology and Biotechnology for their continuous support.

I am also grateful to the **Tempus Foundation** of Hungary for awarding me the Stipendium Hungaricum Scholarship, which made this PhD program possible.

I extend my sincere appreciation to the **Government of Rwanda** for granting me a four-year study leave to pursue this PhD program.

Lastly, I dedicate this work to Almighty God, my wife and my son. Their unwavering love, encouragement and sacrifices, particularly in coping with my prolonged absence, have been the foundation of this achievement.

The experimental work of the present PhD thesis was financed by the Hungarian National Research, Development and Innovation Office - NKFIH, FK 134343 and K 146131 projects.

10. REFERENCES

Abdelbaky I, Elhakeem M, Tayara H, Badr E, Abdul Salam M. Enhanced prediction of hemolytic activity in antimicrobial peptides using deep learning-based sequence analysis. BMC Bioinformatics. 2024;25:368. doi:10.1186/s12859-024-05983-4.

Adler-Moore J, Proffitt RT. AmBisome: liposomal formulation, structure, mechanism of action and pre-clinical experience. J Antimicrob Chemother. 2002;49(Suppl 1):21–30. doi:10.1093/jac/49.suppl_1.21.

Ahmad KM, Ishchuk OP, Hellborg L, Jørgensen G, Skvarc M, Stenderup J, Jørck-Ramberg D, Polakova S, Piškur J. Small chromosomes among Danish *Candida glabrata* isolates originated through different mechanisms. Antonie Van Leeuwenhoek. 2013;104(1):111–122. doi:10.1007/s10482-013-9931-3.

Aimbatov IS. An exciting time for antifungal therapy. Lancet Infect Dis. 2023;23(7):763. doi:10.1016/S1473-3099(23)00380-8.

Almagro Armenteros JJ, Tsirigos KD, Sønderby CK, Petersen TN, Winther O, Brunak S, von Heijne G, Nielsen H. SignalP 5.0 improves signal peptide predictions using deep neural networks. Nat Biotechnol. 2019;37(4):420–423. doi:10.1038/s41587-019-0036-z.

Alsuhibani AA, Alobaid NA, Alahmadi MH, Alqannas JS, Alfreaj WS, Albadrani RF, Alamer KA, Almogbel YS, Alhomaidan A, Guo JJ. Antifungal agents' trends of utilization, spending, and prices in the US Medicaid programs: 2009–2023. Antibiotics (Basel). 2025;14(5):518. doi:10.3390/antibiotics14050518.

Ainaga Andrés MT, Fierro P, Lobo Antuña V, Fierro JF. The antimicrobial activity of human defensins at physiological non-permeabilizing concentrations is caused by the inhibition of the plasma membrane H+-ATPases. Int J Mol Sci. 2024;25(13):7335. doi:10.3390/ijms25137335.

Barbosa MS, Souza BS, Sales ACS, Sousa JDL, Silva FDS, Mendes MGA, Costa KRL, Oliveira TM, Daboit TC, Oliveira JS. Antifungal proteins from plant latex. Curr Protein Pept Sci. 2020;21(5):497–506. doi:10.2174/1389203720666191119101756.

Benedict K, Jackson BR, Chiller T, Beer KD. Estimation of direct healthcare costs of fungal diseases in the United States. Clin Infect Dis. 2019;68(11):1791–1797. doi:10.1093/cid/ciy776.

Bravo A., Likitvivatanavong S, Gill S S, & Soberón M. Bacillus thuringiensis: A story of a successful bioinsecticide. Insect biochemistry and molecular biology.2011; 41(7), 423–431. https://doi.org/10.1016/j.ibmb.2011.02.006

Boman HG. Antibacterial peptides: basic facts and emerging concepts. J Intern Med. 2003;254(3):197–215. doi:10.1046/j.1365-2796.2003.01228.x.

Bondaryk M, Staniszewska M, Zielińska P, Urbańczyk-Lipkowska Z. Natural antimicrobial peptides as inspiration for design of a new generation antifungal compounds. J Fungi (Basel). 2017;3(3):46. doi:10.3390/jof3030046.

Bongomin F, Gago S, Oladele R, Denning D. Global and multi-national prevalence of fungal diseases—estimate precision. J Fungi (Basel). 2017;3(4):57. doi:10.3390/jof3040057.

Buda De Cesare G, Cristy SA, Garsin DA, Lorenz MC. Antimicrobial peptides: a new frontier in antifungal therapy. mBio. 2020;11(6):e02123-20. doi:10.1128/mBio.02123-20.

Bugeda A, Garrigues S, Gandía M, Manzanares P, Marcos JF, Coca M. The antifungal protein AfpB induces regulated cell death in its parental fungus *Penicillium digitatum*. mSphere. 2020;5(4):e00595-20. doi:10.1128/mSphere.00595-20.

Campoy S, Adrio JL. Antifungals. Biochem Pharmacol. 2016;133:86–96. doi:10.1016/j.bcp.2016.11.019.

Cappelletty D, Eiselstein-McKitrick K. The echinocandins. Pharmacotherapy. 2007;27(3):369–388. doi:10.1592/phco.27.3.369.

Casadevall A. Fungal diseases in the 21st century: the near and far horizons. Pathog Immun. 2018;3(2):183–196. doi:10.20411/pai.v3i2.249.

Chang Y, Yu S, Heitman J, Wellington M, Chen Y. New facets of antifungal therapy. Virulence. 2017;8(2):222–236. doi:10.1080/21505594.2016.1257457.

Chagri S, Maxeiner K, Förch L, Link J, Roth P, Meyer R, Fetzer J, Kaltbeitzel A, Lieberwirth I, Landfester K, Wagner M, Ng DYW, Weil T. Intracellular formation of synthetic peptide nanostructures causes mitochondrial disruption and cell death in tumor spheroids. ChemRxiv. 2024. doi:10.26434/chemrxiv-2024-xkxpb.

Chen SC, Slavin MA, Sorrell TC. Echinocandin antifungal drugs in fungal infections: a comparison. Drugs. 2011;71(1):11–41. doi:10.2165/11585270-000000000-00000.

The UniProt Consortium, Bateman A, Martin M, Orchard S, Magrane M, Adesina A, Ahmad S, et al. UniProt: the Universal Protein Knowledgebase in 2025. Nucleic Acids Res. 2025;53(D1):D609–D617. doi:10.1093/nar/gkae1010.

Costa-Orlandi C, Sardi J, Pitangui N, de Oliveira H, Scorzoni L, Galeane M, Medina-Alarcón K, Melo W, Marcelino M, Braz J, Fusco-Almeida A, Mendes-Giannini M.

Fungal biofilms and polymicrobial diseases. J Fungi (Basel). 2017;3(2):22. doi:10.3390/jof3020022.

Cowen LE, Sanglard D, Howard SJ, Rogers PD, Perlin DS. Mechanisms of antifungal drug resistance. Cold Spring Harb Perspect Med. 2015;5(7):a019752. doi:10.1101/cshperspect.a019752.

Danhier F, Ansorena E, Silva JM, Coco R, Le Breton A, Préat V. PLGA-based nanoparticles: an overview of biomedical applications. J Control Release. 2012;161(2):505–522. doi:10.1016/j.jconrel.2012.01.043.

Datta K., Rhee P., Byrnes E., Garcia-Effron G., Perlin, D S., Staab, J F., & Marr K A. Isavuconazole Activity against Aspergillus lentulus, Neosartorya udagawae, and Cryptococcus gattii, Emerging Fungal Pathogens with Reduced Azole Susceptibility. Journal of Clinical Microbiology.2013;51(9),3090–3093. https://doi.org/10.1128/JCM.01190-13

Denning DW. Global incidence and mortality of severe fungal disease. Lancet Infect Dis. 2024;24(7):e428–e438. doi:10.1016/S1473-3099(23)00692-8.

Denning DW. The ambitious '95-95 by 2025' roadmap for the diagnosis and management of fungal diseases. Thorax. 2015;70(7):613–614. doi:10.1136/thoraxjnl-2015-207305.

Fisher M C & Denning, D W. The WHO fungal priority pathogens list as a game-changer. Nature Reviews Microbiology.2023;21(4), 211-212. https://doi.org/10.1038/s41579-023-00861-x

Duvaud S, Gabella C, Lisacek F, Stockinger H, Ioannidis V, Durinx C. Expasy, the Swiss Bioinformatics Resource Portal, as designed by its users. Nucleic Acids Res. 2021;49(W1):W216–W227. doi:10.1093/nar/gkab225.

Érica de Oliveira Mello É, Taveira GB, de Oliveira Carvalho A, Gomes VM. Improved smallest peptides based on positive charge increase of the γ-core motif from PνD1 and their mechanism of action against Candida species. Int J Nanomedicine. 2019;14:407–420. doi:10.2147/IJN.S187957.

Emri T, Majoros L, Tóth V, Pócsi I. Echinocandins: production and applications. Appl Microbiol Biotechnol. 2013;97(8):3267–3284. doi:10.1007/s00253-013-4761-9.

Fernández de Ullivarri M, Arbulu S, Garcia-Gutierrez E, Cotter PD. Antifungal peptides as therapeutic agents. Front Cell Infect Microbiol. 2020;10:105. doi:10.3389/fcimb.2020.00105.

Fisher MC, Denning DW. The WHO fungal priority pathogens list as a game-changer. Nat Rev Microbiol. 2023;21(4):211–212. doi:10.1038/s41579-023-00861-x.

Fisher MC, Gurr SJ, Cuomo CA, Blehert DS, Jin H, Stukenbrock EH, Stajich JE, Kahmann R, Boone C, Denning DW, Gow NAR, Klein BS, Kronstad JW, Sheppard DC, Taylor JW, Wright GD, Heitman J, Casadevall A, Cowen LE. Threats posed by the fungal kingdom to humans, wildlife, and agriculture. mBio. 2020;11(3):e00449-20. doi:10.1128/mBio.00449-20.

Forche A, Abbey D, Pisithkul T, Weinzierl MA, Ringstrom T, Bruck D, Petersen K, Berman J. Stress alters rates and types of loss of heterozygosity in *Candida albicans*. mBio. 2011;2(4):e00129-11. doi:10.1128/mBio.00129-11.

Forsberg K, Woodworth K, Walters M, Berkow EL, Jackson B, Chiller T, Vallabhaneni S. *Candida auris*: the recent emergence of a multidrug-resistant fungal pathogen. Med Mycol. 2019;57(1):1–12. doi:10.1093/mmy/myy054.

Fuentefria A, Pippi B, Lana DD, Donato K, de Andrade S. Antifungals discovery: an insight into new strategies to combat antifungal resistance. Lett Appl Microbiol. 2017;66(1):2–13. doi:10.1111/lam.12820.

Seagle EE, Williams SL, Chiller TM. Recent trends in the epidemiology of fungal infections. Infect Dis Clin North Am. 2021;35(2):237–260. doi:10.1016/j.idc.2021.03.001.

Gandía M, Garrigues S, Bolós B, Manzanares P, Marcos JF. The myosin motor domain-containing chitin synthases are involved in cell wall integrity and sensitivity to antifungal proteins in *Penicillium digitatum*. Front Microbiol. 2019;10:2470. doi:10.3389/fmicb.2019.02400.

Garrigues S, Gandía M, Borics A, Marx F, Manzanares P, Marcos JF. Mapping and identification of antifungal peptides in the putative antifungal protein AfpB from the filamentous fungus *Penicillium digitatum*. Front Microbiol. 2017;8:592. doi:10.3389/fmicb.2017.00592.

Georgiev V. Membrane transporters and antifungal drug resistance. Curr Drug Targets. 2000;1(3):261–284. doi:10.2174/1389450003349209.

Giner-Llorca M, Gallego del Sol F, Marcos JF, Marina A, Manzanares P. Rationally designed antifungal protein chimeras reveal new insights into structure-activity relationship. Int J Biol Macromol. 2023;225:135–148. doi:10.1016/j.ijbiomac.2022.11.280.

Giner-Llorca M, Locascio A, Alonso Del Real J, Marcos JF, Manzanares P. Novel findings about the mode of action of the antifungal protein PeAfpA against *Saccharomyces cerevisiae*. Appl Microbiol Biotechnol. 2023;107(4):1491–1506. doi:10.1007/s00253-023-12749-0.

Goy RC, Assis OBG. A review of the antimicrobial activity of chitosan. Polímeros. 2009;19(3):241–247. doi:10.1590/S0104-14282009000300013.

Gray KC, Palacios DS, Dailey I, Endo MM, Uno BE, Wilcock BC, Burke MD. Amphotericin primarily kills yeast by simply binding ergosterol. Proc Natl Acad Sci U S A. 2012;109(7):2234–2239. doi:10.1073/pnas.1117280109.

Guevara-Lora I, Bras G, Juszczak M, Karkowska-Kuleta J, Górecki T, Manrique-Moreno M, Dymek J, Pyza E, Kozik A, Rapala-Kozik M. Cecropin D-derived synthetic peptides in the fight against *Candida albicans* cell filamentation and biofilm formation. Front Microbiol. 2022;13:1045984. doi:10.3389/fmicb.2022.1045984.

Guo-xiang C. Structure and function of lactoferrin. Food Drug. 2006;6(12). Available at: https://en.cnki.com.cn/Article_en/CJFDTOTAL-SDPK200612008.htm

Ongena M, Jacques P. Bacillus lipopeptides: versatile weapons for plant disease biocontrol. Trends Microbiol. 2008;16(3):115–125. doi:10.1016/j.tim.2007.12.009.

Hagen S, Marx F, Ram AFJ, Meyer V. The antifungal protein AFP from *Aspergillus giganteus* inhibits chitin synthesis in sensitive fungi. Appl Environ Microbiol. 2007;73(7):2128–2134. doi:10.1128/AEM.02497-06.

Hall TA. BioEdit: a user-friendly biological sequence alignment editor and analysis program for Windows 95/98/NT. Nucleic Acids Symp Ser. 1999;41:95–98.

Hamill RJ. Amphotericin B formulations: a comparative review of efficacy and toxicity. Drugs. 2013;73(9):919–934. doi:10.1007/s40265-013-0069-4.

Hegedűs N, Leiter É, Kovács B, Tomori V, Kwon J, Emri T, Marx F, Batta G, Csernoch L, Haas H, Yu H, Pócsi I. The small molecular mass antifungal protein of *Penicillium chrysogenum* – a mechanism of action-oriented review. J Basic Microbiol. 2011;51(6):561–571. doi:10.1002/jobm.201100041.

Hermanova V, Bárta J, Čurn V. Antifungalni proteiny rostlin: klasifikace, charakteristika, možnosti využití. Chem Listy. 2006;100(7):495–500.

Hossain CM, Ryan LK, Gera M, Choudhuri S, Lyle N, Ali KA, Diamond G. Antifungals and drug resistance. Encyclopedia. 2022;2(4):1722–1737. doi:10.3390/encyclopedia2040118.

Houšť J, Spížek J, Havlíček V. Antifungal drugs. Metabolites. 2020;10(3):106. doi:10.3390/metabo10030106.

Holzknecht J, Kühbacher A, Papp C, Farkas A, Váradi G, Marcos JF, Manzanares P, Tóth G, Galgóczy L, Marx F. The *Penicillium chrysogenum* Q176 antimicrobial protein PAFC effectively inhibits the growth of the opportunistic human pathogen Candida albicans. J Fungi (Basel). 2020;6(3):141. doi:10.3390/jof6030141.

Ignasiak K, Maxwell A. *Galleria mellonella* (greater wax moth) larvae as a model for antibiotic susceptibility testing and acute toxicity trials. BMC Res Notes. 2017;10(1):428. doi:10.1186/s13104-017-2757-8.

Iliopoulos G, Moellering RC Jr. Antimicrobial combinations. In: Lorian V, editor. Antibiotics in Laboratory Medicine. Baltimore: Williams & Wilkins; 1996. p. 330–396.

Jackson A, Nussbaum JC, Phulusa J, Namarika D, Chikasema M, Kanyemba C, Jarvis JN, Jaffar S, Hosseinipour MC, van der Horst C, Harrison TS. A phase II randomized controlled trial adding oral flucytosine to high-dose fluconazole, with short-course amphotericin B, for cryptococcal meningitis. AIDS. 2012;26(11):1363–1370. doi:10.1097/QAD.0b013e328354b419.

Johnson MD, Perfect JR. Caspofungin: first approved agent in a new class of antifungals. Expert Opin Pharmacother. 2003;4(5):807–823. doi:10.1517/14656566.4.5.807.

Jumper J, Evans R, Pritzel A, Green T, Figurnov M, Ronneberger O, Tunyasuvunakool K, Bates R, Žídek A, Potapenko A, et al. Highly accurate protein structure prediction with AlphaFold. Nature. 2021;596(7873):583–589. doi:10.1038/s41586-021-03819-2.

Juvvadi PR, Lamoth F, Steinbach WJ. Calcineurin as a multifunctional regulator: unraveling novel functions in fungal stress responses, hyphal growth, drug resistance, and pathogenesis. Fungal Biol Rev. 2014;28(2–3):56–69. doi:10.1016/j.fbr.2014.02.004.

Kainz K, Bauer MA, Madeo F, Carmona-Gutierrez D. Fungal infections in humans: the silent crisis. Microb Cell. 2020;7(6):143–145. doi:10.15698/mic2020.06.718.

Kaiserer L, Oberparleiter C, Weiler-Görz R, Burgstaller W, Marx F. Characterization of the *Penicillium chrysogenum* antifungal protein PAF. Arch Microbiol. 2003;180(3):204–210. doi:10.1007/s00203-003-0584-8.

Kakadia PG, Conway BR. Solid lipid nanoparticles: a potential approach for dermal drug delivery. Am J Pharmacol Sci. 2014;2(5A):1–7.

Khanna D, Bharti S. Luliconazole for the treatment of fungal infections: an evidence-based review. Core Evid. 2014;9:113–124. doi:10.2147/CE.S49629.

Kneale M, Bartholomew JS, Davies E, Denning DW. Global access to antifungal therapy and its variable cost. J Antimicrob Chemother. 2016;71(12):3599–3606. doi:10.1093/jac/dkw325.

Kodedová M, Valachovič M, Csáky Z, Sychrová H. Variations in yeast plasma-membrane lipid composition affect killing activity of three families of insect antifungal peptides. Cell Microbiol. 2019;21(12):e13093. doi:10.1111/cmi.13093.

Kumar P, Mishra S, Singh S. Advanced acuity in microbial biofilm genesis, development, associated clinical infections and control. J Des Anti-infectieux. 2017;19(1):20–31. doi:10.1016/j.antinf.2017.01.002.

Lamiable A, Thévenet P, Rey J, Vavrusa M, Derreumaux P, Tufféry P. PEP-FOLD3: faster *de novo* structure prediction for linear peptides in solution and in complex. Nucleic Acids Res. 2016;44(W1):W449–W454. doi:10.1093/nar/gkw329.

Lara HH, Ayala-Nuñez NV, Ixtepan-Turrent L, Rodriguez-Padilla C. Mode of antiviral action of silver nanoparticles against HIV-1. J Nanobiotechnology. 2010;8:1. doi:10.1186/1477-3155-8-1.

Leonardelli F, Macedo D, Dudiuk C, Cabeza MS, Gamarra S, Garcia-Effron G. *Aspergillus fumigatus* intrinsic fluconazole resistance is due to the naturally occurring T301I substitution in Cyp51Ap. Antimicrob Agents Chemother. 2016;60(9):5420–5426. doi:10.1128/AAC.00905-16.

Li T, Li L, Du F, Sun L, Shi J, Long M, Chen Z. Activity and mechanism of action of antifungal peptides from microorganisms: a review. Molecules. 2021;26(11):3438. doi:10.3390/molecules26113438.

Ilahverdiyev AM, Abamor ES, Bagirova M, Ustundag CB, Kaya C, Kaya F, et al. Antileishmanial effect of silver nanoparticles and their enhanced antiparasitic activity under ultraviolet light. Int J Nanomedicine. 2011;6:2705–2714. doi:10.2147/IJN.S23883.

Lu J, Dang MQ, Samuel E. Side effects of antifungals. Side Effects Drugs Annu. 2023;45:273–278. doi:10.1016/bs.seda.2023.08.012.

Maiga AW, Deppen S, Scaffidi BK, Baddley J, Aldrich MC, Dittus RS, Grogan EL. Mapping *Histoplasma capsulatum* exposure, United States. Emerg Infect Dis. 2018;24(10):1835–1839. doi:10.3201/eid2410.180032.

Mayr A, Lass-Flörl C. Epidemiology and antifungal resistance in invasive aspergillosis according to primary disease – review of the literature. Eur J Med Res. 2011;16(4):153. doi:10.1186/2047-783X-16-4-153.

Miles AJ, Ramalli SG, Wallace BA. DichroWeb, a website for calculating protein secondary structure from circular dichroism spectroscopic data. Protein Sci. 2022;31(1):37–46. doi:10.1002/pro.4153.

Moreno AB, Del Pozo AM, Borja M, Segundo BS. Activity of the antifungal protein from *Aspergillus giganteus* against *Botrytis cinerea*. Phytopathology. 2003;93(11):1344–1353. doi:10.1094/PHYTO.2003.93.11.1344.

Naik SS, Kashyap D, Deep J, Darwish S, Cross J, Mansoor E, Garg VK, Honnavar P. Utilizing next-generation sequencing: advancements in the diagnosis of fungal infections. Diagnostics (Basel). 2024;14(15):1664. doi:10.3390/diagnostics14151664.

Ng TB, Cheung RCF, Wong JH. Recent progress in research on plant antifungal proteins: a review. In: Razzaghi-Abyaneh M, Rai M, editors. Antifungal Metabolites from Plants. Berlin, Heidelberg: Springer; 2013. doi:10.1007/978-3-642-38076-1_7.

Niimi K, Maki K, Ikeda F, Holmes AR, Lamping E, Niimi M, Monk BC, Cannon RD. Overexpression of *Candida albicans* CDR1, CDR2, or MDR1 does not produce significant changes in echinocandin susceptibility. Antimicrob Agents Chemother. 2006;50(4):1148–1155. doi:10.1128/AAC.50.4.1148-1155.2006.

Niño-Vega G, Padró-Villegas L, López-Romero E. New ground in antifungal discovery and therapy for invasive fungal infections: innovations, challenges, and future directions. J Fungi (Basel). 2024;10(12):871. doi:10.3390/jof10120871.

Odds FC, Brown AJ, Gow NA. Antifungal agents: mechanisms of action. Trends Microbiol. 2003;11(6):272–279. doi:10.1016/S0966-842X(03)00117-3.

Parums DV. Editorial: The World Health Organization (WHO) Fungal Priority Pathogens List in Response to Emerging Fungal Pathogens During the COVID-19 Pandemic. Med Sci Monit. 2022 Dec 1;28:e939088. doi: 10.12659/MSM.939088. PMID: 36453055; PMCID: PMC9724454

Pavela O, Juhász T, Tóth L, et al. Mapping of the lipid-binding regions of the antifungal protein NFAP2 by exploiting model membranes. J Chem Inf Model. 2024;64(16):6557–6569. doi:10.1021/acs.jcim.4c00229.

Perea S, Patterson TF. Antifungal resistance in pathogenic fungi. Clin Infect Dis. 2002;35(9):1073–1080. doi:10.1086/344050.

Pfaller MA, Pappas PG, Wingard JR. Invasive fungal pathogens: current epidemiological trends. Clin Infect Dis. 2006;43(Suppl 1):S3–S14. doi:10.1086/504490.

Perlin DS, Rautemaa-Richardson R, Alastruey-Izquierdo A. The global problem of antifungal resistance: prevalence, mechanisms, and management. Lancet Infect Dis. 2017;17(12):e383–e392. doi:10.1016/S1473-3099(17)30316-X.

Perlin DS, Shor E, Zhao Y. Update on antifungal drug resistance. Curr Clin Microbiol Rep. 2015;2(2):84–95. doi:10.1007/s40588-015-0015-1.

Pettersen EF, Goddard TD, Huang CC, Couch GS, Greenblatt DM, Meng EC, Ferrin TE. UCSF Chimera—a visualization system for exploratory research and analysis. J Comput Chem. 2004;25(13):1605–1612. doi:10.1002/jcc.20084.

Pianalto KM, Alspaugh JA. New horizons in antifungal therapy. J Fungi (Basel). 2016;2(4):26. doi:10.3390/jof2040026.

Polvi EJ, Li X, O'Meara TR, Leach MD, Cowen LE. Opportunistic yeast pathogens: reservoirs, virulence mechanisms, and therapeutic strategies. Cell Mol Life Sci. 2015;72(12):2261–2287. doi:10.1007/s00018-015-1860-z.

Puumala E, Fallah S, Robbins N, Cowen LE. Advancements and challenges in antifungal therapeutic development. Clin Microbiol Rev. 2024;37(1):e00142-23. doi:10.1128/cmr.00142-23.

Raghupathi KR, Koodali RT, Manna AC. Size-dependent bacterial growth inhibition and mechanism of antibacterial activity of zinc oxide nanoparticles. Langmuir. 2011;27(7):4020–4028. doi:10.1021/la104825u.

Rai M, Yadav A, Gade A. Silver nanoparticles as a new generation of antimicrobials. Biotechnol Adv. 2009;27(1):76–83. doi:10.1016/j.biotechadv.2008.09.002.

Richardson MD. Changing patterns and trends in systemic fungal infections. J Antimicrob Chemother. 2005;56(Suppl 1):i5–i11. doi:10.1093/jac/dki218.

Robbins N, Caplan T, Cowen LE. Molecular evolution of antifungal drug resistance. Annu Rev Microbiol. 2017;71:753–775. doi:10.1146/annurev-micro-030117-020345.

Ropero-Pérez C, Bolós B, Giner-Llorca M, Locascio A, Gimenez Garrigues S, Gandía M, Manzanares P, Marcos JF. Transcriptomic profile of *Penicillium digitatum* reveals novel aspects of the mode of action of the antifungal protein AfpB. Microbiol Spectr. 2023;11(3):e04846-22. doi:10.1128/spectrum.04846-22.

Rochard C, Bigot J, Balloy V, Hennequin C, Guitard J. Antimicrobial peptides: a new alternative for the treatment of aspergillosis. Rev Mal Respir. 2024;41(5):e69–e80. doi:10.1016/j.rmr.2024.02.011.

Rodrigues ML, Nosanchuk JD. Fungal diseases as neglected pathogens: a wake-up call to public health officials. PLoS Negl Trop Dis. 2020;14(2):e0007964. doi:10.1371/journal.pntd.0007964.

Ryder NS, Wagner S, Leitner I. In vitro activities of terbinafine against cutaneous isolates of *Candida albicans* and other pathogenic yeasts. Antimicrob Agents Chemother. 1998;42(5):1057–1061. doi:10.1128/AAC.42.5.1057.

Sagaram US, Pandurangi R, Kaur J, Smith TJ, Shah DM. Structure-activity determinants in antifungal plant defensins MsDef1 and MtDef4 with different modes of action against *Fusarium graminearum*. PLoS One. 2011;6(4):e18550. doi:10.1371/journal.pone.0018550.

Sanglard D, Coste AT. Activity of isavuconazole and other azoles against *Candida* clinical isolates and yeast model systems with known azole resistance mechanisms. Antimicrob Agents Chemother. 2016;60(1):229–238. doi:10.1128/AAC.02157-15.

Sanglard D, Coste AT, Ferrari S. Antifungal drug resistance mechanisms in fungal pathogens from the perspective of transcriptional gene regulation. FEMS Yeast Res. 2009;9(7):1029–1050. doi:10.1111/j.1567-1364.2009.00578.x.

Sekkides O. The ambitious '95–95 by 2025' roadmap for the diagnosis and management of fungal diseases. Lancet Infect Dis. 2015;15(8):884–885. doi:10.1016/S1473-3099(15)00165-6.

Selitrennikoff CP. Antifungal proteins. Appl Environ Microbiol. 2001;67(7):2883–2894. doi:10.1128/AEM.67.7.2883-2894.2001.

Selmecki A, Forche A, Berman J. Aneuploidy and isochromosome formation in drug-resistant *Candida albicans*. Science. 2006;313(5785):367–370. doi:10.1126/science.1128242.

Singh N. Trends in the epidemiology of opportunistic fungal infections: predisposing factors and the impact of antimicrobial use practices. Clin Infect Dis. 2001;33(10):1692–1696. doi:10.1086/323895.

Singh K, Rani J. Sequential and structural aspects of antifungal peptides from animals, bacteria and fungi based on bioinformatics tools. Probiotics Antimicrob Proteins. 2016;8(2):85–101. doi:10.1007/s12602-016-9212-3.

Sionov E, Lee H, Chang YC, Kwon-Chung KJ. *Cryptococcus neoformans* overcomes stress of azole drugs by formation of disomy in specific multiple chromosomes. PLoS Pathog. 2010;6(4):e1000848. doi:10.1371/journal.ppat.1000848.

Slezina MP, Istomina EA, Kulakovskaya EV, Korostyleva TV, Odintsova TI. The γ-core motif peptides of AMPs from grasses display inhibitory activity against human and plant pathogens. Int J Mol Sci. 2022;23(15):8383. doi:10.3390/ijms23158383.

Slezina MP, Istomina EA, Korostyleva TV, Odintsova TI. The γ-core motif peptides of plant AMPs as novel antimicrobials for medicine and agriculture. Int J Mol Sci. 2023;24(1):483. doi:10.3390/ijms24010483.

Sonderegger C, Váradi G, Galgóczy L, Kocsubé S, Posch W, Borics A, Dubrac S, Tóth GK, Wilflingseder D, Marx F. The evolutionary conserved γ-core motif influences the anti-*Candida* activity of the *Penicillium chrysogenum* antifungal protein PAF. Front Microbiol. 2018;9:1655. doi:10.3389/fmicb.2018.01655.

Sousa F, Ferreira D, Reis S, Costa P. Current insights on antifungal therapy: novel nanotechnology approaches for drug delivery systems and new drugs from natural sources. Pharmaceuticals (Basel). 2020;13(9):248. doi:10.3390/ph13090248.

Sreerama N, Woody RW. Estimation of protein secondary structure from circular dichroism spectra: comparison of CONTIN, SELCON, and CDSSTR methods with an expanded reference set. Anal Biochem. 2000;287(2):252–260. doi:10.1006/abio.2000.4880.

Starke S, Velleman L, Dobbert B, Seibert L, Witte J, Jung S, Meyer V. The antifungal peptide AnAFP from *Aspergillus niger* promotes nutrient mobilization through autophagic recycling during asexual development. Front Microbiol. 2025;15:1490293. doi:10.3389/fmicb.2024.1490293.

Struyfs C, Cammue BPA, Thevissen K. Membrane-interacting antifungal peptides. Front Cell Dev Biol. 2021;9:649875. doi:10.3389/fcell.2021.649875.

Tamura K, Stecher G, Kumar S. MEGA11: molecular evolutionary genetics analysis version 11. Mol Biol Evol. 2021;38(7):3022–3027. doi:10.1093/molbev/msab120.

Theis T, Wedde M, Meyer V, Stahl U. The antifungal protein from *Aspergillus giganteus* causes membrane permeabilization. Antimicrob Agents Chemother. 2003;47(2):588–593. doi:10.1128/AAC.47.2.588-593.2003.

Tóth L, Boros É, Poór P, Ördög A, Kele Z, Váradi G, Holzknecht J, Bratschun-Khan D, Nagy I, Tóth GK, Rákhely G, Marx F, Galgóczy L. The potential use of the *Penicillium chrysogenum* antifungal protein PAF, the designed variant PAFopt and its γ-core peptide Pγopt in plant protection. Microb Biotechnol. 2020;13(5):1403–1414. doi:10.1111/1751-7915.13559.

Tóth L, Kele Z, Borics A, Nagy L, Váradi G, Virágh M, Takó M, Vágvölgyi C, Galgóczy L. NFAP2, a novel cysteine-rich anti-yeast protein from *Neosartorya fischeri* NRRL 181: isolation and characterization. AMB Express. 2016;6(1):75. doi:10.1186/s13568-016-0250-8.

Tóth L, Poór P, Ördög A, Váradi G, Farkas A, Papp C, Bende G, Tóth GK, Rákhely G, Marx F, Galgóczy L. The combination of *Neosartorya* (*Aspergillus*) *fischeri* antifungal proteins with rationally designed γ-core peptide derivatives is effective for plant and crop protection. BioControl. 2022;67(2):249–262. doi:10.1007/s10526-022-10132-y.

Tóth L, Váradi G, Boros É, Borics A, Ficze H, Nagy I, Tóth GK, Rákhely G, Marx F, Galgóczy L. Biofungicidal potential of *Neosartorya* (*Aspergillus*) *fischeri* antifungal protein NFAP and novel synthetic γ-core peptides. Front Microbiol. 2020;11:820. doi:10.3389/fmicb.2020.00820.

Urban K, Chu S, Scheufele C, Giesey RL, Mehrmal S, Uppal P, Delost GR. The global, regional, and national burden of fungal skin diseases in 195 countries and territories: A cross-sectional analysis from the Global Burden of Disease Study 2017. JAAD Int. 2020 Nov 30;2:22-27. doi: 10.1016/j.jdin.2020.10.003. PMID: 34409349; PMCID: PMC8362308.

Utesch T, de Miguel Catalina A, Schattenberg C, Paege N, Schmieder P, Krause E, Miao Y, McCammon JA, Meyer V, Jung S, Mroginski MA. A computational modeling approach predicts interaction of the antifungal protein AFP from *Aspergillus giganteus* with fungal membranes via its γ-core motif. mSphere. 2018;3(5):e00377-18. doi:10.1128/mSphere.00377-18.

van der Weerden NL, Bleackley MR, Anderson MA. Properties and mechanisms of action of naturally occurring antifungal peptides. Cell Mol Life Sci. 2013;70(19):3545–3570. doi:10.1007/s00018-013-1260-1.

Vandeputte P, Ferrari S, Coste AT. Antifungal resistance and new strategies to control fungal infections. Int J Microbiol. 2012;2012:713687. doi:10.1155/2012/713687.

Vanzolini T, Magnani M. Old and new strategies in therapy and diagnosis against fungal infections. Appl Microbiol Biotechnol. 2024;108(1):147. doi:10.1007/s00253-023-12884-8.

Váradi G, Bende G, Borics A, Dán K, Rákhely G, Tóth GK, Galgóczy L. Rational design of antifungal peptides based on the γ-core motif of a *Neosartorya* (*Aspergillus*) *fischeri* antifungal protein to improve structural integrity, efficacy, and spectrum. ACS Omega. 2024;9(6):7206–7214. doi:10.1021/acsomega.3c09377.

Váradi G, Kele Z, Czajlik A, Borics A, Bende G, Papp C, Rákhely G, Tóth GK, Batta G, Galgóczy L. Hard nut to crack: solving the disulfide linkage pattern of the *Neosartorya* (*Aspergillus*) *fischeri* antifungal protein 2. Protein Sci. 2023;32(7):e4692. doi:10.1002/pro.4692.

Varadi M, Bertoni D, Magana P, Paramval U, Pidruchna I, Radhakrishnan M, Tsenkov M, Nair S, Mirdita M, Yeo J, et al. AlphaFold Protein Structure Database in 2024: providing structure coverage for over 214 million protein sequences. Nucleic Acids Res. 2024;52(D1):D368–D375. doi:10.1093/nar/gkad1011.

Váradi G, Tóth GK, Batta G. Structure and synthesis of antifungal disulfide β-strand proteins from filamentous fungi. Microorganisms. 2019;7(1):5. doi:10.3390/microorganisms7010005.

Vermes A. Flucytosine: a review of its pharmacology, clinical indications, pharmacokinetics, toxicity and drug interactions. J Antimicrob Chemother. 2000;46(2):171–179. doi:10.1093/jac/46.2.171.

Verstrepen KJ, Klis FM. Flocculation, adhesion and biofilm formation in yeasts. Mol Microbiol. 2006;60(1):5–15. doi:10.1111/j.1365-2958.2006.05072.x.

Wall G, Lopez-Ribot JL. Current antimycotics, new prospects, and future approaches to antifungal therapy. Antibiotics (Basel). 2020;9(8):445. doi:10.3390/antibiotics9080445.

Wang G, Li X, Wang Z. APD3: the antimicrobial peptide database as a tool for research and education. Nucleic Acids Res. 2016;44(D1):D1087–D1093. doi:10.1093/nar/gkv1278.

Waterhouse AM, Procter JB, Martin DM, Clamp M, Barton GJ. Jalview Version 2—a multiple sequence alignment editor and analysis workbench. Bioinformatics. 2009;25(9):1189–1191. doi:10.1093/bioinformatics/btp033.

Webb BJ, Ferraro JP, Rea S, Kaufusi S, Goodman BE, Spalding J. Epidemiology and clinical features of invasive fungal infection in a US health care network. Open Forum Infect Dis. 2018;5(8):ofy187. doi:10.1093/ofid/ofy187.

Whelan S, Goldman N. A general empirical model of protein evolution derived from multiple protein families using a maximum-likelihood approach. Mol Biol Evol. 2001;18(5):691–699. doi:10.1093/oxfordjournals.molbev.a003851.

Williams CJ, Headd JJ, Moriarty NW, Prisant MG, Videau LL, Deis LN, Verma V, Keedy DA, Hintze BJ, Chen VB, et al. MolProbity: more and better reference data for

improved all-atom structure validation. Protein Sci. 2018;27(1):293–315. doi:10.1002/pro.3330.

Wong JH, Ng TB. Plant biochemistry: antifungal proteins protecting plants from fungal pathogens. In: Plant Biochemistry, Vol. 4. 2011:745–756. doi:10.1016/B978-0-08-088504-9.00013-1.

Wong J, Ng TB, Cheung RCF, Ye X, Wang HX, Lam S, Lin P, Chan YS, Fang EF, Ngai PHK, Xia L, Ye X, Jiang Y, Liu F. Proteins with antifungal properties and other medicinal applications from plants and mushrooms. Appl Microbiol Biotechnol. 2010;87(4):1221–1235. doi:10.1007/s00253-010-2690-4.

Zhao G, Jia C, Zhu C, Fang M, Li C, Chen Y, He Y, Han S, Gao JS, Wang T, Wang C, Wang J. γ-core guided antibiotic design based on human enteric defensin 5. Membranes (Basel). 2023;13(1):51. doi:10.3390/membranes13010051.

Zhu P, Li Y, Guo T, Liu S, Tancer RJ, Hu C, Zhao C, Xue C, Liao G. New antifungal strategies: drug combination and co-delivery. Adv Drug Deliv Rev. 2023;198:114874. doi:10.1016/j.addr.2023.114874.

Zhu Y, Hao W, Wang X, Ouyang J, Deng X, Yu H, Wang Y. Antimicrobial peptides, conventional antibiotics, and their synergistic utility for the treatment of drug-resistant infections. Med Res Rev. 2022;42(4):1377–1422. doi:10.1002/med.21879.

11. LIST OF PUBLICATIONS

11.1. Publication related to thesis work

Karemera JK, Váradi G, Bende G, Merber R, Dán K, Papp C, Farkas A, Maróti G, Tóth GK, Borics A, Galgóczy L. Screening the γ-core motif peptides of ascomycetous antifungal proteins for antifungal activity and potential therapeutic applicability. Probiotics Antimicrob Proteins. 2026. doi: 10.1007/s12602-025-10890-y. Epub ahead of print. IF_{2024}=4.4 (Q2)

11.2. Other publications

Dán K, Zsindely N, Kele Z, Laczi K, **Karemera JK**, Papp C, Farkas A, Maróti G, Borics A, Bodai L, Galgóczy L. Beyond plasma membrane disruption: novel antifungal mechanism of *Neosartorya* (*Aspergillus*) *fischeri* antifungal protein 2 in *Candida albicans*. Int J Biol Macromol. 2025;327:146558. doi:10.1016/j.ijbiomac.2025.146558. IF_{2024}=8.5 (D1)

Emmanuel M, Parfait C, Callixte Y, **Karemera J**. Contribution of medical wards contamination to wound infection among patients attending Ruhengeri Referral Hospital. Int J Microbiol. 2021:7838763.doi.org/10.1155/2021/7838763. IF_{2021}=0.4 (Q4)

Callixte Y, Thierry H, **Karemera J**, Cedrick I,Monique M , Ange Yvette Uw. Bacteriological identification among patients attending intensive care unit at Nemba District Hospital. Am J Biomed Sci. 2019;11(2):65–73.DOI: 10.5099/aj190200065.
Callixte Y, François N, Ange Y U, Karemera J, Françoise A, Emmanuel M, Thierry H. Bacteriological identification between human and sheep living in the same shelter: Cyuve Sector, Musanze, Rwanda. Int J Res Stud Biosci. 2019;7(5):1–8.DOI:10.20431/2349-0365.0705001.

Karemera J, Neel GR. Assessment of intestinal parasitic infections and risk factors among suspected patients attending Kirambo Health Center. Int J Pharma Res Health Sci. 2018;6(1):2338–2341. DOI:10.21276/ijprhs. 2018.01.44.

Karemera J, G R Neel, Cedric Izere. Contamination of currency, notes and coins as sources of transmissible diseases. Int J Pharma Res Health Sci. 2018;6(1):2334–2337.DOI: 10.21276/ijprhs.

Karemera JK, Kumar R, Shrestha S, Chaudhari SR. Bacteriological implication of antibiogram on otitis media. Sch J Appl Med Sci. 2017;5(7D):2756–2762.DOI: 10.36347/sjams.2017.v05i07.051.

Karemera JK, Kumar R, Shrestha S, Chaudhari S. Study of ventilator associated pneumonia: its etiology and antibiogram profile. Sch J Appl Med Sci. 2017;5(12B):4924–4927.DOI: 10.36347/sjams.2017.v05i12.027

Janviere K**, Karemera JK**, Cedrick I, Clementine Y. Impact of antioxidant activity of Sechium edule (chayote) in prevention of cancer. Int J Res AYUSH Pharm Sci. 2017;1(6):196–198.http://ijraps.in

12. SUPLEMENTARY MATERIAL

Table S1: Statistical analysis of *Candida albicans* SC5314-infected larval survival treated with γAFP^{B6GXZ8}, terbinafine (TRB), and their combination.

IPS *vs. C. albicans* SC5314 + IPS		
Log-rank (Mantel-Cox) test		
Chi square	24.2	
df	1	
P value	<0.0001	
P value summary	****	
Are the survival curves sig different?	Yes	
Gehan-Breslow-Wilcoxon test		
Chi square	24.12	
df	1	
P value	<0.0001	
P value summary	****	
Are the survival curves sig different?	Yes	
Median survival		
IPS	Undefined	
C. albicans + IPS	4.5	
Hazard Ratio (Mantel-Haenszel)	**B/C**	**C/B**
Ratio (and its reciprocal)	0.09657	10.36
95% CI of ratio	0.03805 to 0.2451	4.080 to 26.28
Hazard Ratio (logrank)	**B/C**	**C/B**
Ratio (and its reciprocal)	0.06881	14.53
95% CI of ratio	0.02793 to 0.1696	5.898 to 35.81
IPS *vs. C. albicans* SC5314 + γAFP^{B6GXZ8}		
Log-rank (Mantel-Cox) test		
Chi square	7.999	
df	1	
P value	0.0047	
P value summary	**	
Are the survival curves sig different?	Yes	
Gehan-Breslow-Wilcoxon test		
Chi square	8.148	
df	1	
P value	0.0043	
P value summary	**	
Are the survival curves sig different?	Yes	
Median survival		
IPS	Undefined	
C. albicans + γAFP^{B6GXZ8}	Undefined	
Hazard Ratio (Mantel-Haenszel)	**B/D**	**D/B**
Ratio (and its reciprocal)	0.1887	5.3
95% CI of ratio	0.05939 to 0.5993	1.669 to 16.84

Hazard Ratio (logrank)	**B/D**	**D/B**
Ratio (and its reciprocal)	0.1531	6.53
95% CI of ratio	0.04889 to 0.4796	2.085 to 20.45
IPS *vs. C. albicans* SC5314 + TRB		
Log-rank (Mantel-Cox) test		
Chi square	4.516	
df	1	
P value	0.0336	
P value summary	*	
Are the survival curves sig different?	Yes	
Gehan-Breslow-Wilcoxon test		
Chi square	4.521	
df	1	
P value	0.0335	
P value summary	*	
Are the survival curves sig different?	Yes	
Median survival		
IPS	Undefined	
C. albicans + TRB	Undefined	
Hazard Ratio (Mantel-Haenszel)	**B/E**	**E/B**
Ratio (and its reciprocal)	0.256	3.907
95% CI of ratio	0.07284 to 0.8995	1.112 to 13.73
Hazard Ratio (logrank)	**B/E**	**E/B**
Ratio (and its reciprocal)	0.2204	4.536
95% CI of ratio	0.06366 to 0.7633	1.310 to 15.71
IPS *vs. C. albicans* SC5314 + γAFP^{B6GXZ8} + TRB		
Log-rank (Mantel-Cox) test		
Chi square	3.736	
df	1	
P value	0.0533	
P value summary	ns	
Are the survival curves sig different?	No	
Gehan-Breslow-Wilcoxon test		
Chi square	3.71	
df	1	
P value	0.0541	
P value summary	ns	
Are the survival curves sig different?	No	
Median survival		
IPS	Undefined	
C. albicans + γAFP^{B6GXZ8} + TRB	Undefined	
Hazard Ratio (Mantel-Haenszel)	**B/F**	**F/B**
Ratio (and its reciprocal)	0.2906	3.442
95% CI of ratio	0.08297 to 1.017	0.9828 to 12.05
Hazard Ratio (logrank)	**B/F**	**F/B**
Ratio (and its reciprocal)	0.2477	4.037

95% CI of ratio	0.07172 to 0.8557	1.169 to 13.94
***C. albicans* SC5314 +IPS *vs. C. albicans* SC5314 +γAFP^{B6GXZ8}**		
Log-rank (Mantel-Cox) test		
Chi square	5.093	
df	1	
P value	0.024	
P value summary	*	
Are the survival curves sig different?	Yes	
Gehan-Breslow-Wilcoxon test		
Chi square	5.057	
df	1	
P value	0.0245	
P value summary	*	
Are the survival curves sig different?	Yes	
Median survival		
C. albicans + IPS	4.5	
C. albicans + γAFP^{B6GXZ8}	Undefined	
Hazard Ratio (Mantel-Haenszel)	C/D	D/C
Ratio (and its reciprocal)	2.472	0.4045
95% CI of ratio	1.126 to 5.426	0.1843 to 0.8878
Hazard Ratio (logrank)	C/D	D/C
Ratio (and its reciprocal)	2.273	0.4399
95% CI of ratio	1.078 to 4.793	0.2086 to 0.9274
***C. albicans* SC5314 + IPS *vs. C. albicans* SC5314 + TRB**		
Log-rank (Mantel-Cox) test		
Chi square	10.13	
df	1	
P value	0.0015	
P value summary	**	
Are the survival curves sig different?	Yes	
Gehan-Breslow-Wilcoxon test		
Chi square	10.75	
df	1	
P value	0.001	
P value summary	**	
Are the survival curves sig different?	Yes	
Median survival		
C. albicans + IPS	4.5	
C. albicans + TRB	Undefined	
Hazard Ratio (Mantel-Haenszel)	**C/E**	**E/C**
Ratio (and its reciprocal)	3.791	0.2638
95% CI of ratio	1.668 to 8.614	0.1161 to 0.5994
Hazard Ratio (logrank)	**C/E**	**E/C**
Ratio (and its reciprocal)	3.375	0.2963
95% CI of ratio	1.540 to 7.396	0.1352 to 0.6494
***C. albicans* SC5314 +IPS *vs. C. albicans* SC5314 + γAFP^{B6GXZ8} + TRB**		

Log-rank (Mantel-Cox) test		
Chi square	12.7	
df	1	
P value	0.0004	
P value summary	***	
Are the survival curves sig different?	Yes	
Gehan-Breslow-Wilcoxon test		
Chi square	13.75	
df	1	
P value	0.0002	
P value summary	***	
Are the survival curves sig different?	Yes	
Median survival		
C. albicans + IPS	4.5	
C. albicans+γAFP^{B6GXZ8} + TRB	Undefined	
Hazard Ratio (Mantel-Haenszel)	**C/F**	**F/C**
Ratio (and its reciprocal)	4.515	0.2215
95% CI of ratio	1.970 to 10.35	0.09665 to 0.5075
Hazard Ratio (logrank)	**C/F**	**F/C**
Ratio (and its reciprocal)	3.857	0.2592
95% CI of ratio	1.739 to 8.558	0.1168 to 0.5751
***C. albicans* SC5314 + γAFP^{B6GXZ8} *vs. C. albicans* SC5314 + TRB**		
Log-rank (Mantel-Cox) test		
Chi square	0.7003	
df	1	
P value	0.4027	
P value summary	ns	
Are the survival curves sig different?	No	
Gehan-Breslow-Wilcoxon test		
Chi square	0.8203	
df	1	
P value	0.3651	
P value summary	ns	
Are the survival curves sig different?	No	
Median survival		
C. albicans + γAFPB^{6GXZ8}	Undefined	
C. albicans + TRB	Undefined	
Hazard Ratio (Mantel-Haenszel)	**D/E**	**E/D**
Ratio (and its reciprocal)	1.5	0.6666
95% CI of ratio	0.5803 to 3.878	0.2579 to 1.723
Hazard Ratio (logrank)	**D/E**	**E/D**
Ratio (and its reciprocal)	1.47	0.6804
95% CI of ratio	0.5816 to 3.714	0.2693 to 1.719
***C. albicans* SC5314 + γAFP^{B6GXZ8} *vs. C. albicans* SC5314 + γAFPB^{6GXZ8} + TRB**		
Log-rank (Mantel-Cox) test		
Chi square	1.252	

df	1	
P value	0.2632	
P value summary	ns	
Are the survival curves sig different?	No	
Gehan-Breslow-Wilcoxon test		
Chi square	1.493	
df	1	
P value	0.2217	
P value summary	ns	
Are the survival curves sig different?	No	
Median survival		
C. albicans + γAFP^{B6GXZ8}	Undefined	
C. albicans + γAFP^{B6GXZ8} + TRB	Undefined	
Hazard Ratio (Mantel-Haenszel)	**D/F**	**F/D**
Ratio (and its reciprocal)	1.724	0.58
95% CI of ratio	0.6640 to 4.476	0.2234 to 1.506
Hazard Ratio (logrank)	**D/F**	**F/D**
Ratio (and its reciprocal)	1.672	0.5982
95% CI of ratio	0.6571 to 4.252	0.2352 to 1.522
***C. albicans* SC5314 + TRB *vs. C. albicans* SC5314 + γAFP^{B6GXZ8} + TRB**		
Log-rank (Mantel-Cox) test		
Chi square	0.07	
df	1	
P value	0.7913	
P value summary	ns	
Are the survival curves sig different?	No	
Gehan-Breslow-Wilcoxon test		
Chi square	0.08884	
df	1	
P value	0.7657	
P value summary	ns	
Are the survival curves sig different?	No	
Median survival		
C. albicans + TRB	Undefined	
C. albicans + γFPB6GXZ8 + TRB	Undefined	
Hazard Ratio (Mantel-Haenszel)	**E/F**	**F/E**
Ratio (and its reciprocal)	1.145	0.8735
95% CI of ratio	0.4203 to 3.118	0.3207 to 2.379
Hazard Ratio (logrank)	**E/F**	**F/E**
Ratio (and its reciprocal)	1.138	0.8785
95% CI of ratio	0.4263 to 3.039	0.3290 to 2.346

Table S2: Statistical analysis of *Aspergillus fumigatus* CBS 101355-infected larval survival treated with γAFP^{A0A2J5HZT4}, fluconazole (FLC), and their combination.

IPS *vs.* *A. fumigatus* CBS 101355 + IPS		
Log-rank (Mantel-Cox) test		
Chi square	33.76	
df	1	
P value	<0,0001	
P value summary	****	
Are the survival curves sig different?	Yes	
Gehan-Breslow-Wilcoxon test		
Chi square	31.61	
df	1	
P value	<0,0001	
P value summary	****	
Are the survival curves sig different?	Yes	
Median survival		
IPS	Undefined	
A. fumigatus + IPS	4	
Hazard Ratio (Mantel-Haenszel)	**B/C**	**C/B**
Ratio (and its reciprocal)	0.09077	11.02
95% CI of ratio	0,0404 to 0,2039	4,904 to 24,75
Hazard Ratio (logrank)	**B/C**	**C/B**
Ratio (and its reciprocal)	0.0544	18.38
95% CI of ratio	0,02523 to 0,1173	8,524 to 39,64
IPS *vs.* *A. fumigatus* CBS 101355 + γAFP^{A0A2J5HZT4}		
Log-rank (Mantel-Cox) test		
Chi square	16.12	
df	1	
P value	<0,0001	
P value summary	****	
Are the survival curves sig different?	Yes	
Gehan-Breslow-Wilcoxon test		
Chi square	15.56	
df	1	
P value	<0,0001	
P value summary	****	
Are the survival curves sig different?	Yes	
Median survival		
IPS	Undefined	
A. fumigatus + γAFP^{A0A2J5HZT4}	Undefined	
Hazard Ratio (Mantel-Haenszel)	**B/D**	**D/B**
Ratio (and its reciprocal)	0.1398	7.153
95% CI of ratio	0,05351 to 0,3653	2,738 to 18,69
Hazard Ratio (logrank)	**B/D**	**D/B**

Ratio (and its reciprocal)	0.09573	10.45
95% CI of ratio	0,03769 to 0,2431	4,113 to 26,53
IPS *vs. A. fumigatus* CBS 101355 + FLC		
Log-rank (Mantel-Cox) test		
Chi square	30.71	
df	1	
P value	<0,0001	
P value summary	****	
Are the survival curves sig different?	Yes	
Gehan-Breslow-Wilcoxon test		
Chi square	29.09	
df	1	
P value	<0,0001	
P value summary	****	
Are the survival curves sig different?	Yes	
Median survival		
IPS	Undefined	
A. fumigatus + FLC	4	
Hazard Ratio (Mantel-Haenszel)	**B/E**	**E/B**
Ratio (and its reciprocal)	0.09203	10.87
95% CI of ratio	0,03958 to 0,214	4,673 to 25,27
Hazard Ratio (logrank)	**B/E**	**E/B**
Ratio (and its reciprocal)	0.05922	16.89
95% CI of ratio	0,02665 to 0,1316	7,599 to 37,53
IPS *vs. A. fumigatus* CBS 101355 + γAFP^{A0A2J5HZT4}+ FLC		
Log-rank (Mantel-Cox) test		
Chi square	10.95	
df	1	
P value	0.0009	
P value summary	***	
Are the survival curves sig different?	Yes	
Gehan-Breslow-Wilcoxon test		
Chi square	10.65	
df	1	
P value	0.0011	
P value summary	**	
Are the survival curves sig different?	Yes	
Median survival		
IPS	Undefined	
A. fumigatus + FLC + γAFP^{A0A2J5HZT4}	Undefined	
Hazard Ratio (Mantel-Haenszel)	**B/F**	**F/B**
Ratio (and its reciprocal)	0.1737	5.757
95% CI of ratio	0,06158 to 0,4899	2,041 to 16,24
Hazard Ratio (logrank)	**B/F**	**F/B**
Ratio (and its reciprocal)	0.1257	7.954
95% CI of ratio	0,04546 to 0,3477	2,876 to 22

***A. fumigatus* CBS 101355 + IPS *vs.* *A. fumigatus* CBS 101355 + γAFP^{A0A2J5HZT4}**		
Log-rank (Mantel-Cox) test		
Chi square	4.328	
df	1	
P value	0.0375	
P value summary	*	
Are the survival curves sig different?	Yes	
Gehan-Breslow-Wilcoxon test		
Chi square	4.047	
df	1	
P value	0.0442	
P value summary	*	
Are the survival curves sig different?	Yes	
Median survival		
A. fumigatus + IPS	4	
A. fumigatus + γAFP^{A0A2J5HZT4}	Undefined	
Hazard Ratio (Mantel-Haenszel)	**C/D**	**D/C**
Ratio (and its reciprocal)	2.048	0.4883
95% CI of ratio	1,042 to 4,023	0,2486 to 0,9594
Hazard Ratio (logrank)	**C/D**	**D/C**
Ratio (and its reciprocal)	1.816	0.5507
95% CI of ratio	0,9828 to 3,355	0,298 to 1,018
***A. fumigatus* CBS 101355 + IPS *vs.* *A. fumigatus* CBS 101355 + FLC**		
Log-rank (Mantel-Cox) test		
Chi square	0.003893	
df	1	
P value	0.9503	
P value summary	ns	
Are the survival curves sig different?	No	
Gehan-Breslow-Wilcoxon test		
Chi square	0.02008	
df	1	
P value	0.8873	
P value summary	ns	
Are the survival curves sig different?	No	
Median survival		
A. fumigatus + IPS	4	
A. fumigatus + FLC	4	
Ratio (and its reciprocal)	1	1
95% CI of ratio	0,5676 to 1,762	0,5676 to 1,762
Hazard Ratio (Mantel-Haenszel)	**C/E**	**E/C**
Ratio (and its reciprocal)	1.021	0.9798
95% CI of ratio	0,5377 to 1,937	0,5162 to 1,86
Hazard Ratio (logrank)	**C/E**	**E/C**
Ratio (and its reciprocal)	1.016	0.9842
95% CI of ratio	0,5768 to 1,79	0,5588 to 1,734

A. fumigatus CBS 101355 + IPS *vs. A. fumigatus* CBS 101355 + γAFP^{A0A2J5HZT4} +FLC		
Log-rank (Mantel-Cox) test		
Chi square	8.061	
df	1	
P value	0.0045	
P value summary	**	
Are the survival curves sig different?	Yes	
Gehan-Breslow-Wilcoxon test		
Chi square	7.467	
df	1	
P value	0.0063	
P value summary	**	
Are the survival curves sig different?	Yes	
Median survival		
A. fumigatus + IPS	4	
A. fumigatus + FLC + γAFP^{A0A2J5HZT4}	Undefined	
Hazard Ratio (Mantel-Haenszel)	**C/F**	**F/C**
Ratio (and its reciprocal)	2.732	0.366
95% CI of ratio	1,365 to 5,468	0,1829 to 0,7325
Hazard Ratio (logrank)	**C/F**	**F/C**
Ratio (and its reciprocal)	2.381	0.4201
95% CI of ratio	1,256 to 4,513	0,2216 to 0,7963
***A. fumigatus* CBS 101355 + γAFP^{A0A2J5HZT4} *vs. A. fumigatus* CBS 101355 + FLC**		
Log-rank (Mantel-Cox) test		
Chi square	3.651	
df	1	
P value	0.056	
P value summary	ns	
Are the survival curves sig different?	No	
Gehan-Breslow-Wilcoxon test		
Chi square	4.012	
df	1	
P value	0.0452	
P value summary	*	
Are the survival curves sig different?	Yes	
Median survival		
A. fumigatus + γAFP^{A0A2J5HZT4}	Undefined	
A. fumigatus + FLC	4	
Hazard Ratio (Mantel-Haenszel)	**D/E**	**E/D**
Ratio (and its reciprocal)	0.5094	1.963
95% CI of ratio	0,2551 to 1,017	0,9828 to 3,92
Hazard Ratio (logrank)	**D/E**	**E/D**
Ratio (and its reciprocal)	0.5713	1.75
95% CI of ratio	0,304 to 1,073	0,9316 to 3,289
***A. fumigatus* CBS 101355 + γAFP^{A0A2J5HZT4} *vs. A. fumigatus* CBS 101355 + FLC + γAFP^{A0A2J5HZT4}**		

Log-rank (Mantel-Cox) test		
Chi square	0.6143	
df	1	
P value	0.4332	
P value summary	ns	
Are the survival curves sig different?	No	
Gehan-Breslow-Wilcoxon test		
Chi square	0.5733	
df	1	
P value	0.449	
P value summary	ns	
Are the survival curves sig different?	No	
Median survival		
A. fumigatus + γAFP^{A0A2J5HZT4}	Undefined	
A. fumigatus + FLC + γAFP^{A0A2J5HZT4}	Undefined	
Hazard Ratio (Mantel-Haenszel)	**D/F**	**F/D**
Ratio (and its reciprocal)	1.361	0.7345
95% CI of ratio	0,6294 to 2,945	0,3396 to 1,589
Hazard Ratio (logrank)	**D/F**	**F/D**
Ratio (and its reciprocal)	1.317	0.7593
95% CI of ratio	0,6358 to 2,729	0,3665 to 1,573
***A. fumigatus* CBS 101355 +FLC *vs. A. fumigatus* CBS 101355 + FLC + γAFP^{A0A2J5HZT4}**		
Log-rank (Mantel-Cox) test		
Chi square	6.928	
df	1	
P value	0.0085	
P value summary	**	
Are the survival curves sig different?	Yes	
Gehan-Breslow-Wilcoxon test		
Chi square	7.064	
df	1	
P value	0.0079	
P value summary	**	
Are the survival curves sig different?	Yes	
Median survival		
A. fumigatus + FLC	4	
A. fumigatus + FLC +γ AFP^{A0A2J5HZT4}	Undefined	
Hazard Ratio (Mantel-Haenszel)	**E/F**	**F/E**
Ratio (and its reciprocal)	2.604	0.384
95% CI of ratio	1,277 to 5,311	0,1883 to 0,7832
Hazard Ratio (logrank)	**E/F**	**F/E**
Ratio (and its reciprocal)	2.272	0.4402
95% CI of ratio	1,176 to 4,388	0,2279 to 0,8504